Initiation of ligament engineering using novel silk scaffolds

Ainsworth, Benjamin James

Award date:
2007

Awarding institution:
University of Bath

Initiation of ligament engineering using novel silk scaffolds

Benjamin James Ainsworth

A thesis submitted for the degree of Doctor of Philosophy

University of Bath

Department of Chemical Engineering

October 2007

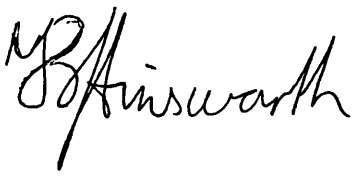

ProQuest LLC
789 East Eisenhower Parkway
P.O. Box 1346
Ann Arbor, MI 48106-1346

ABSTRACT

Three dimensional cell culture holds great promise both as a method for constructing better *ex vivo* models of tissues, and as a method for creating *de novo* tissue to repair damaged tissue. One of the major issues in biology is that many biological systems are controlled by multiple variables, yet it is normal to design univariate experiments. This problem can be reduced by designing multivariate experiments.

This thesis describes the creation of porous silk scaffolds in which both the pore structure can be varied from film-like to fibrous and the pore size can be controlled by using 20% v/v formic acid as a solvent and salt particles with a defined particle size range to produce salt leached scaffolds. Furthermore, Fourier transform infrared spectroscopy indicates that the chemistry of these scaffolds remains identical, and image analysis of sections through the scaffolds shows that the porosity remains constant. In order to confirm that the scaffolds were not cytotoxic, three cell types: primary ligament fibroblasts osteoblast and chondrocyte cell lines were grown on scaffold with different pore structures and constant pore size. DNA quantification suggests that differences in pore structure affect cell attachment and subsequent proliferation.

To better understand how ligament fibroblasts respond to differences in pore size and pore structure, a high pressure liquid chromatography protocol for quantifying glycosaminoglycans was adapted for use as tissue engineering outcome measure. It proved possible to analyse glycosaminoglycans following papain digestion with approximately an order of magnitude improvement in the sensitivity of the assay. On the basis of a literature review it was predicted that if ligament engineering follows the same pattern as development hyaluronic acid content should start high and drop rapidly, and the glycosaminoglycan : hydroxyproline ratio should also start high and drop rapidly.

Three different pore sizes and three different pore structures were combined in all possible combinations to make nine different types of scaffold for fabricated for the final experiment. These scaffolds were seeded with ligament fibroblasts from six different animals, and sacrificed after 1 day, 1 week, 2 weeks and 3 weeks. DNA, hydroxyproline, hyaluronic acid and chondroitin sulphate were quantified. Four different independent variables were analysed: time, animal, pore size and pore structure. Time, animal and pore size and their interactions affected DNA content. Time and animal and time x animal affected hydroxyproline and chondroitin sulphate content. Averaged over all the scaffolds glycosaminoglycan/hydroxyproline fraction started at 7 at the end of week 1 and dropped to 0.05 by the end of week 3, but the hyaluronic acid content was undetectable in most samples at all time points. The outcome variables were correlated; hydroxyproline content at week 1 and week 2 was not significantly correlated with hydroxyproline content at week 3; the only variable from the first two weeks to correlate significantly with DNA, hydroxyproline, and chondroitin sulphate at week 3 was chondroitin sulphate at week 1 (correlations of 0.281, 0.443 and 0.383 respectively). This data suggests that ligament engineering is a multistage process, and that the amount of collagen in the first two weeks of ligament engineering is unimportant.

ACKNOWLEDGMENTS

First, and formnost, I wish to thank Julian Chaudhuri for both allowing me the freedom to plough my own furrow, and keeping the furrows straight and narrow. I am incredibly grateful for the advice and friendship of Rachel Locklin. Thanks to past and present members of the tissue engineering group, especially Andy, Karina, Moreica, Holly and Richard. I am grateful for the help of my project students, Andy and Debbie. The advice of Ann O'Reily, and Ursula Potter on SEM was invaluable, as was the help of Alexei Lapkin with FTIR. Finally, I wish to acknowledge the help of the technicians: Feranando, Richard, Mac, Bob and Suzanne.

I gratefully acknowledge funding from the EPSRC and the University of Bristol

"The dogmas of the quiet past are inadequate to the stormy present. The occasion is piled high with difficulty, and we must rise with the occasion. As our case is new, so we must think anew and act anew."

Abraham Lincoln 1809-1865

TABLE OF CONTENTS

LIST OF FIGURES

LIST OF TABLES

LIST OF EQUATIONS

ABBREVIATIONS

Abbreviation	Full name
ANOVA	Analysis of variance
bFGF	Basic Fibroblast Growth Factor (also known as Fibroblast Growth Factor 2)
BMSC	Bone Marrow Stromal Cell
CFU-F	Colony Forming Units Fibroblastic
CS	Chondroitin Sulphate
DNA	Deoxyribonucleic Acid
ECM	Extracellular Matrix
EDTA	Ethylenediamine tetraacetic acid
EGF	Epidermal Growth Factor
EGFR	Epidermal Growth Factor Receptor
FA	Formic acid
HFIP	Hexafluoroisopropanol
HPLC	High Pressure Liquid Chromatography
HSP-70	Heat Shock Protein 70
Hy	Hydroxyproline
MCL	Medial Collateral Ligament
mRNA	Messenger Ribonucleic Acid
PBS	Phosphate Buffered Saline
PGE2	Prostaglandin E2
roH2O	Reverse osmosis water
SLRP	Small Leucine Rich Proteoglycan
SMC	Smooth Muscle Cell
TGF-β1	Transforming Growth Factor β1
Tris	Tris(hydroxymethyl)aminomethane
α-SMA	α-Smooth Muscle Actin

1 Introduction

Much of the interest in engineering replacement ligaments and tendons has focused on one of the ligaments inside the knee, the Anterior Cruciate Ligament (ACL), as it is frequently ruptured (over 200,000 cases in the USA per annum (Weitzel et al. 2002). The ACL accounts for 50% of ligament injuries, mostly as the result of sports injuries, and many of these injuries lead to permanent disability (Bollen 1998). An addition area of interest is that it is thought that osteoarthritis might result from damage to soft tissues such as the ACL (Brandt et al. 2006), and by extension, that early intervention to restore normal function to damaged soft tissue could prevent osteoarthritis.

The preferred option when surgically reconstructing a ruptured ACL is to use an autograft of either hamstring tendon or patellar tendon (Dopirak et al. 2004; Fu et al. 1999; Fu et al. 2000; Spindler et al. 2004). Two recent long term studies of soccer players with ruptured ACLs (Lohmander et al. 2004; Von Porat et al. 2004) suggest that the soccer players are at high risk of developing osteoarthritis regardless of surgical reconstruction. Cadaveric models suggest that these problems might be caused by failure to replicate the anatomy of the ACL (Yagi et al. 2002; Yamamoto et al. 2004).

In some patients neither hamstring tendon nor patellar tendon is suitable for harvesting and use as an autograft, these problems are particularly common when multiple ligaments are being reconstructed, or the original reconstruction requires revision. For this population several options are available including: allografts, which remain controversial, due to the possibility of infection and high cost (Barber 2003; Johnson 2003; McGuire 2003), and the Leeds-Keio polyester ligament which has poor long term outcomes (Murray and Macnicol 2004), possibly because the tissue inside the ligament is still immature 60 months postoperatively (Nomura et al. 2005).

1.1 Aims and Objectives

Tissue engineering offers a new approach to solve these problems, but the understanding of the cell and matrix biology necessary to engineer ligaments is far behind the understanding of cell and matrix biology necessary to engineer bone or cartilage. There has also been a much greater research effort targeted at bone and cartilage tissue engineering. For these reasons, in comparison to cartilage and bone tissue engineering, many fundamental questions about ligament engineering remain unanswered. This thesis attempts to answer some of these fundamental questions based on the mainstream tissue engineering techniques of seeding cells onto scaffolds. It is argued that scaffolds with high porosity will result in better cellular response (see Section 7.1.3), so this thesis focuses on highly porous scaffolds. It is commonly assumed that scaffolds with small (~100μm) pores are superior for fibrous tissue engineering, but this assumption is based on the formation of fibrous tissue in work trying to regenerate bone in an osteogenic environment. Therefore the central question investigated in this thesis is the effect of pore size and pore structure on ligament fibroblast cells. In order to understand this effect, both cell proliferation and matrix synthesis were quantified. In setting up this study much effort was put into the question of what would constitute a good outcome, the decision was to investigate to what extent hydroxyproline and glycosaminoglycan production in engineered ligaments mirrored the results published for these biomarkers in fibrous tissue development.

1.2 Outline of the thesis

The next chapter (Chapter 2) is a literature review covering: the biology of the ACL; how biomarkers have been used to understand ligament engineering and development; the use of bioreactors and biomaterials for ligament engineering, and finally a section introducing the multivariate statistics used in this thesis. The third chapter introduces the statistics used in this thesis. Chapter 4, Materials and Methods, reports the reagents and procedures used in this research.

In the first results chapter, (Chapter 5), a HPLC assay for glycosaminoglycans is adapted to work in a tissue engineering context. The second results chapter, (Chapter 6), reports with the development of a novel highly porous silk scaffold, in which both pore size, and pore structure can be varied. The final results chapter (Chapter 7) uses the techniques developed in the first two chapters to understand the effect of pore size and pore structure on ligament fibroblast proliferation and matrix synthesis.

The final chapter (Chapter 8) summarises the work carried out in this thesis, and makes suggestions for future work.

2 Literature Review

2.1 Biology of Ligament Engineering

2.1.1 Anatomy of the Anterior Cruciate Ligament

The ACL is a helical intraarticular ligament named for its attachment to anterior intercondylar area of the tibia. From this attachment it extends upwards, backwards and laterally (Figure 2-1) past the posterior cruciate ligament (PCL). Together with the PCL it forms the main bond between the femur and tibia (Snell 2000).

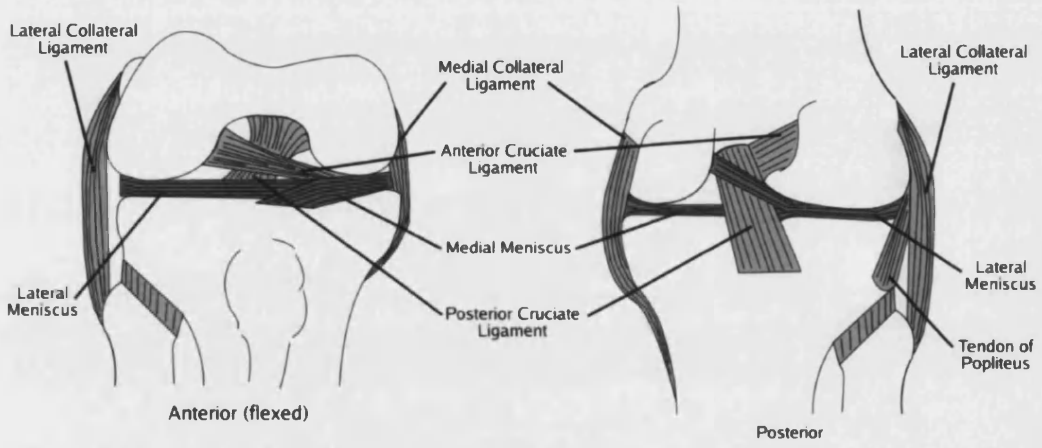

Diagram of the ligaments and menisci in the right knee

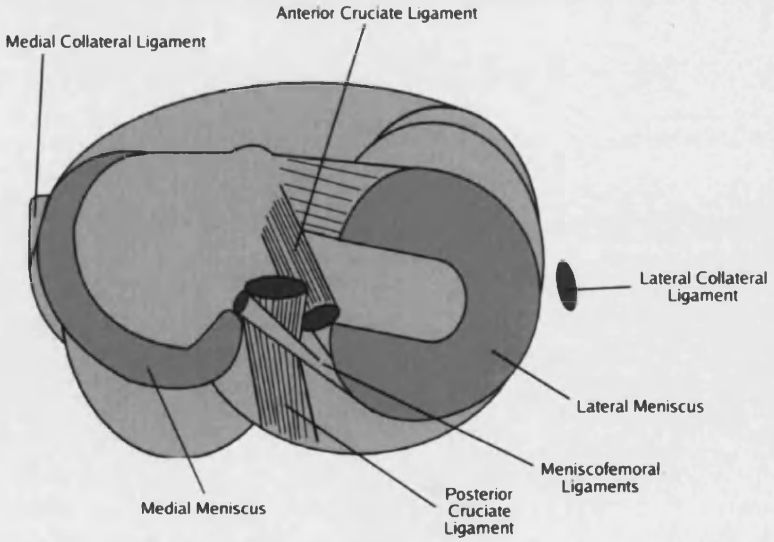

Cross Sectional diagram of the ligaments and menisci in the right knee seen from above

Figure 2-1 Diagram of the ligaments and menisci in the right knee. (After Snell (2000))

The anatomy of the ACL will be described by moving from a description of the arrangement of collagen molecules at the smallest scale moving up to larger scales until the anatomy is described (Figure 2-2). This description is based on the work of Clark and Sidles (1990), this agrees with the description used by Benjamin and Ralphs (2000) and Silver et al. (2003) although the three papers use different terminology. The notable difference between this description and that of Yahia and Drouin (1989) is that Clark and Sidles could not find the sub-fascicles described by Yahia and Drouin, this is possibly an artefact of differences in staining procedure.

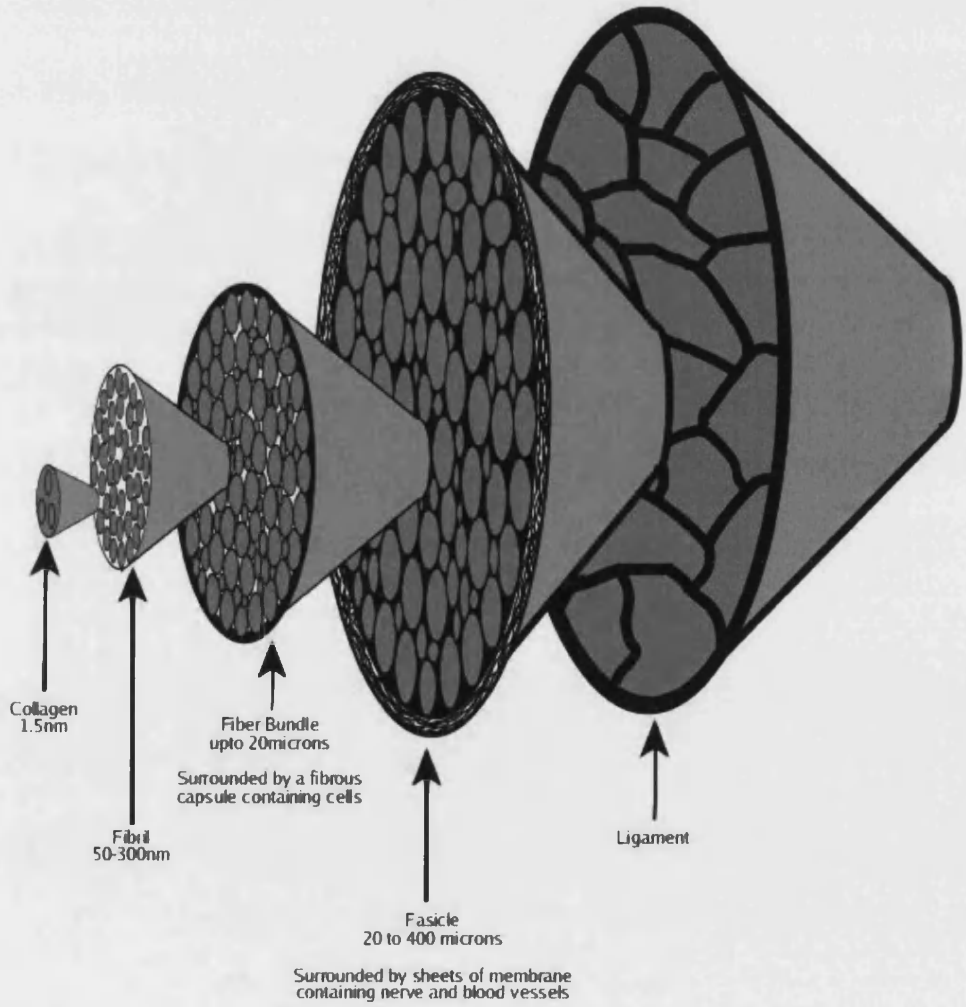

Figure 2-2 The 5 levels of organisation found by Clark and Sidles (1990)

Collagen molecules are arranged into fibrils, with the molecules arranged in rows and quarter staggered. These fibrils are from 50-300nm in diameter. The fibrils themselves are not straight, but run in a wavy pattern; this pattern is known as crimp. The wave is typically two dimensional, although in some fascicles the wave takes a helical form (Yahia and Drouin 1989).

Fibrils themselves are tightly packed to form bundles known as fibre bundles. These fibre bundles are surrounded by a fibrous capsule that are largest in the fibrocartilaginous regions near the insertion of the ligament, becoming more compact and elongated further away from the insertion. The fibrous capsules contain cells arranged in rows.

Fibre bundles are packed together to form fascicles, which have a diameter of 20 to 400μm. The fascicles are separated by a membranous septae, the number of membranes varies within the ligament, normally there are several layers separated by empty space, occasionally fascicles are separated by one or even no layers of membrane. Within the membranous septae lie the blood and nerve vessels. The divisions between fascicles become more prominent closer to the insertion, as the membranes separating them become more numerous.

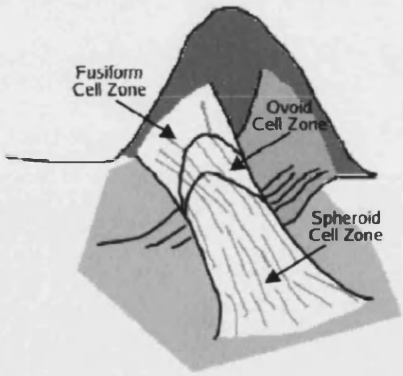

Figure 2-3 Distribution of cells within ACL (after Murray and Spector (1999))

The ACL can be divided up into three zones based on the shape of the cells within the ligament (Murray and Spector 1999). Moving along the ligament from the femur to the tibia, the cells start out looking like typical fibroblasts –

spindle shaped, the cells become more rounded as the tibia is approached becoming first ovoid and then spherical (see Figure 2-3). These ovoid and spherical cells occur in the regions of fibrocartilage where the ligament is being compressed during movement of the knee. It is worth noting that the cell density is five times higher in the fusiform cell zone than the spheroid cell zone. The proportion of different shaped cells can change with exercise, the ratios of spindle shaped to ovoid cells changed significantly comparing biped rats forced to exercise on treadmill and those without exercise (Sakuma et al. 1993).

The "enthesis" is where the ligament connects to bone, also known as the "insertion". It is thought to balance the different elastic moduli of ligament and bone so that local peaks in tension are avoided; at the enthesis the ligament becomes fibrocartilaginous and the ligament spread outs out (Benjamin et al. 2002).

The ACL is mostly composed of collagen (80% by dry weight (Vunjak-Novakovic et al. 2004)), this is ~90% collagens I and ~10% collagen III (Riechert et al. 2001). Although tendons and ligaments are similar, ligaments are thought to be slightly more metabolically active containing more cells, and glycosaminoglycans, but slightly less total collagen (Amiel et al. 1984).

2.1.2 Biomechanics of the ACL

The ACL has two roles: it is the primary restraint on anterior tibial displacement and is a secondary restraint of axial rotation. This section will explore the biomechanics of ACL at the level of the fibre bundle, the fascicle and as a tissue, using analogies with other ligaments and tendons where necessary.

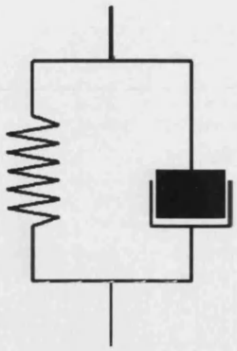

Figure 2-4 Simplest viscoelastic model – a spring and damper in parallel

Ligaments are viscoelastic materials; the simplest model of this behaviour is to imagine a spring and damper in parallel (Figure 2-4); the properties of the damper mimic the way viscoelastic materials flow, the spring models the way viscoelastic materials stretch elastically, and the spring and damper are in parallel, not series as they ultimately return to their original length.

The three phenomena most associated with viscoelasticity are shown in Figure 2-5:

- Creep - a ligament held a constant force will get extended with time
- Stress relaxation - a ligament held at constant length will progressively exert less force on its restraint
- Strain rate dependence, if ligaments are strained at low rates then they are absorb less energy, fail at a lower ultimate load and less stiff than at high strain rates.

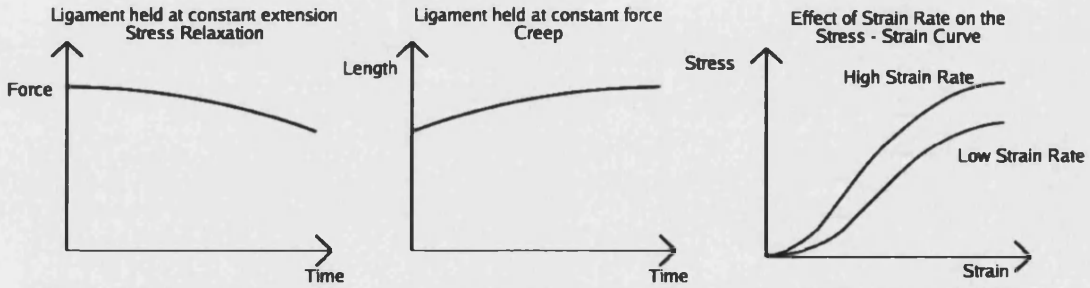

Figure 2-5 Stress relaxation, creep and strain rate dependence (after Woo et al (1997))

The recent work of Screen et al. (2004) provides evidence of what occurs to the fibre bundles when a ligament or tendon is under tensile strain. They

used cell nuclei as markers to enable them to estimate the strain field within a fibre bundle by comparing the position of nuclei next to the same fibre bundle and the displacement of adjacent fibre bundles by comparing the position of cell nuclei either side of a fibre bundle. They found that the strain within a fibre bundle was small only reaching ~1% when the fascicle was strained 8%. On the other hand the displacement between fibre bundles was much larger reaching ~4% when the fascicle was strained 8%. It is important to note that this appears to raise an important question about much of the work looking at the effects of tensile strain on tendon /ligament fibroblasts, the experiments often expose cells to 10% or greater strains when the fibroblasts are only strained by ~1% inside a tendon. Figure 2-6 summarises the current model of how the fibre bundles within a tendon respond to strain:

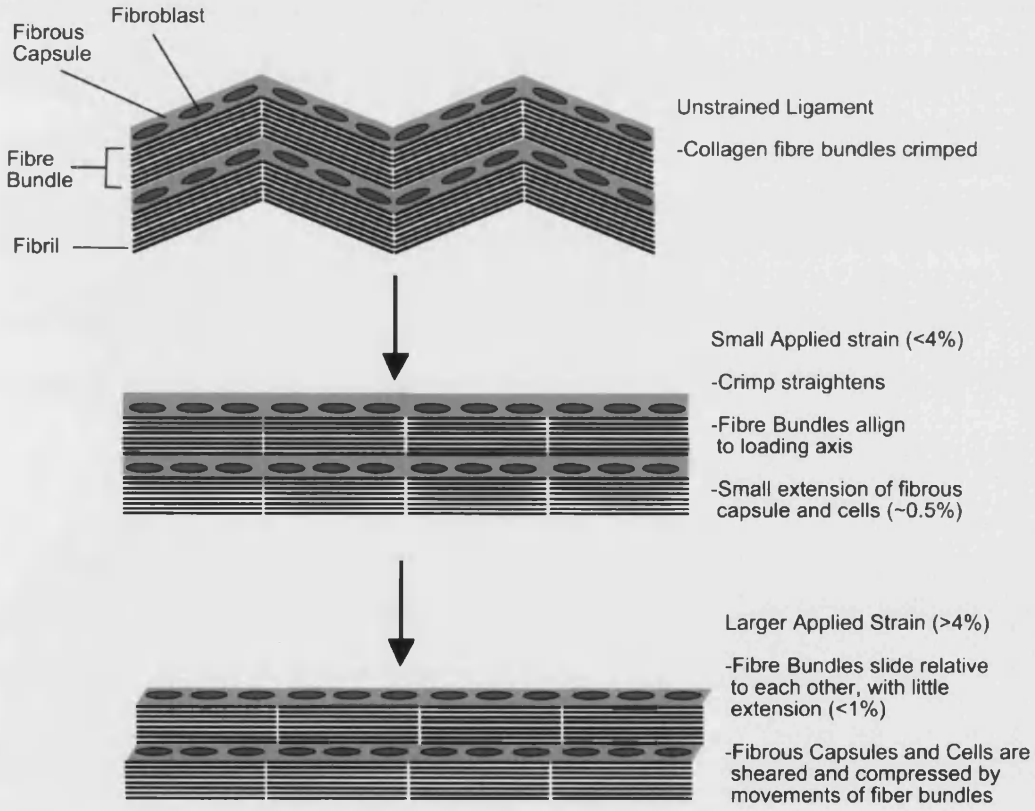

Figure 2-6 Effect of strain on the organisation of tendon (after Screen et al. (2004))

The work of Yamamoto et al. (1999) suggests how ligaments might behave at the level of fascicles. They compared the behaviour of fascicles isolated from rabbit patellar tendon with whole rabbit patellar tendon. They found that

the fascicles had 42% of the ultimate tensile strength and 179% of the ultimate tensile strain of the whole tendon. They suggest these differences are due to the ground substances between the fascicles, mechanical interactions between fascicles or different crimp structures. However more work is necessary to understand how single fascicles interact to form a tendon.

The ACL's role as the primary restraint of anterior tibial displacement has been widely investigated, and the force varies with the angle of flexion (Takai et al. 1993). The secondary role of the ACL in resisting internal axial rotation fits with its helical structure and lateral position. When the knee is passively flexed the ACL generates an internal torque of up to 1.4 Nm (Fukubayashi et al. 1982). This is complicated by the effect of compression of the knee upon the ACL, which has recently been investigated by Fleming et al. (2001) in order to understand the effects of weight bearing. The compression induced a 2% strain in otherwise unloaded ACLs and increased ACL strain at low anterior tibial loadings (loads < 40N) and low internal torques (torque < 2Nm).

One major complication when engineering a replacement ACL will be replicating the different functions and behaviours of the anteromedial and posterolateral bundles. The response of the posterolateral bundle to anterior tibial loading varies with the angle of knee flexion and the in-situ force in the posterolateral bundle is larger than the anteromedial bundle between 0° and 45° (Sakane et al. 1997). The anteromedial bundle shows a very constant response to anterior tibial loading at knee flexions between 0° and 90° (Sakane et al. 1997), it has been hypothesised that the anteromedial bundle plays a role in guiding the ACL (Takai et al. 1993). Recent evidence suggests that the current methods of ACL repair are failing due to failure to replicate the functions of both of these bundles and to position the autograft in the correct anatomical position (Yagi et al. 2002; Yamamoto et al. 2004).

The ACL, like many other ligaments, has a section of fibrocartilage. This is formed by simultaneous tension and compression. This compression is

generated *in vivo* by loading around a pulley (Benjamin and Ralphs 1998; Wren et al. 2000). It is not yet known whether the pattern of fibrocartilage in ligaments will have to be recreated *in vitro* when engineering ligaments, instead it might be possible to rely upon adaptation to compressive loads after surgical insertion of the engineered ligament.

2.1.3 Cell sources for ligament engineering

Three comparisons of different cell sources for ligament engineering have been published. The first study compared ACL fibroblasts, adherent bone marrow stromal cells (BMSCs) and skin fibroblasts seeded onto a braided resorbable suture material (poly(L-lactide/glycolide) multifilaments). On day 12, total collagen and DNA content were the highest for BMSC seeded scaffolds, and least for scaffolds seeded with ACL fibroblasts (van Eijk et al. 2004). Mean DNA content using BMSCs was nearly twice that using ACL fibroblasts, and mean total collagen was almost six times higher with BMSCs. Neither glycosaminoglycan nor proteoglycan synthesis was considered in this paper. These results were supported by the second study which found higher proliferation and collagen excretion for BMSCs than ACL or medial collateral ligament (MCL) fibroblasts (Ge et al. 2005). The third study compared fibroblasts from patellar tendon, Achilles tendon, MCL and ACL seeded onto 3D braided poly-l-lactic acid (PLLA) scaffolds and cultured for 21 days (Cooper et al. 2006). This study found that ACL fibroblasts proliferated slower than the other types of fibroblast, but expressed significantly more mRNA for fibronectin and collagens I, & III at 14 days.

There is much debate about what a BMSC is. The standard technique, which was used by Van Eijk et al. (2004), is to aspirate the cells from bone marrow, and retain the adherent cells. However non-adherent cells treated with prostaglandin E2 (PGE2) become adherent and can differentiate into oestoblasts (Scutt and Bertram 1995), beyond this their differentiation potential has not been characterised. The wisdom of removing non-adherent cells has been questioned by the finding that twice as many stem cells as assessed by the number of colony forming units fibroblastic (CFU-F) could

be obtained from BMSCs grown on fibronectin at low cell densities when non-adherent cells were kept (D'Ippolito et al. 2004). This could either be non-adherent cells becoming adherent, non-adherent cells dividing to become adherent or the influence of cytokines produced by the non-adherent cells.

There is increasing evidence for the view that phenotype of the subpopulation of BMSCs with the highest potential for multipotent differentiation are small with little cytoplasm from several different groups using different methods (Colter et al. 2001; D'Ippolito et al. 2004; Zohar et al. 1997). Although it should be noted that these cells are more multipotent and proliferate better than larger cells, the larger cells are still multipotent to some extent. There is some evidence whilst the smallest spindle shaped cells are best for adipogenesis; slightly wider and older cells are superior for chondrogenesis (Sekiya et al. 2002).

More sophisticated methods for isolating stem cells have relied on generating antibodies that can be used to separate cells based on cell surface markers. This allows enrichment to increase the proportion of CFU-F. Selecting CD49+ cells appears to offer the greatest single step enrichment of CFU-F (Stewart et al. 2003). However the disadvantage is that not all of the CFU-F are recovered, CD49+ fraction recovers less than a quarter of CFU-F; the STRO-1+ fraction contains more CFU-F (and a higher percentage non-CFU-F reducing the enrichment) than the CD49+ fraction, but still recovers less than half of the CFU-F. There are also methods based on selecting CFU-F by plating cells at low densities, in these conditions CFU-F proliferate much faster, simply as the definition of CFU-F is a cell that forms a colony at low cell densities (D'Ippolito et al. 2004; Sekiya et al. 2002). The down side to these techniques are that they require a huge area of plastic. Finally, it should be noted that roughly twice as many CFU-F can be removed from bone marrow by centrifuging it than by aspiration (Dobson et al. 1999).

BMSCs have not been compared with other multipotent cells for the purposes of ligament engineering; the other major source of autologous primitive mesenchymal cells is adipose tissue-derived stromal cells (ATSCs). ATSCs have several advantages over BMSCs (Strem and Hedrick 2005):

- low morbidity upon harvest;
- stem cell frequency is higher than bone marrow (2% vs. 0.002%) meaning that sufficient ATSCs can be harvested without expansion *in vitro*; and
- higher proliferation rates.

The current major disadvantage of ATSCs is that they are poorly characterised compared to BMSCs. It is not yet clear if either ATSCs or BMSCs have superior differentiation potential. Comparison of osteogenesis and chondrogenesis by BMSCs and ATSCs has yielded ambiguous results: (Im et al. 2005) found that BMSCs differentiated better towards bone and cartilage than ATSCs as assessed by the bone biomarkers alkaline phosphatase and Von Kossa staining, and histological cartilage biomarkers for collagen II and GAGs. Whereas (Hattori et al. 2004) found that they were equivalent for osteogenesis as assessed by alkaline phosphatase, osteocalcin production, and mineral deposition; (Lee et al. 2004b) also found that ATSCs and BMSCs were similar when it came to osteogenesis and chondrogenesis and both cell types expressed CD29, CD44, CD90, and CD105. It is possible that differences in the isolation techniques used in the two papers account for the differences. Im et al. (2005) used an erythrocyte lysis buffer to remove erythrocytes (red blood cells); Lee et al. (2004b) removed non-adherent cells including erythrocytes by washing with phosphate buffered saline (PBS). One option to improve the isolation of multipotent ATSCs would be to plate ATSCs at low cell densities to select CFU-F.

There remains a substantial problem with using BMSCs for ligament and tendon engineering: the differentiation of BMSCs into ligament fibroblasts is far from fully understood. This problem manifests itself in two ways: BMSCs sometimes form bone when implanted in collagen gels into tendon defects

(Harris et al. 2004); and very similar conditions to those claimed to differentiate BMSCs into ligament fibroblasts are claimed to differentiate BMSCs into smooth muscle cells (SMCs).

Harris et al (2004) hypothesised that the formation of ectopic bone was due to the large number of cells used, resulting in excessive contraction of the collagen gel. This hypothesis was supported by two subsequent papers. The formation of ectopic bone by BMSCs do not appear to be a function of the age of the animal used to supply the cells (Dressler et al. 2005). Reducing the cell-collagen ratio appears to eliminate the formation of ectopic bone (Juncosa-Melvin et al. 2005). It remains unclear whether this will be a generic problem, or it is limited to highly contractible biomaterials such as the collagen gels used in these studies. It might be anticipated that BMSCs could be seeded at higher densities on stiffer materials without being contracted. Alternatively, it could be that the formation of ectopic bone is driven by the increased stiffness of the collagen gel, resulting from the contraction of the collagen gel. Matrix stiffness is known to be able to control BMSC differentiation (Engler et al. 2006), with stiffer environments promoting osteogenesis. The role of biological factors in formation of ectopic bone is largely unknown; it might be possible to block this process by the addition of specific growth factors, or by selecting BMSCs with specific surface markers (the BMSCs that formed ectopic bone were adherent BMSCs that had not been selected further for specific surface markers).

Perhaps more problematic is the reported differentiation of BMSCs into SMCs under almost identical conditions to those reported to differentiate BMSCs into ligament fibroblasts. Cyclical tensile strain combined with cyclical torsion has been reported to differentiate BMSCs into ligament fibroblasts (Altman et al. 2002b). Similarly, cyclical uniaxial tensile strain has been reported to differentiate cells into smooth muscle cells (Kurpinski et al. 2006). There has also been a report of differentiation into smooth muscle cells by transforming growth factor β1 (TGF-β1), one of the principal signals responsible for cellular responses to cyclical tension (Ross et al. 2006). Given that it is unlikely that the difference in cell type can be explained by the

differences in mechanical loading environment as many ligaments and tendons are not rotated; the data are more persuasive that cells have been differentiated into smooth muscle cells than ligament fibroblasts. One of the key markers for making this attribution is the presence of α-smooth muscle actin (α-SMA), a protein associated within contraction. One of the cell types within ligament, myofibroblasts, also express α-SMA; but these α-SMA positive myofibroblasts only account for 10-20% of ACL cells (Murray and Spector 1999). There is no data on the number of α-SMA positive cells in the reports above, but Zhang et al (2005) who culture BMSCs on intestinal sub-mucosa, which is rich in basic fibroblast growth factor (bFGF) and TGF-β (Voytik-Harbin et al. 1997), report that over 95% of the cells are α-SMA positive. A report of BMSC differentiation towards a ligament / tendon fibroblast phenotype triggered by low doses of bFGF also found elevated α-SMA levels (Hankemeier et al. 2005). Further, Ross et al (2006) report high levels of smoothelin-B mRNA, which is a smooth muscle cell marker reported to be absent in myofibroblasts. In conclusion, neither growth factors, nor mechanical stimulation have been conclusively demonstrated to differentiate BMSCs into ligament fibroblasts; on the contrary, there is evidence that BMSCs are differentiating into smooth muscle cells, not ligament fibroblasts.

Due to the lack of conclusive evidence for the differentiation of BMSCs into ligament fibroblasts, primary ligament fibroblasts will be used for this study as they are already differentiated. Table 2-1 summarises the advantages and disadvantages of cell types discussed in this section. Human primary tissue is unavailable for this study (although potentially ACL fibroblasts could be harvested from ruptured ligaments for clinical use), so ovine tissue will be used as sheep are closer to human scale than mice or rats, and are extensively reared in the UK. This allows them substantial freedom of movement, which should make them a more appropriate model for ligament repair than more sedentary animals as ligament injury is primarily a sports injury.

Table 2-1 Possible cell sources for ligament tissue engineering

Cell source	Advantages	Disadvantages
Skin Fibroblasts	Easily to isolate and culture Higher matrix synthesis and proliferation than ACL fibroblasts (van Eijk et al. 2004)	It is unclear how they differ from ACL fibroblasts Trans-differentiation pathway is unknown
BMSCs	Higher matrix synthesis and proliferation than ACL fibroblasts (van Eijk et al. 2004) Multipotent	Heterogeneous phenotype (Colter et al. 2001) Can form ectopic bone in tendon repair (Harris et al. 2004) Unclear to what extent phenotype in "ligament" differentiation is that of a smooth muscle cell not a ligament fibroblast
ATSCs	Multipotent High stem cell frequency	No published research on ligament differentiation
MCL or tendon fibroblasts	Higher proliferation than ACL fibroblasts (Cooper et al. 2006)	Lower matrix synthesis than ACL fibroblasts (Cooper et al. 2006)
ACL fibroblasts	Higher matrix synthesis than MCL and tendon fibroblasts (Cooper et al. 2006) Already differentiated to the correct phenotype	Lower matrix synthesis and proliferation than BMSCs or skin fibroblasts (van Eijk et al. 2004)

2.1.4 Biomarkers for ligament engineering

As the confusion between BMSCs differentiating into ligament fibroblasts and smooth muscle cells in the above section demonstrates, appropriate choice of biomarkers is essential in regenerative medicine, and results can be highly misleading if this is insufficient or inappropriate biomarkers are used. This section will consider the use of extracellular matrix (ECM) molecules as markers for ligament engineering. Beyond their role purely as biomarkers, it will also discuss how these molecules are synthesised, and their function. Biomarkers will be discussed further in Chapter 5. Table 2-2 summarises this section.

Table 2-2 Summary of selected biomarkers for ligament engineering

Biomarker	Notes	Desired outcome
Collagen	Major component of ligament Unclear what mRNA levels mean	90% collagen I : 10% collagen III
Collagen crosslinks	Different tissues have specific patterns of collagen crosslinks	high dihydroxylysinonorleucine low histidinohydroxymerodesmosine
Proteoglycans	Many proteoglycans can be measured such as decorin, fibromodulin, aggrecan and lumican	Positive for decorin and biglycan Negative for aggrecan
Glycosaminoglycans	Longitudinal data exists on glycosaminoglycan levels in collagen fibrogenesis	High dermatan sulphate in mature in tissue See section 7.1.4 for more detail
Glycoproteins	A variety of different glycoproteins are present in the matrix	Positive for Tenascin C if mechanically stimulated Negative for bone sialoprotein

2.1.5 Collagen

The most widely measured biomarkers for ligament engineering are various measures of collagen synthesis since the ACL is mostly composed of collagen (80% by dry weight (Vunjak-Novakovic et al. 2004)). Of this, ~90% collagen I and ~10% collagen III (Riechert et al. 2001). The most common assays for collagen are quantifying mRNA for collagen I and III. The limitation of this approach is that mRNA for collagens I and III are necessary for their synthesis, but they are not sufficient. It is hard to draw conclusions about collagen synthesis from collagen mRNA levels. In Moreau et al (2005b) various combinations of growth factors were applied to BMSCs seeded onto bundles of twisted silk fibres. Significant differences were found by a ELISA for collagen I between combinations in which TGF-β1 was used and combinations in which TGF-β1 was not used, but no significant

differences were found by quantifying collagen I mRNA. The process of collagen synthesis is outlined below.

Collagen synthesis is a complex process with several post-translation modifications occurring. This section will focus on synthesis and crosslinking of the fibrillar collagens type I and III. The first of these is hydroxylation of some of the lysine and proline residues by lysyl hydroxylase and prolyl 4-hydroxylase respectively (Kagan 2000). The activity of prolyl 4-hydroxylase is dependent on both coenzyme A and vitamin C (ascorbate). Collagen synthesis can be increased by increasing the concentration of coenzyme A (Mio et al. 2001) and by adding ascorbate to the media (Fermor et al. 1998). The hydroxylation of lysine by lysyl hydroxylase requires iron (Knott and Bailey 1998). Some of the hydroxylysine residues are further modified by glycosylation, which can by catalysed by either a glycosyl transferase or lysyl hydroxylase 3 (Wang et al. 2002). The function of these glycosylated residues is unclear; control of fibril diameter has been suggested as a possible function (Knott and Bailey 1998).

A signal peptide is cleaved as collagen is secreted to the ECM. In the ECM the *N* and *C* propeptides are removed by procollagen *N* & *C* proteinases. The *N* and *C* propeptides serve two functions: they increase the solubility of collagen, and they limit lateral growth of the fibril (Silver et al. 2003). *N*-proteinase cleaves the *N*-propeptide from collagens I and II, but does not cleave denatured collagen I or II and it has been suggested this might act as a quality control step (Prockop et al. 1998). The main source of collagen for tissue engineering experiments - collagen obtained from animal tissue by acid hydrolysis, has been shown to be denatured by the failure of *N*-proteinase to remove the *N*-propeptide (Prockop et al. 1998).

Collagen crosslinking *in vivo* is started by the deamination of lysine or hydroxylysine to create reactive aldehyde groups (allysine or hydroxyallysine). These aldehyde groups then react with either: lysine, hydroxylysine, allysine or hydroxyallysine. The main reducible crosslink in the ACL is dehydroxylysinonorleucine (Fujii et al. 1994), created by an

allysine group reacting with a hydroxylysine group, or a hydroxyallysine group reacting with a lysine (Reiser et al. 1992). One or two further reactions with a nearby histidine or hydroxylysine will result in a reduced crosslink (which amino acid and the number of further reactions depend upon the type of crosslink). In the ACL, hydroxypyridinium is the most common non-reducible crosslink. Hydroxypyridinium is formed by the reaction of hydroxyallysine with hydroxylysine to form dehydrodihydroxylysinonorleucine. Dehydrodihydroxylysinonorleucine then reacts with hydroxylysine to form hydroxypyridinium (Reiser et al. 1992). Some degree of control of crosslinking is given by the differences in hydroxylation of lysine residues in different tissues, different amounts of hydroxylation result in different crosslinks (Pornprasertsuk et al. 2004). The position of crosslinking is determined by a precise sequence of amino acids, these limited positions correspond to the quarter staggered arrangement of collagen fibrils. As tissues age they undergo crosslinking by non-enzymatic glycation, this changes the mechanical properties of tendon and ligament and is thought to be involved in some connective tissue disorders (Reddy 2003).

Collagen fibrils are normally assembled outside the cell. One exception is in the embryo, where tendon collagen fibrils are initially assembled inside the cell in the Golgi to plasma membrane carriers known as fibripositors. In the fibripositors, collagen is assembled into 28nm fibrils, with the *N* and *C* propeptides cleaved inside the cell. These fibripositors are not present in postnatal tendons (Canty et al. 2004).

Understanding the process of collagen synthesis suggests several other possible biomarkers beyond mRNA for collagen I and III, such as the collagen crosslinks. By measuring mRNA for the various steps in collagen synthesis it might be possible to understand better how to improve processes to synthesise more collagen. The pattern of lysine hydroxylation and subsequent collagen crosslinking is tissue specific, for instance patellar tendon has low dihydroxylysinonorleucine and high histidinohydroxymerodesmosine whereas the ACL has high

dihydroxylysinonorleucine and low histidinohydroxymerodesmosine (Amiel et al. 1986). These patterns might be used to help to distinguish the various types of ligament and tendon from one another.

2.1.6 Glycosaminoglycans and proteoglycans: role in collagen fibre bundles

Tendons and ligaments are commonly classified as "fibre reinforced composites" (a fibre such as collagen, glass or carbon are deposited in a resin or viscous matrix; fibreglass is a fibre reinforced composite) and this description of their material properties is used to model their mechanical behaviour (Ker 1999). However, research into the role of proteoglycans in ligaments and tendons is beginning to suggest that they are much more complex structures and this research provides a more satisfactory explanation of their exceptional properties.

The proteoglycans of particular interest to ligament engineering are the small leucine rich proteoglycans (SLRPs). These are currently thought to have three major roles:

- regulation of collagen fibrillogenesis by controlling fibril diameter,
- binding transforming growth factor to prevent fibrosis
- controlling cell proliferation – decorin (an SLRP) interacts with the epidermal growth factor receptor (EGFR) to increase p21 which itself causes an arrest in cell cycle (Iozzo 1999).

Recent evidence suggests that proteoglycans are important in determining the mechanical properties of ligaments and tendons (Scott 2003).

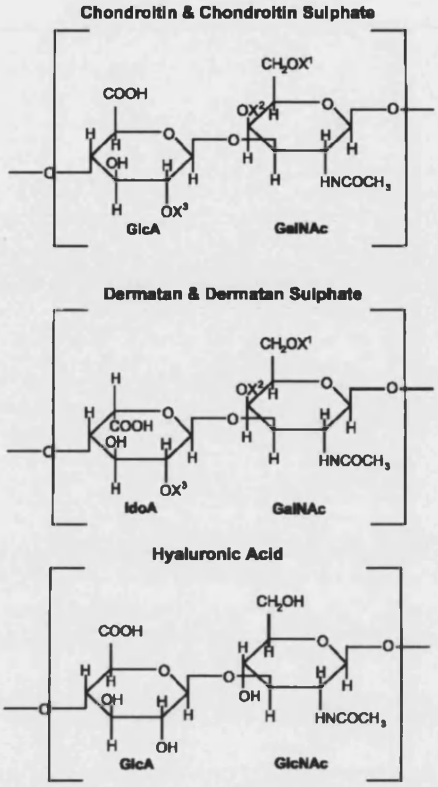

Disaccharide	X_1	X_2	X_3
ΔDi-0S	H	H	H
ΔDi-4S	H	SO_3^-	H
ΔDi-6S	SO_3^-	H	
ΔDi-UA2S	H	H	SO_3^-
ΔDi-disE	SO_3^-	SO_3^-	H
ΔDi-disB	H	SO_3^-	SO_3^-
ΔDi-disD	SO_3^-	H	SO_3^-
ΔDi-triS	SO_3^-	SO_3^-	SO_3^-

Figure 2-7 GAG structures. Table shows the structures of chondroitin sulphate disaccharides (after Esko (1999)).

Proteoglycans consist of a protein core linked to a glycosaminoglycan (GAG) – a polysaccharide that consists of a repeated chain of disaccharides: one uronic acid and one acetylated amino sugar. Chondroitin / dermatan sulphate is the main GAG present in tendon and ligament. Chondroitin sulphate (CS) consists of a chain of the disaccharide [*-4* glucuronic acid (GlcA) *β1-3 N-*

acetylgalactosamine (GalNAc) *β1-*], with sulphation of some hydroxyl residues (see Figure 2-7). Dermatan sulphate (DS) is formed by a modification of the CS polymer by epimerizing some of the GlcA sugars to Idouronic Acid (IdoA), which increases the flexibility of the polymer (Vynios et al. 2002). CS and DS are linked to a serine residue in the protein core by an O-linked tetrasaccharide.

The strongest evidence for a role of proteoglycans in creating the mechanical properties of ligament comes from studies of knock-out mice. The role of single knock-outs of proteoglycans is far from straightforward: biglycan and fibromodulin knock out mice show a reduction in the ultimate tensile strength and stiffness of tendons in knock-out mice (Jepsen et al. 2002; Young et al. 2002), whereas decorin knock out mice show an increase in ultimate tensile strength and stiffness (Robinson et al. 2004b). There is evidence that knocking out one proteoglycans increases expression of other proteoglycans to compensate: lumican expression increases in fibromodulin knock-out mice and lumican fibromodulin double knock out mice have weaker tendons than single knock out mice (Jepsen et al. 2002). There is also some evidence of an interaction between biglycan and decorin which might explain the increased ultimate tensile strength of decorin knockout mice: a synergistic effect upon bone of biglycan and decorin double knock out has been found (Corsi et al. 2002). Analysing the effects of various factors on the mechanical strength of tendon from decorin knock-out mice showed that the GAG content was the most important factor in determining the load at failure and the stiffness of the tendon (Robinson et al. 2004a).

One possibility for the involvement of proteoglycans in ligament strength is their role in fibril fusion. This effect changes during development. In the mouse flexor digitorium tendon, both lumican and fibromodulin initially limit the diameter of collagen fibrils as they are being assembled. When fibrils begin to fuse, lumican initially promotes this fusion. However, as the mouse matures lumican expression drops to a barely detectable levels, and fibromodulin promotes fibril growth. Mature lumican knock-out mice have tendon phenotypes similar to wild-type mice, but mature fibromodulin knock

out mice have smaller fibrils than wild-type (Ezura et al. 2000). It has also been suggested that the prevalence of different types of GAGs might affect fibril fusion. During development, hyaluronic acid is the predominant GAG when the ligament is young and the fibrils are narrow (average diameter less than 60 microns). This is replaced by chondroitin sulphate, which is thought to limit the expansion of tendon fibrils beyond ~150nm. Above this limit, chondroitin sulphate is replaced by dermatan sulphate (Parry et al. 1982).

Intriguingly, HA improves the mechanical strength of the bone-tendon junction in a healing patellar tendon after three weeks, but not six weeks (Yagishita et al. 2005). This result, combined with the fact that HA is produced by very immature tendons suggests that HA is important to initiate tendon formation.

Chondroitin sulphate and dermatan sulphate have been shown to from bridges between adjacent fibrils (Cribb and Scott 1995). The molecular nature of these bridges is as yet unknown. However the bridges would need to be extensible to play a role in the mechanical strength of the ligament, several possibilities for the molecular nature of these bridges exist:

- L-iduronate has alternative conformations that would allow it to extend under tension; there is a higher ratio of IdoUA/GlcUA in extensible tissues such as tendon and skin than rigid ones such as cartilage and cornea (Scott 2003).
- Some chondroitin sulphate and dermatan sulphate molecules self-aggregate to from bridges between adjacent collagen fibrils. The preferred state of these bridges is one of minimal energy, when all the hydrogen and hydrophobic binding sites are involved. Mechanical stress can extend these CS/DS bridges by moving them to less favourable arrangements (Scott 2003).
- A computational model of chondroitin-6-sulphate polymer suggests that the molecule itself is highly extensible, as extension from a wavy form at low strain to a linear molecule at 800% strain could be modelled (Redaelli et al. 2003).

The role of these bridges has yet to be elucidated. Tendon fascicles treated with chondroitinase ABC, to remove hyaluronic acid, chondroitin sulphate and dermatan sulphate, do not become significantly weaker, although they appear to have lower stiffness than normal. The picture might be complicated by the removal of GAGs allowing new non-physiological interactions between the fibrils (Screen et al. 2005b). It is possible that glycosaminoglycans are predominately acting through interactions with cells to determine mechanical properties, and are principally determining the stiffness, but not the strength of the ECM.

As biomarkers, the SLRPs decorin and biglycan have been used (Moreau et al. 2005a). However it is not clear what different levels of these SLRPs mean, nor is it clear what the levels of these SLRPs should be. Aggrecan has also been used (Moreau et al. 2005a), as it is useful as a negative biomarker for the presence of large amounts of aggrecan would suggest the formation of either fibrocartilage or cartilage. Glycosaminoglycans have potential as biomarkers for ligament and tendon engineering, which will be discussed further in Chapter 5.

2.1.7 Glycoproteins as biomarkers

Another biomarker of ligament engineering is fibronectin (Cristino et al. 2005). This is a glycoprotein that appears to be important for linking the ECM to cells via a domain that binds integrins (Mardilovich et al. 2006). In normal tendons, the levels of fibronectin are higher in the membrane that surrounds the fibrous core than the fibrous core, and higher still in the synovium surrounding the membrane (Brigman et al. 1994). Early synthesis of fibronectin appears to help BMSCs respond to mechanical tension (Chen et al. 2006), although this work has not prevented fibronectin synthesis to prove that fibronectin is important. This early synthesis fits with what is known about tendon healing, in response to injury, fibronectin levels increase early in the membrane (epitenon) surrounding the fibrous core (endotenon) of the tendon, there is also a delayed increase in fibronectin levels in the endotenon (Gelberman et al. 1991). Thus, elevated levels of fibronectin that

subsequently decline can be considered a marker for tendon repair, which might be important to tendon and ligament engineering. The membranes that surround the fibrous core of the tendon / ligament should be richer in fibronectin than the fibrous core.

Laminin has also been used as a biomarker (Cristino et al. 2005). Laminin is so rare in the ACL that it has been used as a way of identifying blood vessels in the ACL by staining their basement membranes (Petersen and Tillmann 1999). In contrast to fibronectin, laminin does not appear to be up-regulated in response to tendon injury (Jozsa et al. 1989). As an outcome marker, laminin would come into its own to identify blood vessels if the co-culture of ligament cells and endothelial cells was being studied.

Tenascin is found in a number of tissues exposed to mechanical stress (Chiquet-Ehrismann and Tucker 2004). Tenascin-C levels are higher in regions of tendons subject to compression (Mehr et al. 2000). In general, levels of tenascin-c are elevated in parts of tissues subject to tension, and highest in fibrocartilaginous regions, subject to both tension and compression (Jarvinen et al. 2000), part of the function of tenascin-C appears to be inhibition of cell attachment (Chiquet-Ehrismann and Tucker 2004), so its presence might explain the spherical morphology of cells in fibrocartilaginous regions (Mehr et al. 2000). Western-blotting identifies two isoforms of tenascin-C, a 200kDa form and a 300kDa form, the 200kDa is found in normal and degenerating tendons, whilst the 300kDa form was only found in degenerating tendons (Riley et al. 1996). Thus tenascin-C could be used to detect cells responding to mechanical stress. High levels of tenascin-C might indicate the presence of fibrocartilage; this could be confirmed with histology. Western blotting might be able to detect aberrant regeneration by detecting the 300kDa form of tenascin-C.

Finally, bone sialoprotein is used in a similar way to aggrecan as a negative marker of ligament differentiation, although its absence indicates that cells are not differentiating into bone (Altman et al. 2002b; Cristino et al. 2005). However bone sialoprotein is a late marker of bone differentiation (Young et

al. 2002). Therefore elevated levels of bone sialoprotein may not be detected immediately even when cells are differentiating into osteoblasts to form bone.

2.2 Biomaterials

The ideal biomaterial for ligament engineering would have several properties:

- Good mass transfer of nutrients and waste
- Means of attaching cells throughout the scaffold
- Appropriate mechanical behaviour
- Degradation rate suited to ligament synthesis
- Sites to stimulate cell surface receptors
- High Specific Surface Area
- Low immunogenicity
- Optimal pore size

There are other properties that might be advantageous that have not been proven to be advantageous yet. For instance, many scaffolds include glycosaminoglycans, as glycosaminoglycans are self-aggregating (Scott 1992) these scaffolds might provide "hooks" on the scaffold for newly synthesised ECM to bond with.

Mass transfer, the diffusion of nutrients to cells through biomaterials, is a major limitation in tissue engineering (Yang et al. 2001), as the time taken for nutrient diffusion is proportional to the square of the distance travelled. *In vivo* there are blood vessels in the fascicles (Clark and Sidles 1990), so cells are no further than 200μm from a blood supply. *In vitro* there is no vasculature, presenting a major problem as assemblies of cell aggregates larger than 1mm diameter invariably develop necrotic cores in conventional bioreactors due to insufficient oxygen (Unsworth and Lelkes 2000); the axial diameter of ACL averages 4.7mm in women and 5.6mm in men (Anderson et al. 2001). This is complicated by the fact that the importance of nutrient transfer in the ACL is poorly understood. On one hand ACL fibroblasts are metabolically relatively inactive (Fermor et al. 1998), and low oxygen tensions increase proliferation and collagen synthesis. On the other hand

poor vascularisation is thought to be a limiting factor in ACL healing (Bray et al. 2003), and primitive ligament cells differentiated from marrow stromal cells may proliferate and mature faster at normal oxygen tensions (21%). In addition, adding sodium bicarbonate to the culture medium to increase its buffering capacity against acidification improves the quality of engineered cartilage (Robinson et al. 2004a). This suggests that it might be the increased concentration of lactic acid from anaerobic respiration that is harmful, not the lack of oxygen (as with ligament reducing the oxygen tension can increase matrix synthesis (Saini and Wick 2004); adding lactic acid to reduce the extracellular pH does reduce matrix synthesis, this reduction can be prevented if the lactic acid is buffered by sodium bicarbonate (Wilkins and Hall 1995).

A review of cartilage engineering concludes that higher initial cell density improves final matrix quality, although it does not affect the final cell density (Darling and Athanasiou 2003). A higher cell density will require more nutrients and a scaffold with good mass transfer properties. There are three main ways of modifying a biomaterial to increase mass transfer through it:

- Larger pore size facilitates convection in the presence of fluid flow within the biomaterial, which makes mass transfer faster.
- High porosity will not only help improve flow in the scaffold, but provide empty space to be filled by newly synthesised ECM.
- Better interconnected pores. This is measured by tortuosity -the distance the molecule has to travel divided by the thickness of the material.

For the cells to grow on the scaffold they first need to attach to it. Two factors are known to affect this. First the diameter of the fibres within a scaffold has been shown to affect the attachment of some cell types, such as osteoblasts (Ma et al. 2005). Secondly, attachment of MC3T3-E1 cells shows a strong correlation with the specific surface area of collagen-GAG scaffolds (O'Brien et al. 2005). Unfortunately there's a trade off between optimal specific surface area and optimal mass transfer. According to the Hagen-Poiseuille

equation, (which produces good approximations of permeability from the material properties for porous structures with porosities of less than 80%) the intrinsic permeability is inversely proportional to the square of specific surface area (Sander and Nauman 2003).

There are two options for the mechanical behaviour of the biomaterial: either start with a material with a low stiffness and ultimate tensile strength and rely on the ligament engineering process to make the construct stiffer and increase in ultimate tensile strength. This approach was used by Altman et al (2002b) and Goulet et al (2000) when they chose a hardened collagen gel as a biomaterial (if a collagen gel containing cells is left for a couple of days the cells will contract it: which increases collagen concentration and helps align collagen fibres (Wallace and Rosenblatt 2003). Hardened collagen gels did result in ligament-like constructs.

The alternative is to start with a biomaterial whose mechanical properties are similar to those of a ligament, this approach has been taken by Altman et al (2002a) and Chen et al (2003) who used silk as a biomaterial. A direct comparison between these approaches has yet to be carried out, but comparing between the results published in the two separate papers (by the same group) it seems that the collagen gel system expresses twice as much collagen I at 14 days as the best silk system, although this does not control for other variables such as the degradation rates of the two different polymers.

If cyclical stretching is used it will also be necessary to ensure that the mechanical properties of the biomaterial are compatible with the stretching protocol. The biomaterial must be capable of taking at least at much strain as the protocol uses. Furthermore the material should not be permanently deformed by repeated stretching. (Kim and Mooney 2000) compared Poly(L-lactic acid)-bonded polyglycolide fibre-based scaffolds and type I collagen sponges as scaffolds for engineering smooth muscle and found that cyclic strain permanently deformed the polymer scaffold, but not the collagen gel

and that cells grown on the polymer scaffold contained less elastin than those grown on the collagen I sponges.

Work on tissues other than ligament suggests that the rate at which the scaffold degrades is a critical variable. Work on peripheral nerve regeneration looked at varying the degradation rate of a collagen scaffold by varying the extent of cross-linking showed that nerve regeneration was best at an intermediate rate of degradation (Harley et al. 2004). The rate of scaffold degradation has also been shown to be a critical variable in skin regeneration (Yannas et al. 1989). There's limited evidence that the same is true for chondrocytes (Tognana et al. 2005).

The biomaterial needs to be bioactive to have some way of emulating the ECM-cell interactions. Whereas a collagen gel will interact with cells, as the collagens process binding sites the cells recognise, a biomaterial such as silk will not possess these same binding sites. However materials such as silk can be chemically modified to include binding sites. Chen et al (2003) modified their silk based biomaterial with RGD sites that many integrins recognise. This modification with RGD almost trebled the amount of collagen I expressed by ACL fibroblasts and resulted in nearly a five-fold increase in collagen I expression by bone marrow stromal cells.

The material should have low immunogenicity so as not trigger an immune response when the implant is inserted.

Finally, there is no sound evidence as to the optimal pore size for ligament engineering. Cooper et al (2005) suggested that a size of 200-250μm was ideal. However this conclusion was based upon an a limited investigation that looked at replacing tendons with a woven tape made of fine-gauge stainless steel using two weaving designs to give two different porosities; the tape was inserted into the metacarpals of beagle hounds. The only result given was that the greatest interfacial bonding strength occurred after twelve weeks with the tape with a pore size of 250μm (Konikoff et al. 1974); the pore size of the other tape was not given. This would not be a good test of

pore size for tendon or ligament engineering, as the interfacial bonding strength would be determined by the extent of bone ingrowth, not tendon regeneration. This conclusion is supported by the evidence on the effect of pore size on bone ingrowth: a pore size of at least 150μm is thought to be necessary for bone ingrowth into a scaffold (Petite et al. 2000), and a pore size of over 300μm is thought to be optimal (Karageorgiou and Kaplan 2005). This issue will be returned to in Chapter 7.

There is also the issue of how to attach the construct, when the ACL has ruptured. One option that has been studied in a goat model is to use demineralised bone as a biomaterial inserted into bone (Jackson et al. 1996), but regeneration was found to be slow in this system, and the same questions arise about using demineralised bone as any other xenograft. Another option that might promote faster and better healing would be to tissue engineer the enthesises; Mutsuzaki (2004) have developed a technique that hybridises calcium phosphate with a tendon graft that replicates at least some of the features of the enthesis. Table 2-3 summarises the materials that have been used for ligament engineering.

Table 2-3 Materials used for ligament engineering

Material	Advantages	Disadvantages
Hardened collagen gel	Promotes collagen synthesis	Poor mechanical properties
Twisted silk fibres	Good mechanical properties	Low porosity Lower collagen synthesis than hardened collagen gel
Twisted silk fibres with RGD decoration	Good mechanical properties Better collagen synthesis than silk	Worse collagen synthesis than silk

2.2.1 Silk

Silk is composed of three major components: the core fibre made up of a heterodimer of silk fibroin heavy chain and light chain proteins, 6 heterodimers bind non-covalently with the glycoprotein P25 (Inoue et al. 2004), and the sericin coat a glue like protein (Altman et al. 2003). This section will consider the properties of silk fibroin from the silkworm, *Bombyx mori,* in more detail.

The sericin component appears to be responsible for almost all problems with biocompatibility and hypersensitivity (Altman et al. 2003). Fortunately it is easily removed by a degumming process (Altman et al. 2002a). Little is known about the role of P25. Silk fibroin has a number of properties that make it a very interesting biomaterial: biocompatible (Altman et al. 2003), biodegradable ((Altman et al. 2003), thermally stable (Nakamura et al. 1994), with good mechanical properties (Altman et al. 2003).

Silk fibroin has a long history of use as a suture (Altman et al. 2003), and as surgical thread (Bunning et al. 1994). Silk films implanted into rats trigger an milder inflammatory response than either PLA or collagen films, further *in vitro* cells grown on silk films express lower levels of the inflammation markers Interleukin-1β and COX-2 (Meinel et al. 2005).

According to the US Pharmacopoeia, an absorbable biomaterial is one that "loses most of its tensile strength within 60 days post-implantation". Under this definition silk fibroin is not an absorbable biomaterial, but it does degrade within a longer timeframe, losing most of its tensile strength within a year and being unrecognizable at the site of implantation within two years (Altman et al. 2003). Recently, a silk biomaterial has been developed where the silk is dissolved in an aqueous solvent rather than the traditional organic solvents. This biomaterial is degraded by proteases within 21 days, much faster than biomaterials made with organic solvents, although the time for absorption *in vivo* of this new material is unknown (Kim et al. 2005b).

Silk fibroin is a very thermally stable protein, intramolecular and intermolecular hydrogen bonds are broken between 150 and 180°C, then the silk filament begins to gradually lose weight at 175 °C (Nakamura et al. 1994). These properties are in stark contrast to the typical properties of proteins which undergo conformational change well below 100°C. This thermal stability of silk has been exploited as part of the degumming process for removing sericin (Altman et al. 2002a). Further it suggests that it would be possible to sterilise silk-based biomaterials by autoclaving them, rather than merely sanitising them with 70% ethanol solution, which is the usual method for tissue engineering scaffolds.

Perhaps the major reason for interest in silk is its exceptional mechanical properties. These depend somewhat upon the method of fabrication, but ultimate tensile strengths of typically over 500 MPa, combined with Young's moduli of 5-17 GPa and %strain at break of 4-20% have been reported (Altman et al. 2003). As silk is stronger than the tendon, porous scaffolds can be made of silk that possess similar mechanical properties to ligament (Altman et al. 2002a). One of the unique properties of silk is its strength in compression (Altman et al. 2003; Bunning et al. 1994), this would make it an attractive option for both the ligament itself and the bony enthesises.

Silk fibroin has at least three crystalline structures: Silk I, Silk II and random coil (Magoshi et al. 1994). Silk II, consisting of β-sheets, is the most stable form and is insoluble in water. To make silk-based biomaterials silk is normally regenerated in a strong salt solution: this changes the crystalline structure of silk fibroin from type II to type I, a distorted β-turn structure. Type I is soluble in water and organic acids such as *1,1,1,3,3,3* hexafluoro-2-propanol (HFIP). Freeze drying below -20°C promotes a shift to random coils. Once the silk is in solution as random coils or silk I, it can be cast as a film or scaffold and converted to silk II by methanol (Ha et al. 2005), the shear stress creating by drawing silk into fibres can also convert it to silk II (Magoshi et al. 1994).

2.2.2 Cross-linking

Crosslinking of collagen is much better understood than crosslinking of silk. In the case of collagen, crosslinking can chemically link adjacent collagen molecules changing the material properties of the scaffold. Crosslinking can also be used to add useful molecules to the scaffold such as GAGs or RGD peptides. The effect of crosslinking is hard to predict a priori, for instance crosslinking of Dermal Sheep Collagen was found to decrease its tensile strength (Olde Damink et al. 1996), whereas it can strengthen collagen gels (Charulatha and Rajaram 2003). The exact location of the amino acids crosslinked seems to be important (Charulatha and Rajaram 2003); as does whether the crosslinks are between and within collagen molecules or between microfibrils (Sung et al. 2003). A complication when crosslinking silk is that crosslinking can affect the crystalline structure of the molecule and induce a shift from beta sheets to random coils (Sampaio et al. 2005).

Crosslinking can either be done with chemicals or by physical methods, such as heat treatment or irradiation. Physical methods have the advantage that they do not introduce any potentially cytotoxic chemicals, although these processes might induce cytotoxic changes in the materials being crosslinked. The more major disadvantage is that there is a trade off between the extent of crosslinking and potential onset of degradation of the molecules being crosslinked (Khor 1997).

Initially, glutaraldehyde was widely used for crosslinking biomaterials. However when implanted subcutaneously in rats and compared to other crosslinking reagents for crosslinking collagen, it triggered an increased infiltration of neutrophils and became more calcified than the other scaffolds; *N*-(3-dimethylaminopropyl)-*N'*-ethylcarbodiimide hydrochloride (EDC) : *N*-hydroxysuccinimide (NHS) crosslinking on the other hand produced a much milder cellular reaction and an optimal collagen matrix (van Wachem et al. 1994).

EDC/NHS produces a zero-length crosslink between a carboxylic acid group and an amine group. Various factors have been shown to affect the extent of crosslinking with EDC/NHS: pH, the ratio of EDC:NHS, the ratio of EDC:COOH groups, reaction volume, ethanol, and the reaction time (Pieper et al. 2000; Pieper et al. 1999). This is particularly useful for crosslinking compounds containing amine groups, such as peptides to silk fibroin, as silk fibroin is richer in carboxylic acid groups than amine groups (Xia et al. 2004).

Recently there has been a lot of interest in genipin as chemical crosslinker. The chemistry of the crosslinking reaction has not been elucidated in detail, but it appears that it can react with amine groups, further it can react with itself to from bridges between two amine groups (Chen et al. 2004). Genipin has been shown to be much less cytotoxic than glutaraldehyde (Sung et al. 1998); only at high concentrations (50ppm) is it more genotoxic than a negative control, whereas glutaraldehyde is genotoxic (Tsai et al. 2000); although a direct comparison of the relative cytotoxicity of EDC/NHS and Genipin is yet to be made. Genipin has an advantage over EDC/NHS when crosslinking collagen in that it creates more intermicrofibrillar crosslinks which affect the mechanical properties of the scaffold (Sung et al. 2003). The disadvantage of this method for silk crosslinking is that silk fibroin has few amine groups (Xia et al. 2004) limiting the extent of crosslinking.

Another option for crosslinking is to use enzymes. Lysyl oxidase is the enzyme that crosslinks collagen *in vivo*, whilst it has not been purified in sufficient quantity to be applied as a crosslinking reagent, it has been possible to up-regulate lysyl oxidase activity by transfecting cells with additional copies of the lysyl oxidase gene (Elbjeirami et al. 2003). This approach is limited by the limited understanding of how to make gene therapy safe, as shown by the death of a patient on a clinical safety trial (Raper et al. 2003). Tranglutaminase crosslinks glutamine and lysine in the presence of calcium, it has been successfully used to crosslink collagen (Orban et al. 2004), but cannot crosslink protein to other classes of molecule such as polysaccharides. Mushroom tyrosinase has been used to cross-link chitosan (a polysaccharide) to silk, but this induced a change from the β

sheet form of silk to random coils (Sampaio et al. 2005) which is thought to be undesirable.

Table 2-4 Summary of chemical crosslinking methods

Crosslinking agent	Crosslink formed	Notes
Glutaraldehyde	Aldehydes react with hydroxylysine (Zeeman 1998)	Triggers neutrophil infiltration
EDC NHS	Carboxylic acid and amine group	Zero length crosslink
Genipin	Links amine groups and forms bridges between amine groups and existing genipin crosslinks	Low cytotoxicity
Lysyl oxidase	Proline or Hydroxyproline to Lysine or Hydroxylysine	The natural collagen crosslink Enzyme has not been purified in large quantities
Ionic crosslinking	Collagen-Chitosan-Glycosaminoglycan	

The final option is ionic crosslinking; a collagen-chitosan-glycosaminoglycan complex has been made without chemical crosslinking (Berthod et al. 1994). The degree of acetylation of the chitosan controls the strength of the crosslinking (Collombel et al. 1992). Unusually in this case the ionic bonds between the molecules are strong enough to prevent the GAGs from being salted out. Table 2-4 summarises the crosslinking methods discussed in this section.

2.3 Bioreactors

The purpose of using a bioreactor for ligament tissue engineering is to allow a 3D construct to be mechanically manipulated and to control the physiochemical environment (e.g. concentrations of O_2, CO_2, pH and temperature). The process of engineering a ligament can be broken down into three steps:

- differentiation of the cells to ligament cells,
- proliferation of the cells, and
- maturation of the cells into a mature ligament.

One of the aims of bioreactor design is to combine these steps into an efficient process. So far research has focused on maturation and differentiation; there have been two attempts to engineer such a bioreactor.

Several simple bioreactors have been designed that allow cell seeded collagen gels to be cyclically stretched (Cho et al. 2004; Garvin et al. 2003; Langelier et al. 1999; Peperzak et al. 2004; Yahia et al. 1991).

The simplest bioreactors are those that use static strain to mechanically stimulate cells. These consist of two poles in a dish, and biomaterial placed on the dish that contracts to from a three dimensional scaffold suspended between in the two posts. The first of these used a collagen gel as the biomaterial and after twelve weeks the construct had an ultimate tensile strength of 0.14 MPa. Blocking collagen crosslinking with β-aminopropionitrile suggested that much of this increase in ultimate tensile strength was due to collagen crosslinking (Huang et al. 1993). A recent experiment used tendon fibroblasts seeded in monolayer on lumican in culture dishes coated with SYLGARD to allow the tendon monolayer to peel off the dish and contract. This showed that, after four weeks, the tendon fibroblasts *in vitro* could form constructs with ultimate tensile strength of 2 MPa, and morphology resembling embryonic tendon (Calve et al. 2004). It is not clear if it would be possible to scale this technique up to form large ligaments like the ACL.

The cyclical strain bioreactor designed by Langelier et al. (1999) allowed the maturation of ACL fibroblast seeded collagen gels into a tendon-like constructs with cells orientated parallel to the direction of strain (Goulet et al. 2000). Several authors have looked at the effect of 2D cyclical tensile strain upon ligament cells, and the expression of the main protein markers of ligament maturation. Cyclical strain increases gene expression of collagens I and III by ACL fibroblasts. TGF-β1 is a key messenger in this response as the expression of the collagens can be significantly reduced by anti-TGF-β1 antibodies (Hsieh et al. 2000; Kim et al. 2002). Five percent strain at 1Hz has been to shown to upregulate collagen synthesis in tendon fascicles *ex vivo*, without affecting GAG synthesis or cell proliferation (Screen et al. 2005a).

The bioreactor of Altman et al (2002c) is more sophisticated than the other reactors mentioned in other ways: it can both cyclically stretch and twist the construct, and it can control the physicochemical environment including partial pressures of O_2, CO_2 and N_2 (Figure 2-8). This bioreactor allowed them to demonstrate that combined cyclical tensile strain (10%) and rotational strain (90°, 25%) at 0.0167 Hz applied to a collagen gel seeded with mesenchymal progenitor cells into ligament like construct with a helical organisation reminiscent of the ACL. The mesenchymal progenitor cells had apparently differentiated into ligament fibroblasts based on production RNA for tenascin-C, and collagens I and III (Altman et al. 2002b). This reactor allowed them to simultaneously differentiate into ligament-like cells and mature them into a ligament-like construct which had a helical organisation reminiscent of the ACL.

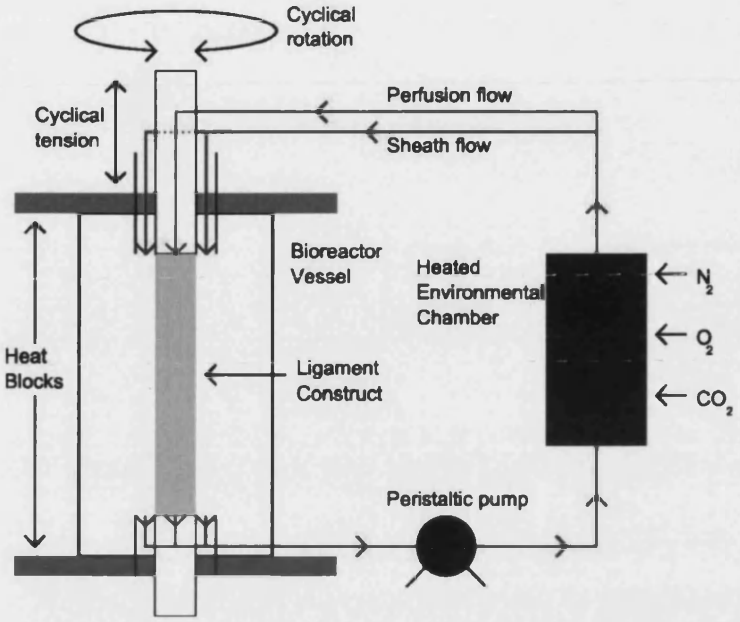

Figure 2-8 Schematic of Altman et al (2002c) bioreactor for ligament production

The effect of different mechanical loading strategies is poorly understood. Howard et al (1998) have looked at the effect of different strains upon periodontal ligament fibroblasts (PDLF), they found that 5% strains increased collagen I and fibronectin production, decreasing tropoelastin production relative to static controls, whilst 10% strains still increased fibronectin production and decreased tropoelastin production, but had no effect on collagen I relative to static controls. Agarwal et al. (2003) found that in osteoblast-like periodontal ligament cells high cyclical tensile strain (10-18.5%) up-regulated proinflammatory signals (cyclooxygenase-2 (COX-2) mRNA expression and PGE2 synthesis) via Interleukin-1ß-induced translocation of the transcription factor nuclear factor-κB, whilst low cyclical tensile strain (2-8%) prevented this translocation. Frequency is another important variable; tenocytes stretched at 5% at 1Hz expressed vascular endothelial growth factor, unlike cells stretched at 0.5Hz (Petersen et al. 2004). Finally, the duration of stretching appears to be important: the proliferation rate and apoptosis increased when tenocytes where stretched by 5% at 1Hz for a day; after two days stretching, heat shock protein 72 was expressed and proliferation and apoptosis decreased (Barkhausen et al. 2003).

As explained in the biomaterials section (Section 2.2) mass transfer of nutrients and waste is a major issue in tissue engineering. However this not just a biomaterials problem, bioreactors also have a role to play. Either the body could used to improve mass transfer as rapid neovascularisation occurs *in vivo*, starting within 20 days of surgery and being complete after 3 months (Fu et al. 1999), this could be used as part of an *in vivo* tissue engineering strategy.

Alternatively, the bioreactor could be designed to improve mass transfer *in vitro*: the design of Altman et al. (2002c) perfuses media through the biomaterial, and around the biomaterial, reducing the distance media has to diffuse through the boundary layer; mechanical stimulation might be used to create negative pressure within the construct, sucking fresh media in (Langberg et al. 1999); or the vasculature could be artificially replicated with biodegradable hollow fibres.

Bioreactor designs utilising fluid flow induced shear stress as the mechanical stimulus have been widely used for cartilage engineering (Darling and Athanasiou 2003), but have yet to tested for ligament engineering. Although it is known that fluid flow triggers nitric oxide and PGE2 release, decreases tissue non-specific alkaline phosphatase activity in PDLF (van der Pauw et al. 2000), and increases intracellular calcium levels in ACL and MCL fibroblasts (Hung et al. 1997), signals that should affect the differentiation, proliferation or maturation of ligaments. However, only an effect on matrix metalloproteinase (MMP) 1 & 3 levels in tendon cells (Archambault et al. 2002) has been shown so far. Fluid flow induced shear stress might be effective because ligament fibroblasts are in the "viscous phase" between the fibre bundles (Puxkandl et al. 2002), and the fibrous capsule is sheared between adjacent fibre bundles (Screen et al. 2003). Mechanically stimulating cells with fluid flow will also allow the cells to benefit from better mass transfer which increases with fluid flow. Table 2-5 summarises the bioreactor discussed in this section.

Table 2-5 Summary of bioreactors for ligament and tendon tissue engineering

Mechanical regime	Key Papers	Advantages and disadvantages
Static tension	Huang et al (1993) Calve et al (2004)	Very simple Stimulates less collagen synthesis than dynamic tension Calve et al (2004) technique appears promising for small constructs
Cyclical tensile strain	Langelier et al. (1999) Screen et al. (2005a)	Increased collagen synthesis relative to static culture
Cyclical tensile and strain	Altman et al (2002c)	Better replicates the mechanical forces on the ACL Differentiates BMSCs into a structure resembling ACL
Fluid flow		Improved mass transfer of nutrients Not yet demonstrated for ligament engineering

2.3.1 Interactions between biomaterials and bioreactors

The work of Screen et al. (2004) described above has shown that the mechanical forces on ligament/tendon fibroblasts *in vivo* are different to those investigated by investigators looking at the effect of mechanical forces upon ligament/tendon fibroblasts. Often the fibroblasts are placed under much greater tensile strains than occur *in vivo* and the effect of the shear stresses created by the displacement of one fibre bundle relative to another have yet to be investigated. Whilst it is known that when tendons & ligaments are compressed between bones their response is to form fibrocartilage, it is not known what effect the compression of the fibroblasts by the movement of

fibre bundles has. Replicating these forces upon the cells *in vitro* will require consideration of both bioreactor and biomaterial.

2.4 Aims and Objectives

The overall aim of this project was to quantify the effects of pore size and pore structure on ligament tissue engineering. An essential part of this project was the data analysis following quantification of ligament tissue engineering.

The work was carried out to meet the following objectives:

- Allowing pore size and pore structure to be controlled within porous silk scaffolds
- Characterisation of the novel silk scaffolds
- Quantification of glycosaminoglycan production within 3d tissue constructs
- Quantification of the effects of pore size and pore structure on ligament fibroblast proliferation and matrix synthesis
- Use of appropriate statistics to study interactions between variables
- Comparison of results to existing literature on ligament development to see if any combincation of pore size and pore structure helps to recapitulate development

3 Statistics: introduction to factorial ANOVA

3.1 Introduction

As the effects of multiple variables on ligament engineering are being considered an appropriate choice of statistics is necessary. There are essentially two problems in statistics when trying to determine if an independent variable has an effect on a dependent variable: type I error: deciding that there is an effect when there is not (i.e. a false positive), and a type II error: concluding that there is no effect when there is an effect (i.e. a false negative). The probability of a type I error should be determined by setting an appropriate alpha level, typically this is 5%. In others words, in the experiment the statistics should be used in such a way that there is a 5% chance of incorrectly concluding that there is an effect when there is not.

Often experiments are designed so that t-tests can be used to determine whether or not there is a significant difference between two groups. However, where there are three or more groups to compare this approach risks increasing the chance of a type I error; every time another group is compared the chance of a type I error increases, if 14 comparisons are made then the chance of type I error is over 50%. One solution to this problem is to make a correction to the level of statistical significance for individual tests; the simplest correction is the Bonferroni correction, in which the alpha level is divided by the number of tests carried out, for 10 separate tests the alpha level would have to be reduced to 0.5% from 5% to ensure that the chance of a type I error is not increased. The problem with this approach is that it greatly increases the chance that a real effect is not detected, a type II error.

The solution to this problem is to use more appropriate statistical tests. For more than two groups this involves using analysis of variance (ANOVA). Modern statistical software calculates ANOVA on the basis of a regression model. When there is a single independent variable, ANOVA tests whether that variable has a significant impact on the dependent variable. This thesis makes extensive use of factorial ANOVA, which compares data on a single

outcome variable when multiple independent variables. A complete explanation of factorial ANOVA is beyond the scope of this section, instead this section will first introduce the mathematics behind factorial ANOVA with a worked example using notation from Field (2005), using additional equations from Cardinal and Aitken (2006) and Hays (1994); it will then use examples to demonstrate how some of the key concepts when using factorial ANOVA.

3.2 Worked example of factorial ANOVA

First, the effect of "Factor A" upon glycosaminoglycan production in chondrocytes and MSCs will be calculated to show how the mathematics works. (All the data for this section has been randomly generated.) The raw data for this calculation is given in Table 3-1. Analysis of variance works by comparing the variance that can be explained by the independent variables with the variance that cannot be explained. To do this first the total sum of squares (SS_T) must be found, this can be broken down into the model sum of squares (SS_M), and the residual sum of squares (SS_R). The total sum of squares is given by the total variance of all the scores (s^2_{grand}), times the degrees of freedom (N-1), see Equation 3-1.

$$SS_T = s^2_{grand}(N-1)$$

Equation 3-1 Total sum of squares

Table 3-1 Glycosaminoglycan production by chondrocytes and MSCs at different concentrations of Factor A

Chondrocytes				
Conc. Factor A (ng)	**8**	**11**	**14**	**17**
	9.82	10.74	13.19	15.38
	11.55	10.57	17.05	18.84
	4.45	6.99	13.88	15.90
	5.80	12.33	15.20	19.05
	6.34	4.49	12.80	19.49
	8.62	8.54	16.59	13.69
Total	**46.58**	**53.67**	**88.70**	**102.35**
Mean ($\bar{x}_{group}$)	**7.76**	**8.94**	**14.78**	**17.06**
Variance (s^2_{group})	**7.23**	**8.23**	**3.17**	**5.70**

MSCs				
Conc. Factor A (ng)	**8**	**11**	**14**	**17**
	12.18	7.62	7.98	8.03
	13.46	9.83	8.93	6.38
	15.76	16.66	12.04	8.72
	14.38	10.11	6.14	11.46
	20.25	13.93	12.14	4.73
	14.81	13.74	16.54	8.10
Total	**90.85**	**71.90**	**63.78**	**47.41**
Mean ($\bar{x}_{group}$)	**15.14**	**11.98**	**10.63**	**7.90**
Variance (s^2_{group})	**7.76**	**11.17**	**13.86**	**5.15**

Treating all of the results as one gives the variance as 17.955 (Table 3-2), there are 48 results so N=48. Hence the total sum of squares is:

SS_T = 17.955(48-1)

= 843.885

The model sum of squares is given by the sum of the number of scores in a group (n_{group}) times the square of mean each group of scores ($\bar{x}_{group}$) minus the mean of all the scores ($\bar{x}_{grand}$; Equation 3-2). Essentially this compares the mean of each group of scores to the overall mean, and then weights the

result to account for the size of the group. The more different the means of each group are to the overall mean the more variance that must be explained.

$$SS_M = \sum n_{group}\left(\bar{x}_{group} - \bar{x}_{grand}\right)^2$$

Equation 3-2 Model sum of squares

Table 3-2 Mean and variance of scores from Table 3-1

9.82	10.74	13.19	15.38
11.55	10.57	17.05	18.84
4.45	6.99	13.88	15.90
5.80	12.33	15.20	19.05
6.34	4.49	12.80	19.49
8.62	8.54	16.59	13.69
12.18	7.62	7.98	8.03
13.46	9.83	8.93	6.38
15.76	16.66	12.04	8.72
14.38	10.11	6.14	11.46
20.25	13.93	12.14	4.73
14.81	13.74	16.54	8.10
Total		565.23	
Mean ($\bar{x}_{grand}$)		11.78	
Variance (s^2_{grand})		17.955	

This can be calculated using the figures from in Tables 3-1 and 3-2:

SS_M = 6 (7.76 - 11.78)^2 + 6(8.94 - 11.78)^2 + 6(14.78 - 11.78)^2 + 6(17.06 - 11.78)^2 + 6(15.14 - 11.78)^2 + 6(11.98 - 11.78)^2 + 6(10.63 - 11.78)^2 + 6(7.90 - 11.78)^2

= 6 (-4.02)^2 + 6(-2.84)^2 + 6(3)^2 + 6(5.28)^2 + 6(3.36)^2 + 6(0.20)^2 + 6(-1.15)^2 + 6(-3.88)^2

= 96.96 + 48.39 + 54 +167.27 + 67.78 + 0.25 + 7.94 + 90.22

= 532.8

For a factorial ANOVA SS_M has to be broken down further into main effects and interactions. The main effects correspond to the two independent

variables: concentration of factor A and cell type; there is one interaction between these variables concentration of factor A x cell type. The sum of squares for each of these effects and interactions needs to be calculated. For main effects this is calculated using the same equation as the SS_M, changing n_{group} and $\bar{x}_{group}$ to reflect the sum of squares being calculated.

Starting with the concentration of factor A (SS_A) the equation now subtracts the mean for each concentration of Factor A($\bar{x}_{column}$) from the overall mean ($\bar{x}_{grand}$), squares the result, and multiplies by the number of results in each column (n_{column};Equation 3-3).

Table 3-3 Glycosaminoglycan production with respect to concentration of Factor A

Conc. Factor A (ng)	8	11	14	17
	9.82	10.74	13.19	15.38
	11.55	10.57	17.05	18.84
	4.45	6.99	13.88	15.90
	5.80	12.33	15.20	19.05
	6.34	4.49	12.80	19.49
	8.62	8.54	16.59	13.69
	12.18	7.62	7.98	8.03
	13.46	9.83	8.93	6.38
	15.76	16.66	12.04	8.72
	14.38	10.11	6.14	11.46
	20.25	13.93	12.14	4.73
	14.81	13.74	16.54	8.10
Total	**145.42**	**136.57**	**166.48**	**166.76**
Mean ($\bar{x}_{column}$)	**11.19**	**10.51**	**12.81**	**12.83**
Variance	**20.77**	**10.42**	**11.54**	**27.05**

$$SS_A = \sum n_{column}\left(\bar{x}_{column} - \bar{x}_{grand}\right)^2$$

Equation 3-3 Sum of squares for concentration of Factor A

Using the values from Tables 3-2 and 3-3:

$SS_A = 12(11.19 - 11.78)^2 + 12(10.51 - 11.78)^2 + 12(12.81 - 11.78)^2 + 12(12.83- 11.78)^2$

$=12(-0.59)^2 + 12(-1.27)^2 + 12(1.03)^2 + 12(1.05)^2$

= 4.1772 + 19.3548 + 12.7308 + 13.23

= 49.49

$$SS_B = \sum n_{row}\left(\bar{x}_{row} - \bar{x}_{grand}\right)^2$$

Equation 3-4 Sum of squares for cell type

Table 3-4 Glycosaminoglycan production with respect to cell type

Chondrocytes			
9.82	10.74	13.19	15.38
11.55	10.57	17.05	18.84
4.45	6.99	13.88	15.90
5.80	12.33	15.20	19.05
6.34	4.49	12.80	19.49
8.62	8.54	16.59	13.69
Total		**291.29**	
Mean ($\bar{x}_{row}$)		**12.14**	
Variance		**21.08**	

MSCs			
12.18	7.62	7.98	8.03
13.46	9.83	8.93	6.38
15.76	16.66	12.04	8.72
14.38	10.11	6.14	11.46
20.25	13.93	12.14	4.73
14.81	13.74	16.54	8.10
Total		**273.94**	
Mean ($\bar{x}_{row}$)		**11.41**	
Variance		**15.34**	

The same process applies to cell type (SS_B) using Equation 3-4 and the data from Table 3-2 and 3-4:

$SS_B = 24(12.14 - 11.78)^2 + 24(11.41 - 11.78)^2$

$= 24(0.36)^2 + 24(-0.37)^2$

$= 3.11 + 3.29$

$= 6.40$

The interaction effect (SS_{AxB}) can be calculated by multiplying the square of the mean for each group minus the means for the relevant row and column plus the overall mean by the number of results in each group (Equation 3-5). Essentially, this is comparing the mean of each group to the mean for each

column and row then weighting them for the number of results in each group. The more that the means of the groups differ from the means predicted by the means of the columns and rows, the greater the interaction effect.

$$SS_{AxB} = \sum n_{group}\left(\bar{x}_{group} - \bar{x}_{column} - \bar{x}_{row} + \bar{x}_{grand}\right)^2$$

Equation 3-5 Sum of squares for the interaction effect

Table 3-5 Mean glycosaminoglycan production by group, row and column

7.76	8.94	14.78	17.06	12.14
15.14	11.98	10.63	7.90	11.41
11.19	10.51	12.81	12.83	

Table 3-5 summarises the means for each group, row and column from Tables 3-1, 3-3, and 3-4, together with the overall mean from Table 3-5 this data can be used with the equation for the sum of squares for the interaction effect (Equation 3-5) to find the interaction effect:

SS_{AxB} = 6(7.76 - 12.14 - 11.19 +11.78)^2 + 6(8.94-12.14-10.51 +11.78)^2 +
6(14.78 - 12.14 – 12.81 +11.78)^2 + 6(17.06 -12.14-12.83+11.78)^2 +
6(15.14 – 11.41– 11.19 +11.78)^2 +6(11.98 – 11.41 -10.51 +11.78)^2 +
6(10.63 – 11.41– 12.81 +11.78)^2 +6(7.90 – 11.41– 12.83+11.78)^2
=6(-3.79)^2 + 6(-1.93)^2 + 6(1.61)^2 + 6(3.87)^2 + 6(4.32)^2 + 6(1.84)^2
+ 6(-1.81)^2 + 6(-4.56)^2
= 86.18 + 22.35 + 15.55 + 89.86 + 111.97 + 20.31 + 19.66 + 124.76
= 490.65

The next step is to calculate the residual sum of squares (SS_R), which represents the variance that is not explained by the two independent variables (and their interaction). This can be calculated as the sum of the group variance (s^2_{group}) times the number of results in each group minus one (Equation 6-7).

$$SS_R = \sum s^2_{group}(n_{group} - 1)$$

Equation 3-6 Residual sum of squares

The residual sum of squares can be calculated with the data from Table 3-1:

SS_R = 7.23(6-1) + 8.23(6-1) + 3.17(6-1) + 5.70(6-1) +7.76(6-1) + 11.17(6-1) +13.86(6-1) + 5.15(6-1)
= 311.35

The next step is to convert the sums of squares into mean squares by dividing the number of degrees of freedom. For the two main effects the number of degrees of freedom is one less than the number of categories in that group, for the interaction effect the number of degrees of freedom is the multiple of the degrees of freedom for the main effects, and for the residual sums of squares it the number of results in each group minus one times the number of groups. Therefore the mean squares are as follows:

MS_A = 49.49 / (4 - 1) = 16.50
MS_B = 6.40 / (2 - 1) = 6.40
MS_{AxB} = 490.65 / (3 x 1) = 163.55
MS_R = 311.35 / (6 x (6-1)) = 10.38

These are then converted into F-ratios by dividing the mean square for the effect or interaction by the residual mean square:

F_A = 16.50 / 10.38 = 1.59
F_B = 6.4 / 10.38 = 0.62
F_{AxB} = 163.55 / 10.38 = 15.76

These F-ratios can be looked up in a table of critical F-ratios in conjunction with the degrees of freedom for the main effect or interaction and the residual to find the probability that the result occurred by chance. Table 3-6 reproduces a small part of this critical F-ratio table relevant to these results, it can be seen that the F-ratios for both of the main effects are below the level necessary for statistical significance (1.59 < 2.92 and 0.62 < 4.17), but the F-ratio for the interaction is significant at the 0.01 level (15.76 > 3.47).

Table 3-6 Critical F-ratios for residual degrees of freedom = 30

	Degrees of freedom (effect / interaction)					
p	1	2	3	4	5	6
.05	4.17	3.32	2.92	2.69	2.53	2.42
.01	7.56	5.39	4.51	4.02	3.70	3.47

3.2.1 Effect size

Calculating the effect size for significant effects determines what proportion of the variance in the experiment they account for, allowing comparison of how important different significant results are. There are multiple definitions of effect size. For simplicity, this thesis will focus on one of the most useful versions: ω^2 (Cardinal and Aitken 2006). This is defined as the proportion of the total *population* variance in Y attributable to effect A (Equation 3-7). As this estimates population variances, this effect size can be generalised beyond the results in a given experiment. The equation used to calculate ω^2 is given in Equation 3-8. *(N.B. This can only be used for fixed effects, for this thesis this is sufficient as there are only fixed effects and no random effects).*

$$\hat{\omega}^2 = \frac{\hat{\sigma}_A^2}{\hat{\sigma}_Y^2}$$

Equation 3-7 Definition of ω^2

$$\hat{\omega}^2 = \frac{SS_A - df_A x MS_{error}}{MS_{error} + SS_{total}}$$

Equation 3-8 Calculation of ω^2

For the interaction between concentration and cell type the effect size is calculated as below:

$\hat{\omega}^2_{AxB}$ = (490.65 – 3 x 10.38) / (10.38 + 843.89)

$\hat{\omega}^2_{AxB}$ = 459.51 / 854.27

$\hat{\omega}^2_{AxB}$ = 0.54

Therefore it is estimated that the interaction between cell type and concentration of Factor A accounts for 54% of the variance in the population. As ω^2 is a measure of the proportion of the population variance an effect accounts for, ω^2 values from an experiment will typically add up to less one, as the experiment will normally be run on a sample from the population, not the entire population

In this thesis results will be reported with an F-ratio and degrees of freedom, together with a significance level (calculated by statistical software) and an effect size where they are significant, this format is shown in Table 3-7 for the above results.

Table 3-7 Results of worked (hypothetical) example showing format for results

Variable / Interaction	F value	Probability	Effect size
Concentration of Factor A	F(3,30) = 1.59		
Cell type	F(1,30) = 0.62		
Concentration of Factor A x Cell type	F(3,30) = 15.76	0.00000003	0.54

These results can also be viewed graphically. Figure 3-1 shows the effect of Factor A on GAG production the absence of a statistically significant difference can be seen from the 95% confidence interval bars. Figure 3-2 shows the effect of cell type on glycosaminoglycan production again it is clear that there are not significantly differences. Figure 3-3a shows the interaction between cell type and Factor A concentration here it is clear that at 8ng/ml of Factor A MSCs produce more GAG than chondrocytes do and at 17ng/ml chondrocytes produce more GAG than MSCs do. This illustrates a key point about interactions: significant interactions indicate that the gradient of two (or more) lines is different this can be shown more clearly with a line chart (Figure 3-3b). In this example there is a dramatic difference in gradient; one of the examples in the next section will show that a more subtle difference in gradient can be significant.

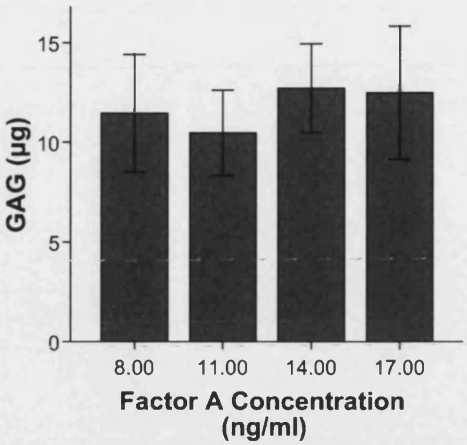

Figure 3-1 Effect of Factor A concentration on glycosaminoglycan production. Error bars show 95% confidence interval.

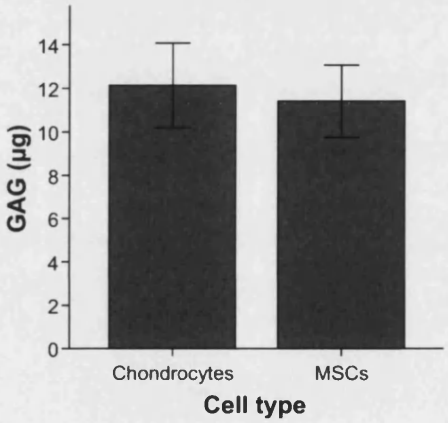

Figure 3-2 Effect of cell type on glycosaminoglycan production. Error bars show 95% confidence interval.

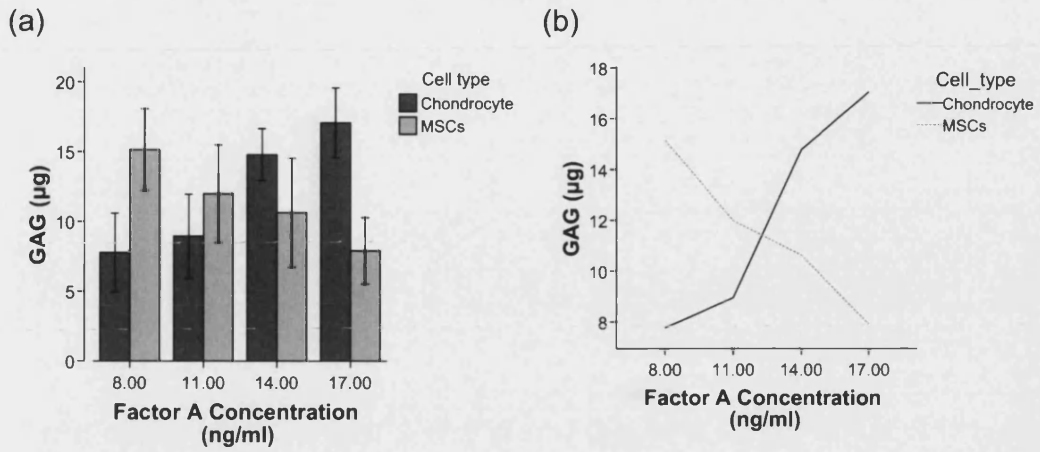

Figure 3-3 The interaction between cell type and Factor A concentration (a) bar chart and (b) line chart. Error bars show 95% confidence intervals.

3.3 Advantages of factorial ANOVA

This section will consider some of the advantages of factorial ANOVA over more widely used methods. A common experiment in tissue engineering and musculoskeletal science is to add a growth factor to cells and then measure the effect of that growth factor at several time points. In the next hypothetical example, Uber Growth Factor is added to chondrocytes and the effect relative to a control on GAG production measured every 5 days for 20 days.

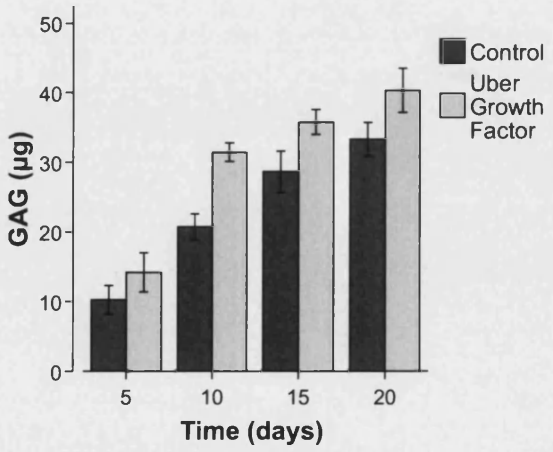

Figure 3-4 Bar chart showing GAG production in response to Uber Growth Factor. Error bars show 95% confidence intervals.

Figure 3-4 summarises the data for this comparison. If this data were analysed in the conventional manner for tissue engineering by independent t-tests to compare the samples the results would be as shown in Table 3-8. If an alpha level of 0.05 is used, these results demonstrate that there's a significant difference between the control and the samples treated with Uber Growth Factor on all four days that GAG was measured. However, as this is one experiment the alpha level of 0.05 needs to be corrected if multiple t-tests are run, using the Bonferroni correction this reduces the alpha level to 0.0125 from 0.05, making the result on day 5 non-significant.

Table 3-8 T-tests of hypothetical Uber Growth Factor experiment

Day	T-test	Probability
5	t(10)=-2.91	0.015
10	t(10)=-12.04	2.83E-7
15	t(10)=-5.33	0.0003
20	t(10)=-4.54	0.001

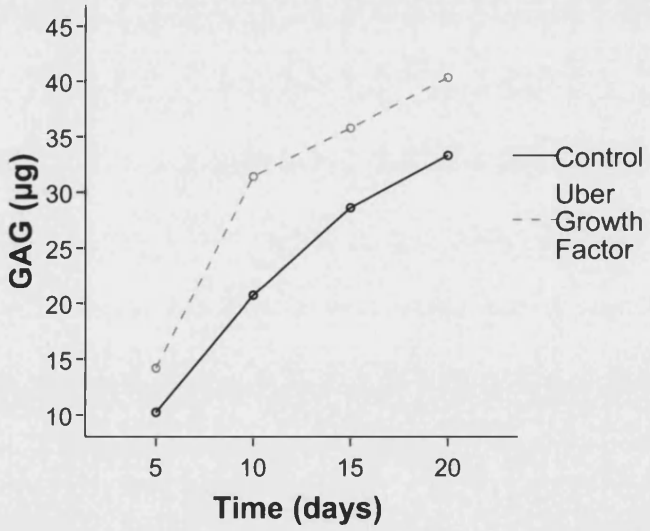

Figure 3-5 Line chart showing GAG production in response to Uber Growth Factor.

Table 3-9 shows the results of a factorial ANOVA carried out on the data. This demonstrates a major advantage of factorial ANOVA, which is that it tests more hypothesises than t-tests do. In addition to showing that the cells

produce more GAG in response to Uber Growth Factor, this ANOVA shows that as time progresses the cells produce more GAG, and that there's an interaction, the gradient of GAG production in response to Uber Growth Factor is different to that of the control. Note that in this example, the difference in gradient is much more subtle than that in the previous example (compare Figures 3-5 and 3-3b), this is reflected in the much smaller effect size for the interaction. The effect size shows that in this experiment, most of the variance (82%) is accounted for by differences due to time (Table 3-9).

Variable / Interaction	F value	Probability	Effect size
Time	F(2,30) = 267.68	1.68E-26	0.82
Uber Growth Factor	F(1,30) = 121.74	1.05E-13	0.12
Time x Uber Growth Factor	F(6,30) = 4.45	0.009	0.01

Table 3-9 Factorial ANOVA of hypothetical Uber Growth Factor experiment

If necessary, a simple effects analysis can be carried out to determine if Uber Growth Factor has an effect on all four days that GAG production was tested. This involves doing a one way ANOVA on each day's result to see if there's an effect of Uber Growth Factor. Table 3-10 shows the results. By analysing the results in this way there is a significant difference between the cells treated on all four days, whereas when t-tests were used, there was no difference on day 5; this is because by analysing multiple variables more of the total variance is accounted for, reducing the residual mean square thus increasing the F-ratio as the mean square for the effect/interaction is divided by a smaller number, thereby increasing the chance of a significant result. By using factorial ANOVA the chance of a type II error is reduced, the alternative would be to use t-tests and run the experiment with a larger sample size, making it more expensive and time consuming.

Variable	F value	Probability
Uber Growth Factor within day 5	F(1,40) = 9.14	0.004
Uber Growth Factor within day 10	F(1,40) = 66.95	<0.001
Uber Growth Factor within day 15	F(1,40) = 30.08	<0.001
Uber Growth Factor within day 20	F(1,40) = 28.91	<0.001

Table 3-10 Simple effects analysis of the effect of day in the hypothetical Uber Growth Factor experiment

3.4 Conclusions

Using multivariate experimental designs and factorial ANOVA gives three major advantages over the conventional statistical analysis for tissue engineering: the chance of a type II error is reduced without expensive increases in sample size; more hypothesises are tested by a single experiment, giving more information; and the calculation of effect size allows comparison of the relative importance of the independent variables. The consensus is that a significant result should have a probability of type I error of level than 0.05; by one widely used convention (Cohen 1988): a small effect explains 1% of the total variance ($\omega^2 = 0.01$), a moderate effect is 6% of the total variance ($\omega^2 = 0.06$), and a large effect explains 25% of the total variance ($\omega^2 = 0.25$).

4 Materials and Methods

4.1 Materials

4.1.1 Materials for cell culture (Section 4.2.1)

Material	Supplier	Code
Ascorbate-2-phosphate	Sigma-Aldrich, Poole, Dorset	A-8960
DMEM	Invitrogen, Paisley, Scotland	32430100
Fetal calf serum (FCS)	Sigma-Aldrich, Poole, UK	F7524
ITS Liquid media supplement	Sigma-Aldrich, Poole, UK	I3146
MEM non-essential amino acid solution	Sigma-Aldrich, Poole, UK	M7145
Penicillin-streptomycin	Sigma-Aldrich, Poole, UK	P0781
Phosphate buffered saline (PBS)	Sigma-Aldrich, Poole, UK	D8537
Serological 6 well plates	Fisher Scientific, Loughborough, UK	TKT-220-006R
Sodium pyruvate	Sigma-Aldrich, Poole, UK	S8636
T150 flasks	Triple red, Long Crendon,, UK	2020300
Tissue culture dishes	Fisher Scientific, Loughborough, UK	TKT-110-070A
Trypan blue	Sigma-Aldrich, Poole, UK	T8154

4.1.2 Materials for silk processing and scaffold preparation (Sections 4.2.2 – 4.2.5)

Material	Supplier	Code
1,1,1,3,3,3-Hexafluoro-2-propanol (HFIP)	Sigma-Aldrich, Poole, UK	105228-100G
Acetic acid	Fisher Scientific, Loughborough, UK	124040025
Ascorbate-2-phosphate	Sigma-Aldrich, Poole, Dorset	A-8960
Crepe silk	Hobbycraft, Bristol, UK	n/a
Formic acid	Fisher Scientific, Loughborough, UK	14793-2500
GRGDS peptide	Merck, Beeston, UK	03-34-0027
Lithium bromide	Sigma-Aldrich, Poole, UK	213225
Methanol	Fisher Scientific,	M/4058/17

	Loughborough, UK	
N-(3-Dimethylaminopropyl)-*N'*-ethylcarbodiimide (EDC)	Sigma-Aldrich, Poole, UK	03449
N-Hydroxysulfosuccinimide (NHS)	Sigma-Aldrich, Poole, UK	130672
Slide-a-Lyzer cassette (3500 MWCO)	Perbio, Cramlington, UK	66130
Sodium carbonate	Sigma-Aldrich, Poole, UK	S7795
Sodium Chloride	Sigma-Aldrich, Poole, UK	S9888
Sodium Chloride (small particles)	British Salt	Fine 60

4.1.3 Materials for scaffold characterisation (Sections 4.3.1 - 4.3.3)

Material	**Supplier**	**Code**
Bijoux tubes		
Eppendorf tubes		
10% Formal saline	VWR, Lutterworth, UK	36136
DPX mountant	VWR, Lutterworth, UK	360294H
Technovit 7100	Taab Laboratories Equipment, Aldermaston, UK	T-218
Potassium bromide	Sigma-Aldrich, Poole, UK	22,186-4

4.1.4 Materials for DNA and hydroxyproline assays (Sections 4.3.4 - 4.3.6)

Material	**Supplier**	**Code**
70% Perchloric acid	Fisher Scientific, Loughborough, UK	P/1280/PB08
Acetic acid	Fisher Scientific, Loughborough, UK	124040025
Chloramine T	Sigma-Aldrich, Poole, UK	31274
Citric acid	Sigma-Aldrich, Poole, UK	C0759
Cysteine hydrochloride	Sigma-Aldrich, Poole, UK	C8005
Ethylenediamine tetraacetic acid (EDTA)	Sigma-Aldrich, Poole, UK	E9884
Hydrochloride acid	Fisher Scientific, Loughborough, UK	H/1200/PB17
l-Hydroxyproline	Sigma-Aldrich, Poole, UK	56250
Methanol	Fisher Scientific, Loughborough, UK	M/4058/17
Papain	Sigma-Aldrich, Poole, UK	P3125

P-Dimethylaminobenzaldehyde	Sigma-Aldrich, Poole, UK	15,647-7
Phosphate buffered saline (PBS)	Sigma-Aldrich, Poole, UK	D8537
Picogreen	Invitrogen, Paisley, UK	P-7589
Poly-l-lysine coated slides	Agar Scientific, Stansted, UK	L4345
Propan-*1*-ol	Sigma-Aldrich, Poole, UK	402893
Sodium acetate ($3H_2O$)	Sigma-Aldrich, Poole, UK	S5889
Sodium Hydroxide	Sigma-Aldrich, Poole, UK	S5881
Sodium phosphate, dibasic	Sigma-Aldrich, Poole, UK	S9763
Tris-EDTA buffer	Sigma-Aldrich, Poole, UK	T-9285

4.1.5 Materials for GAG analysis (Section 4.3.7)

Material	**Supplier**	**Code**
0.5µm frit.	Hichrom, Reading, UK	HI-102
Acetronitrile	Fisher Scientific, Loughborough, UK	A/0626/17
Boric acid	VWR, Lutterworth, UK	27410
Chondroitin sulphate A	Sigma-Aldrich, Poole, UK	C9819
Chondroitin sulphate C	Sigma-Aldrich, Poole, UK	C4384
Ethanol	Fisher Scientific, Loughborough, UK	E/0650DF/17
Hyaluronic acid	Sigma-Aldrich, Poole, UK	17771
Hydrochloride acid	Fisher Scientific, Loughborough, UK	H/1200/PB17
Partisil-5PAC column	Capital analytical	5GM125
Sulphuric acid	Fisons, Ipswitch, UK	
Trizma base	Sigma-Aldrich, Poole, UK	T1503
Unsaturated Chondro-Disaccharide kit	AMS Biotechnology	400571
Δ Di-disB	Dextra Laboratories	C3205
Δ Di-HA	Dextra Laboratories	C3209

4.2 Experimental Methods

4.2.1 Cell culture

Passage 3 anterior cruciate ligament fibroblasts were obtained by explanting the anterior cruciate ligaments from the left and right stifles of a sheep (Graystone Ltd, Hull, UK). Stifles were supplied on ice; within 24 hours of

slaughter; from sheep approximately 10 months old. Each ligament was divided between two tissue dishes (92mm diameter x 17mm high). The cells were grown at 37°C with 5% CO_2 in DMEM supplemented with penicillin-streptomycin, 200μM ascorbate-2-phosphate, 10% fetal calf serum (FCS) and MEM non-essential amino acid solution, which was changed three times a week. At the first passage the cells from the two ligaments were pooled, and transferred to T150 flasks.

MG63 cells (human osteoblast-like cell line) were grown using DMEM supplemented with penicillin-streptomycin, 1mM sodium pyruvate, 10% FCS, and MEM non-essential amino acid solution; ATDC-5 cells (mouse chondrocyte cell line (Atsumi et al. 1990)) were grown in DMEM supplemented with penicillin-streptomycin, ITS liquid media supplement, and 10% FCS.

For the work described in Chapter 6, cells were frozen at passage 3 at 5-10 million cells per cryotube in a mixture of 500μl FCS : 300μl DMEM : 200μl DMSO. For the work reported in Chapter 7 cells were not frozen prior to utilisation. Prior to cell culture, scaffolds were soaked overnight in media with the same composition as the media that would be used for subsequent cell culture on the scaffolds.

To seed the scaffolds with cells, the number of viable cells was counted using trypan blue and a haemocytometer. Seven hundred thousand viable cells were seeded by placing the cells and 3ml of media into a well of a serological 6 well plate (to limit cell attachment to the plate) followed by the scaffold. The 6 well plates were cultured at 37°C, and 5% CO_2 on an orbital shaker set to rotate at 100rpm.

4.2.2 Preparation of regenerated silk fibroin

Regenerated silk fibroin was prepared by a method based on that of Nazarov et al (2004). Crepe silk was first degummed to remove any remaining sericin protein. Two grams of crepe silk were weighed out and cut into strips.

Meanwhile 1L of 0.02M sodium carbonate was brought to boil. The strips of silk were placed into the boiling sodium carbonate solution and boiled for 30 minutes. Then the strips were removed and washed thoroughly in reverse osmosis water (roH_2O; equivalent purity to double distilled water), and left to dry at room temperature (12-25°C).

Next the strips were dissolved in lithium bromide solution by placing them into 10ml of a 9.5M lithium bromide solution and leaving them for four hours to dissolve. To remove the lithium bromide, the solution was dialysised against roH_2O. The solution was injected into a hydrated 3500 molecular weight cut off Slide-a-Lyzer cassette; then the cassette was placed into 2L of roH_2O, which was changed after 2 hours, then changed a second time and left overnight. The resulting solution was then placed into a 100ml freeze dryer bulb, and frozen by rotating the bulb in liquid nitrogen until all the solution was frozen. The bulb was then placed onto the freeze dryer and freeze dried. For the work in Chapter 6, the regenerated silk fibroin (SF) was removed from the bulb and kept sealed in a sample tube at room temperature (15-25°C) until use. For the work in Chapter 7, the SF was used immediately after removal from the bulb.

4.2.3 Solubility of silk in aqueous organic acid solutions

In order to improve the connections between pores, aqueous organic acid solvents were considered to increase the solubility of salt, without increasing to the point that small salt crystals were completely dissolved. Formic acid, acetic acid and *1,1,1,3,3,3* hexafluoro-2-propanol (HFIP) were tested. Approximately 100mg of SF was weighed out, and the exact weight recorded. This weight was used to prepare solvent by mixing 4 volumes of roH_2O to 1 volume of formic acid in a 15ml centrifuge tube to make a 20% v/v formic acid : water solvent; the volume of solvent made was determined to be the quantity required to dissolve all the SF to make a 5% w/v solution. This procedure was repeated changing the ratio of formic acid : water to make 40%, 60% and 80% v/v solutions. 10%w/v and 15%w/v concentrations of silk were also tested with 20%, 40%, 60% and 80% v/v solvents. Aqueous

acetic acid and aqueous HFIP solvents were tested at 10%w/v SF with 20 - 80% v/v acid solvents. Subsequently, the process was repeated with aqueous formic acid saturated with sodium chloride with 10 - 90% formic acid.

4.2.4 Scaffold preparation

First, SF was dissolved in either formic acid or 20% v/v formic acid to make a 10% w/v solution; the solution was left overnight to allow the SF to completely dissolve. Initially, scaffolds were made with 0.3ml of this solution. This was pipetted into a PTFE mould with holes 15 mm diameter by 5 mm high, consisting of two plates: one plate with holes through to make the scaffolds, and a bottom plate that was bolted on to seal it. Then 0.6g of sodium chloride was added. Then scaffolds were left for 10 minutes, after this time they were covered with parafilm for 24 hours. After the parafilm was removed the scaffolds were left for a further 24 hours to allow the solvent to evaporate, at this point the bottom plate of the mould was removed and the scaffolds were left for a further 24 hours to allow all the solvent to evaporate. The scaffolds were then pressed out of the mould into methanol (MeOH) and left for 30 minutes prior to salt leaching. For the salt leaching process the scaffolds were left in roH_2O for 24 hours changing the water four times. The process for regenerating silk and scaffold fabrication is outlined in Figure 4-1.

As the initial procedure did not produce scaffolds with replicable structures, several variations were tried. The variations on the method all involved changing the "Cast in mould using salt as a porogen step" in Figure 4-1.
In the original method (Method A), 0.3ml of 10% w/v silk solution was pipetted into the mould then 0.6g of salt was added and given 10 minutes to settle. In Method B the 0.6g of salt was placed in the mould prior to the addition 0.3ml of the 10% w/v silk solution. Method C was similar to method b, but 1g of salt was used in the place of 0.6g. Method D was another variation of Method B, the 0.6g of salt was placed in the mould followed by 0.6ml of 5% w/v silk solution. In Method E, the 0.6g of salt was placed in the mould followed by 0.4ml of 7.5% w/v silk solution. Method F was a variation of Method A, immediately after the silk solution was added to the salt, a

PTFE lid was placed on top of silk solution. Table 4-1 summarises these methods.

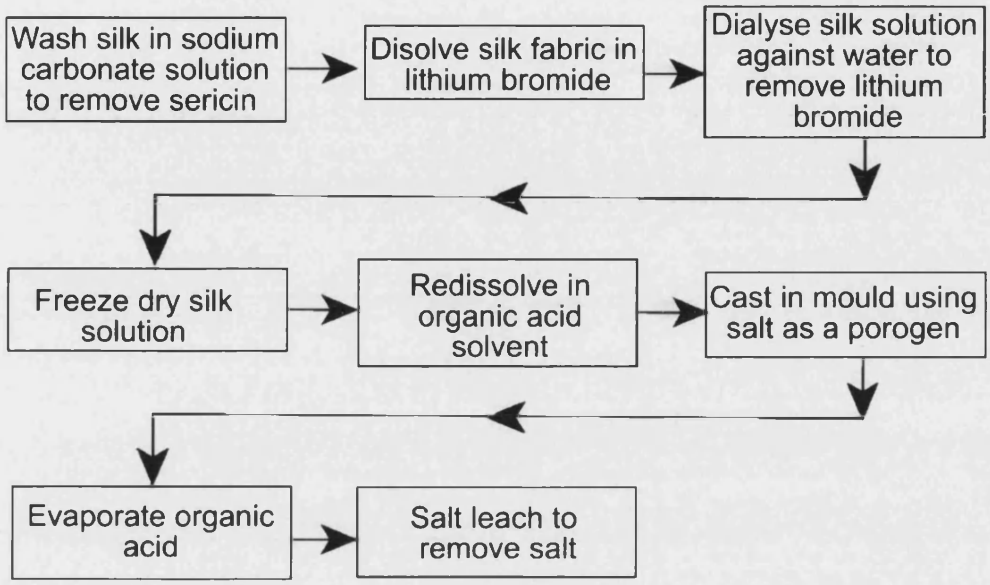

Figure 4-1 Outline of the process for regenerating silk and fabricating porous silk scaffolds

Table 4-1 The five different methods of silk scaffold fabrication with 20% v/v formic acid

Method	Weight of Salt used (g)	Silk before or after Salt	% w/v Silk	Teflon cover
A	0.6	Before	10	No
B	0.6	After	10	No
C	1	After	10	No
D	0.6	After	5	No
E	0.6	After	7.5	No
F	0.6	Before	10	Yes

To understand the effects of saturated silk solutions, scaffolds were also made with Method B with 40% and 80% formic acid saturated with sodium chloride.

For FTIR analysis, scaffolds made with methanol coagulation were compared to scaffolds made without the use of methanol. For cell culture and porosity studies scaffolds were made with 0.05g of SF dissolved at either 7.5% or 10% w/v in 20% v/v formic acid and compared to scaffolds made with 10% w/v silk dissolved in formic acid. These scaffolds were soaked in methanol for 30 minutes, then cut to 2mm height with the aid of a 2mm high polycarbonate guide. In addition, for Chapter 7, a hole punch was used to cut the scaffolds to 7mm diameter. Scaffolds for cell culture were autoclaved to ensure sterility, no changes in scaffold appearance were observed.

4.2.5 RGD decoration

To decorate the silk scaffolds with GRGDS peptide (Merck, Beeston, Nottingham), a solution of *N*-(3-dimethylaminopropyl)-*N'*-ethylcarbodiimide (EDC; 0.5mg/ml) and *N*-hydroxysulfosuccinimide (NHS; 0.7mg/ml) was filter sterilised. Scaffolds were transferred to the EDC:NHS solution at a concentration of 1 scaffold per ml. After 15 minutes the scaffolds were washed with sterile roH_2O and transferred to a sterile solution of GRGDS peptide (0.1mg/ml) in PBS (pH6.5) for 2 hours. After two hours the scaffolds were washed twice with sterile roH_2O.

4.3 Analytical methods

4.3.1 Scanning electron microscopy of silk scaffolds

For the first SEM session, silk scaffolds were removed from roH_2O, cut in half, each half was placed into an Eppendorf tube and the lid of the tube was pierced. The eppendorfs were placed into a 100ml freeze dryer bulb then into a -80°C freezer for two hours to ensure that they were thoroughly frozen. For the subsequent sessions, whole scaffolds were placed into bijoux tubes with their lids pierced; then the tubes were placed into a polycarbonate chamber, which was transferred to -80°C for two hours. The bulb or chamber was then transferred to the freeze dryer and the scaffolds freeze dried overnight. The dry scaffolds were then frozen one at a time in liquid nitrogen, freeze

fractured, mounted and gold coated for SEM. SEM was carried out with a JEOL JSM6310 scanning electron microscope.

4.3.2 Fourier transform infrared spectra of silk scaffolds

Fourier transform infrared (FTIR) spectroscopy can be used to characterise the crystalline structure of silk because the positions of three peaks shift due to hydrogen bonding when the structure changes from random coil to crystalline silk II (Ha et al. 2005). Silk scaffolds were oven dried, then frozen in liquid nitrogen and ground into a powder in a mortar and pestle. FTIR results from this powder suggested that it was contaminated with water, presumably gained during the freezing and grinding. So this powder was then freeze dried with 200µl roH_2O added. Approximately two milligrams of powdered scaffold was added to 30mg of potassium bromide and pressed into a disk. FTIR spectra were measured on a Bruker Equinox 55 spectrophotometer at a resolution of 4cm^{-1} averaging 100 scans.

4.3.3 Light microscopy and image analysis

To ensure that none of the scaffold was lost during the processing of slides for light microscopy, scaffolds were cut into half and embedded into Technovit 7100 after overnight fixation with 10% formal saline (VWR, Lutterworth, Leicestershire). Sections were cut to 5µm thickness and placed onto poly-l-lysine coated slides. Slides were air dried then stained with Methyl Blue, washed in four changes of roH_2O, then air dried a second time, prior to covering with a coverslip and DPX mountant.

Images were analysed with the aid of macros in ImageJ (http://rsb.info.nih.gov/ij) that removed the background, split the image into red, green and blue channels, then selected the red channel, which was automatically thresholded, and recorded the fraction of black pixels in the thresholded image (see Figures 4-2 and 4-3 for an example). This fraction was used to calculate the porosity for each of the images analysed. For each

scaffold 20 images were averaged, and for each type of scaffold measurements from 3 scaffolds were taken.

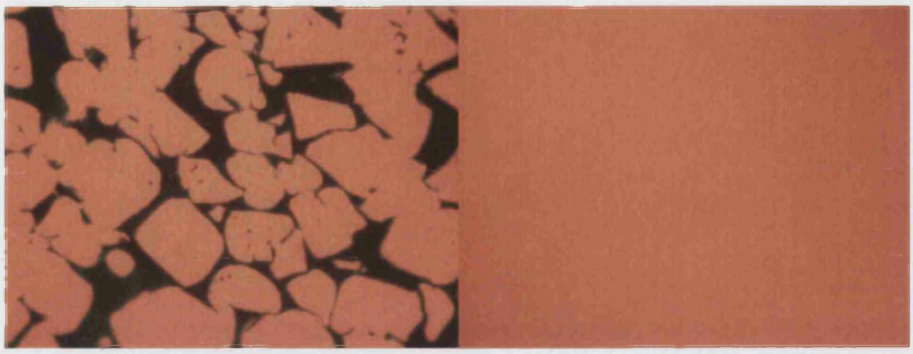

Figure 4-2 Example images for image analysis: left – sample section, and right – background

(a)

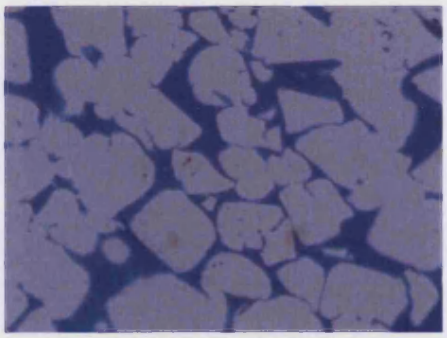

(b)

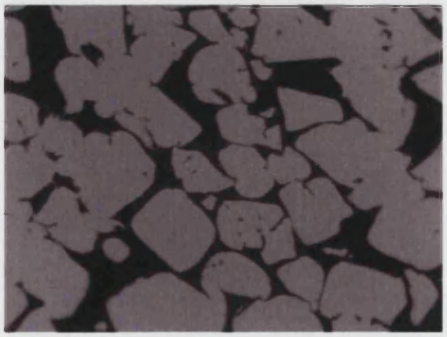

(c)

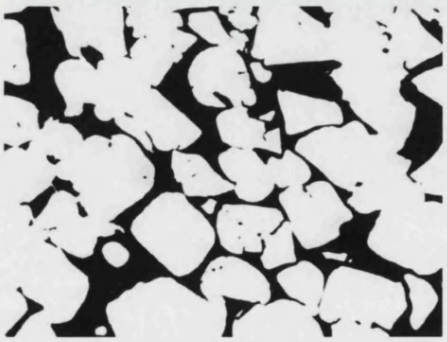

Figure 4-3 Images from Figure 4-2 during processing for image analysis: (a) post-background removal, (b) red channel of image (a), and (c) after thresholding.

4.3.4 DNA quantification

To quantify DNA, scaffolds were rinsed twice with PBS, then the cells were lysed by placing the scaffolds in Tris-EDTA buffer, then freezing at -80°C. Following sample thawing DNA concentration was determined by using Picogreen. DNA standards were made from 10-1000ng/ml. One hundred microlitres of each standard or sample was pipetted into a well of a 96 well plate, and then 30µl of picogreen solution was added. Emission was read at 520nm following excitation at 480nm. Standards were run in triplicate and samples in duplicate. Figure 4-4 shows a representative sample curve.

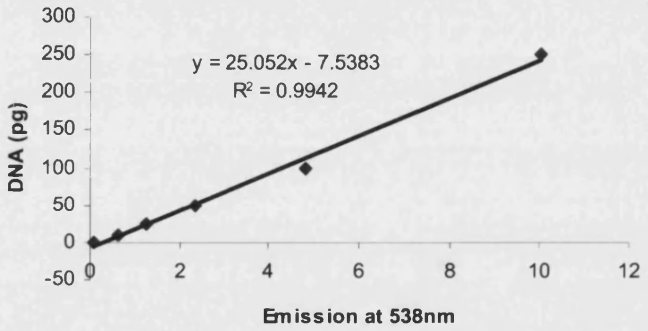

Figure 4-4 Representative standard curve for DNA quantification

4.3.5 Papain digestion

For the work reported in Chapter 7 matrix quantification followed DNA quantification. Scaffolds were removed from the Tris-EDTA buffer and transferred to a microcentrifuge tube containing 0.5ml of papain buffer (see Appendix A) containing 0.5mg of papain. Samples were then transferred to a microcentrifuge tube heater (Grant QBT2) set to 60°C and left for 16 hours. Blank papain digests were run as above without scaffolds, i.e. 0.5mg papain in 0.5ml of papain buffer at 60°C for 16 hours. Samples were then stored at 4°C prior to analysis

4.3.6 Hydroxyproline analysis

One hundred microlitres of papain digest was taken and 100µl of 1.18 specific gravity hydrochloric acid was added to form an approximately 6M solution of hydrochloric acid to hydrolyse the collagen amino acids. This solution was heated to 110°C in sealed eppendorfs in a Grant QBT2 heater. To ensure that the eppendorfs remained sealed their lids were weighted down with a large steel block. After three hours the heater was switched off, and allowed to cool.

Once cool the pH was adjusted to 6.5 with 6M sodium hydroxide. The samples were freeze dried, and dissolved in 200µl of roH_2O. Standards from 0-30µg/ml were prepared with l-hydroxyproline and hydroxyproline assay buffer (Appendix A). Fifty microlitres of standard or sample were aliquoted into wells of a 96 well plate, and 100µl of oxidising solution added to each well. Samples were run in duplicate, and standards were run in triplicate. The plate was shaken for 5 minutes, then 100 µl of Ehrlich's reagent (Appendix A) was added. After the plate was incubated at 60°C in an oven for 45 minutes, absorbance was read at 570nm. Figure 4-5 shows a representative sample curve from this procedure.

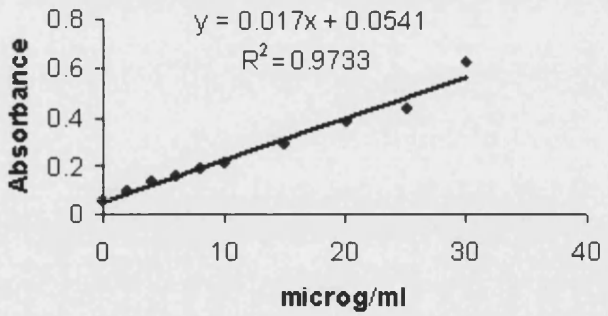

Figure 4-5 Representative standard curve for hydroxyproline analysis

4.3.7 Analysis of glycosaminoglycans

HPLC system

The HPLC system consisted of: a Shimadzu SCL-10AVP system controller, a Shimadzu SPD-10AVVP UV-vis detector, a Shimadzu SIL-10ADVP auto injector, and a Shimadzu LC-10ADVP pump, a Shimadzu DGU-14A degasser, connected to a PC running Shimadzu Class VP V5.032 software for data logging and analysis. A Whatman Partsil-5 PAC column (5µm, 250mm x 4.6mm i.d) was protected by a 0.2µm frit.

Glycosaminoglycan preparation for digestion

A 100µl sample of papain digest was taken and the glycosaminoglycans were precipitated by adding 700µl of ethanol and cooling at -20°C for four hours (Skandalis et al. 2003). The precipitate was pelleted by centrifuging for 10 minutes at 13,400g in a MSE micro-centaur centrifuge. The supernatant was discarded, and the pellet was dissolved in 40µl of roH_2O. Alternatively, for digestion of commercially purified glycosaminoglycans, chondroitin sulphate A or C, or hyaluronic acid was dissolved in roH_2O at 1µg/µl, and 40µl of this solution was used.

Glycosaminoglycan digestion

Either 15 µl of 250µM Tris-HCL (pH 8.0) (Zebrower et al. 1991) or 20µl of 100µM Tris-acetate (pH 8.0) (Koshiishi et al. 1998) were added to the 40 µl of glycosaminoglycan/sample. The desired concentration of enzyme was dissolved in 20µl of roH_2O (0.025U for quantifying ligament matrix production), and the samples were incubated at 37°C for the desired period (16 hours for ligament matrix characterisation). After digestion 300µl of ethanol was added and the solution was kept for four hours at -20°C. The samples were then centrifuged at 13,400g in a MSE micro-centaur centrifuge for 10 minutes to pellet any undigested glycosaminoglycans. The supernatant was kept and evaporated until the samples were dry.

Glycosaminoglycan standard preparation

The standards (Δ Di-0S, Δ Di-4S, Δ Di-6S, Δ Di-diS_E Δ Di-diS_D, and Δ Di-triS from the unsaturated chondro-disaccharide kit, along with Δ Di-diS_B and Δ

Di-HA) were made into stock solutions at 1µg /1µl in roH_2O. To use the standards, the desired amount was added to a microcentrifuge tube, and then dried to remove water.

HPLC of samples

The dry samples were taken and dissolved in 500µl of the mobile phase of 48% acetonitrile, 14% methanol and 38% aqueous buffer (0.5M Tris, 0.1M boric acid, 23.4mM sulphuric acid, adjusted to pH8.0 with HCl). The standards for quantifying glycosaminoglycans following papain digestion were made by dissolving the dried standards in 500µl of mobile phase, the dissolving the dried supernatant from a blank papain digestion in the same 500µl. The HPLC system was operated at a flow rate of 0.7ml/min, and samples were detected by absorbance at 229nm (Zebrower et al. 1991). For Chapter 7, all dissacharides other than ΔDi-HA (see Figure 2-7) were added to calculate total chondroitin sulphate (CS).

4.4 Statistics

For Chapter 6, one or two way analysis of variance was used to determine statistical significance dependent on the number of independent variables. Where data was not homogenous, it was transformed by taking the square root (cell attachment) or the reciprocal (osteochondral). Tukey HSD was used as a post hoc test to better understand the nature of any significant differences.

For Chapter 7, factorial ANOVA was used to determine statistical significance. As there were four dependent variables in this experiment a Bonferroni correction was applied to the alpha level to reduce it from 0.05 to 0.0125. Post hoc analysis was carried out used the Games-Howell test, where the ANOVA indicated there were significant differences. Dependent variables from different days were correlated with Pearson's correlation. Statistics are discussed further in Chapter 3.

5 Implementation of HPLC GAG analysis

5.1 Introduction

5.1.1 Glycosaminoglycans as biomarkers

In order to understand better how to engineer ligament, biomarkers need to be identified that will enable quantitative analysis of ligament engineering processes to determine the strengths and weaknesses of those processes. These biomarkers should ideally possess four characteristics:

1. longitudinal data should be available to enable comparison of the engineered ligament with tissue at several stages of development;
2. the levels of the biomarker should diverge in health and disease;
3. the biomarker should be relevant to the function of the tissue;
4. the biomarker should not confound multiple tissues (especially important when cells are being differentiated).

Not all biomarkers will possess all four properties, but tissue engineering should aim to develop panels of biomarkers for each tissue of interest that combine these properties. An important example of how failure to consider these properties can cause problems is highlighted by the recent work on chondrogenesis showing that BMSCs constitutively express aggrecan, and that type X collagen is sometimes produced by BMSCs undergoing chondrogenesis before they produce type II collagen (Mwale et al. 2006). This means that researchers have potentially been confounding normal BMSC behaviour with differentiation of hypertrophic cartilage.

As discussed in Section 2.1, mRNA of collagen types I, II & III, glycoproteins (bone sialoprotein, tenascin-C, laminin and fibronectin) and proteoglycans (aggrecan, decorin and biglycan) have been as used biomarkers when engineering ligament or tendon (Cristino et al. 2005; Moreau et al. 2005a; Sahoo et al. 2006). A major limitation of this approach is that mRNA does not necessarily result in protein synthesis, for instance, post-translational failure of collagen lysine hydroxylation by prolyl-4-hydroxylase results in collagen being retained in the endoplasmic reticulum (Walmsley et al. 1999).

Therefore, when analysing the ECM it would be better to directly measure ECM components.

(a)

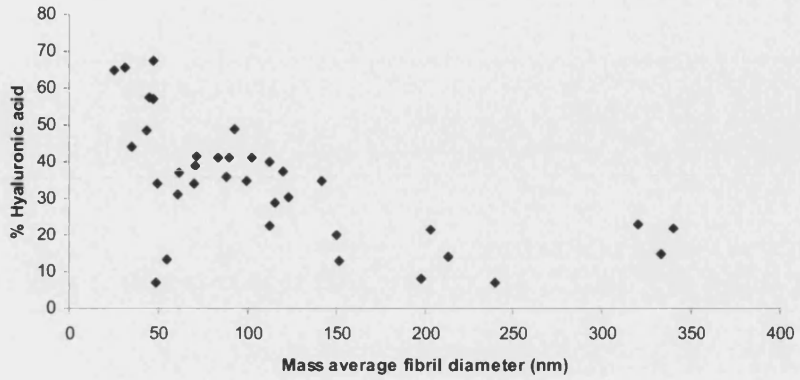

(b)

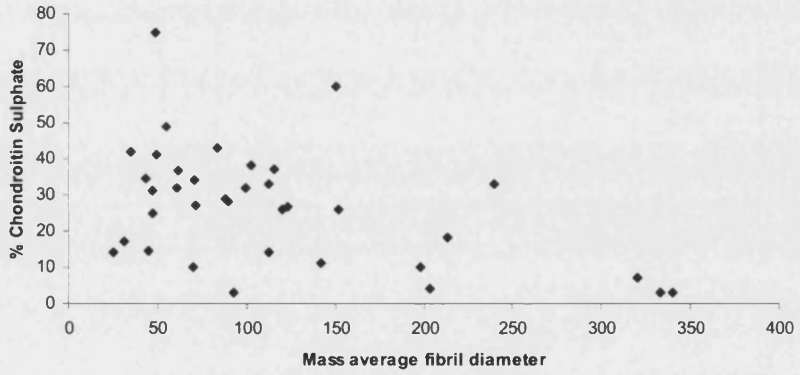

(c)

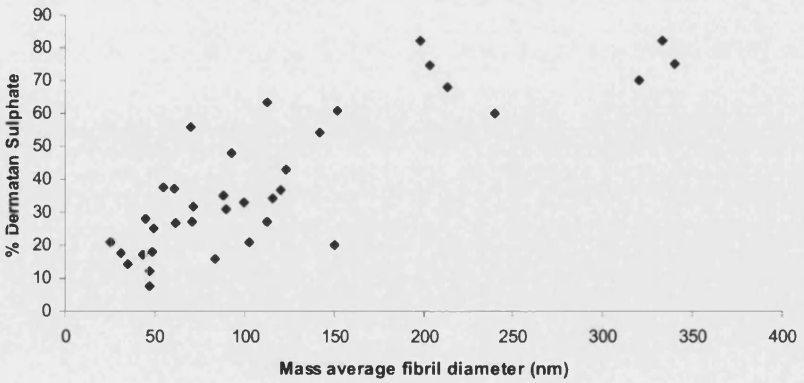

Figure 5-1 Glycosaminoglycan levels against mass-average fibril diameter: (a) hyaluronic acid, (b) chondroitin sulphate, and (c) dermatan sulphate. Plotted from data from Parry et al (1982), excludes data points for Dupuytren's contracture.

The current biomarkers for ligament suffer from several other limitations: ligament differentiation is indicated by a higher ratio of collagen III : collagen I than skin or tendon (Altman et al. 2002b), but fibrosis potentially increases the collagen III:I ratio (el Nabout et al. 1989). Bone sialoprotein, collagen II and aggrecan are potentially useful as negative markers of stem cell differentiation; their sustained presence would suggest that the stem cells are not differentiating correctly. For the other biomarkers, the problem is one of limited information about how much of the biomarker should be present at any given stage of ligament engineering. Perhaps the most extensively studied of these biomarkers is decorin. Both increased and decreased decorin levels can result in fibrotic changes (Reed and Iozzo 2002), but there is not the longitudinal data necessary to specify required levels of decorin during ligament engineering. It would be very useful to have a biomarker for ligament engineering with extensive longitudinal data.

The literature review for this work identified glycosaminoglycans as useful biomarkers for ligament engineering. The key paper from this literature review provides longitudinal data for glycosaminoglycan levels across several species in both skin and tendon (Parry et al. 1982). This paper showed a consistent pattern of glycosaminoglycan levels as the collagen fibrils matured (Figure 5-1). Thin, immature fibrils contain mostly hyaluronic acid, with some chondroitin sulphate. As the fibrils mature and grow laterally the percentage of glycosaminoglycan that is hyaluronic acid drops. Hyaluronic acid is replaced by chondroitin sulphate and dermatan sulphate. Above fibril diameters of about 200nm, the percentage of chondroitin sulphate begins to drop and dermatan sulphate becomes the dominant glycosaminoglycan. These results are supported by work from a different group that identified a strong relationship between age and glycosaminoglycan levels rat tail tendon (Scott et al. 1981). This work showed a rapid drop of hyaluronic acid levels, and an increasing percentage of glycosaminoglycan as dermatan sulphate (Figure 5-2), although the method used appears to underestimate the amount of hyaluronic acid compared to other work on rat tail tendon (Aukland 1991; Aukland et al. 2001; Parry et al. 1982), and human rotator cuff tendons (Riley et al. 1994);

this might be due to a the cetylpyridinium chloride precipitation method used in the Scott et al (1981) paper not precipitating all the hyaluronic acid (Huey et al. 1990). In addition, the Scott et al (1981) paper shows that levels of both sulphated glycosaminoglycans and hyaluronic acid drop as the tendon ages. Unfortunately there is no longitudinal work on glycosaminoglycan levels in ligaments, but the consistency across species and tissues suggests this as a useful biomarker.

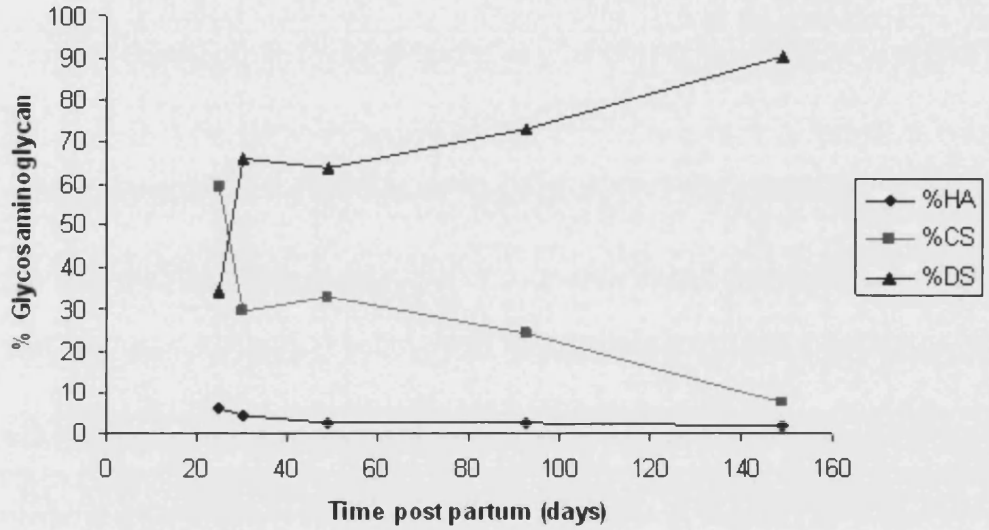

Figure 5-2 Percentage of total glycosaminoglycan content as hyaluronic acid (HA), chondroitin sulphate (CS) and dermatan sulphate (DS) against time in rat tail tendon using data plotted from Scott et al. (1981).

Glycosaminoglycans meet the other requirements of an ideal biomarker at least in part. It has been shown the rotator cuff tendonitis results in elevated levels of hyaluronic acid, chondroitin sulphate and dermatan sulphate (Riley et al. 1994). This suggests that abnormal glycosaminoglycan levels might be common to fibrotic conditions beyond tendonitis, although there is no published work to confirm or deny this.

There is some evidence for glycosaminoglycans playing an important role in ligament and tendons. Hyaluronic acid based biomaterials appear to enhance the differentiation of BMSCs towards a ligament fibroblast phenotype (Cristino et al. 2005); hyaluronic acid also appears capable of

improving tendon healing (Yagishita et al. 2005). These results fit with a role for hyaluronic acid in initiating ligament development and repair. Chondroitin sulphate has been shown to be a better predictor of structural mechanical properties (failure load, and stiffness) of rat tail tendon than fibril diameter, fibril area, or hydroxyproline content (Robinson et al. 2004a); similarly chondroitin sulphate per unit mass of tendon is a better predictor of material properties (failure stress, and modulus) than fibril diameter, fibril area, or hydroxyproline content per unit mass (Robinson et al. 2004a). This strongly suggests that chondroitin sulphate levels are associated with the mechanical function of tendon, and probably ligament.

Glycosaminoglycan levels vary from tissue to tissue, making it them potentially useful markers of differentiation. Cartilage contains much more sulphated glycosaminoglycan than ligament (Price et al. 1996), and sulphated glycosaminoglycan levels are widely measured as an useful biomarker in cartilage tissue engineering (Dickinson et al. 2005). In bone glycosaminoglycans are catabolised prior to matrix mineralisation (Baylink et al. 1972), whilst synovium has high levels of hyaluronic acid (Price et al. 1996). These differences between musculoskeletal tissues show that glycosaminoglycans are useful as biomarkers to help to distinguish differentiation pathways.

5.1.2 Options for GAG analysis

The simplest methods for quantifying glycosaminoglycans rely on their differing physicochemical properties. Several methods exist to precipitate specific glycosaminoglycans at different concentrations of solvents or salts, for instance using acetone (Volpi 1994), alcian blue in combination with guanidine-HCL (Bjornsson 1993), or cetylpyridinium chloride (Cleland and Sherblom 1977). These methods have the advantage of simplicity, but more recent techniques provide more information about the precise composition of the glycosaminoglycans. There are also questions about whether all these tests precipitate all the glycosaminoglycan of interest (Huey et al. 1990).

Perhaps the most widely used test for glycosaminoglycans in tissue engineering is to quantify sulphated glycosaminoglycans with dimethylmethylene blue (Dickinson et al. 2005). The advantage of this technique is its simplicity and speed. The disadvantages are that it does not quantify the separate glycosaminoglycan disaccharides or distinguish chondroitin sulphate, dermatan sulphate, keratin sulphate, or heparin from each other, and by definition it does not detect unsulphated glycosaminoglycans.

More powerful techniques use enzymes to break glycosaminoglycans into disaccharides. The most widely used enzyme is chondroitinase ABC, which has the ability to degrade hyaluronic acid, chondroitin sulphate and dermatan sulphate into disaccharides (Figure 2-7 shows the structure of these dissacharides). Heparin, heparan sulphate and keratin sulphate cannot be analysed with the use of this enzyme, but for ligament engineering the most interesting glycosaminoglycans are those that can be broken down by chondroitinase ABC. A variation on using chondroitinase ABC, is to use chondroitinase AC and chondroitinase B separately, this allows more precise quantification of the levels of dermatan sulphate (Lee et al. 2004a).

One of the most powerful of all the glycosaminoglycan analysis techniques is fluorophore-assisted carbohydrate electrophoresis. This combines gel electrophoresis with a fluorescent probe following enzymatic digestion and chemical modification of the disaccharides (Calabro et al. 2000). The major advantage of this technique over the other techniques considered is that the non-reducing termini of chondroitin sulphate can also be quantified allowing estimation of the average length of chondroitin sulphate chains.

The final option considered was high performance chromatography (HPLC) which uses the HPLC columns to separate the glycosaminoglycans, which are then detected and quantified by either their absorbance of UV light at approximately 230nm (Imanari et al. 1996), or by coupling them to a fluorophore, exciting the fluorophore and then measuring the emission (Volpi 2000). Of these two alternatives, fluorescence is the more sensitive

technique (Imanari et al. 1996), but is limited by the availability of fluorescent detectors. The alternative is to use UV detection. One of the limitations of using UV detection is that most of the published methods do not separate all the disaccharides produced by chondroitinase ABC (Imanari et al. 1996), a particular problem is the separation of the unsulphated chondroitin sulphate disaccharide from the hyaluronic acid as the are isomers (Figure 2-7). Two methods were considered in more detail (Murata and Yokoyama 1987; Zebrower et al. 1991) as they separated hyaluronic acid from chondroitin sulphate, and quantified more of the chondroitin sulphate disaccharides than other methods (Imanari et al. 1996). Of these two methods the Zebrower et al (1991) method results better separated peaks, so this was selected as the method to implement. A minor issue is that the ΔDi-UA2S and ΔDi-6S disaccharides run at almost the some time; this is of limited importance as ΔDi-UA2S is typically much rarer than ΔDi-6S, and both are monosulphated chondroitin sulphate disaccharides.

5.1.3 Outline of experimental work

It was decided to modify the HPLC method used by Zebrower et al (1991) to determine GAGs in tissue engineering ligaments due to the availability of the appropriate equipment. This method has previously been to quantify glycosaminoglycans in chicken tendons (Hae Yoon et al. 2003), but no record exists of it being used for analysis of constructs produced by tissue engineering. There are two issues to resolve: first, the enzymatic digestion protocol used by Zebrower et al (1991) used 0.5U of chondroitinase ABC for 16 hours per sample. This is prohibitively expensive for analysing large numbers of samples. Second, the analysis needs to be coupled to a method for digesting the construct suitable for other quantitative analyses. The review of glycosaminoglycan analysis by HPLC carried out by Imanari et al. (1996) states that 0.05U of chondroitinase ABC for three hours is sufficient to digest 100μg of glycosaminoglycan. Therefore the first task will be to determine how different amounts of chondroitinase ABC affect the digestion of glycosaminoglycans separated with the Zebrower et al. (1991) method. The second task is to couple the glycosaminoglycan digestion to a method

for digesting tissue engineered constructs. Papain digestion is commonly used to digest constructs (Hoemann et al. 2002), so this chapter will attempt to couple papain digestion to HPLC analysis of glycosaminoglycans.

5.2 Materials and Methods

Methods for papain digestion are detailed in Section 4.3.5. Methods for HPLC analysis of glycosaminoglycans are detailed in Section 4.3.7.

5.3 Results

This section details the results found when establishing that the HPLC protocol could correctly separate disaccharides; that glycosaminoglycans could be digested into their constituent disaccharides, and that glycosaminoglycans could be extracted with papain without affecting the results.

5.3.1 Initial studies – to obtain reproducible separation of peaks

Initially, it was decided to digest chondroitin sulphate A and C to attempt to replicate the separation of the peaks published in Zebrower et al (1991). As the original paper used a quantity of enzyme that would have been prohibitively expensive, digestions were tested with much less enzyme, as complete digestion was possible with much less enzyme (Koshiishi et al. 1998). Figure 5-3 shows the results of digesting chondroitin sulphate A with 0.05U and 0.0005U of chondroitinase ABC for 16 hours. The identity of these peaks was based on their running order, this order was later confirmed by running disaccharide standards on the column (Figure 5-5). These results show that the largest peak is ΔDi-4S, the major component of chondroitin sulphate A. Some of the peaks appear to be different sizes, but this is complicated by the rising baseline. If the peaks are different sizes, it suggests that amount of enzyme affects the results of the digestion.

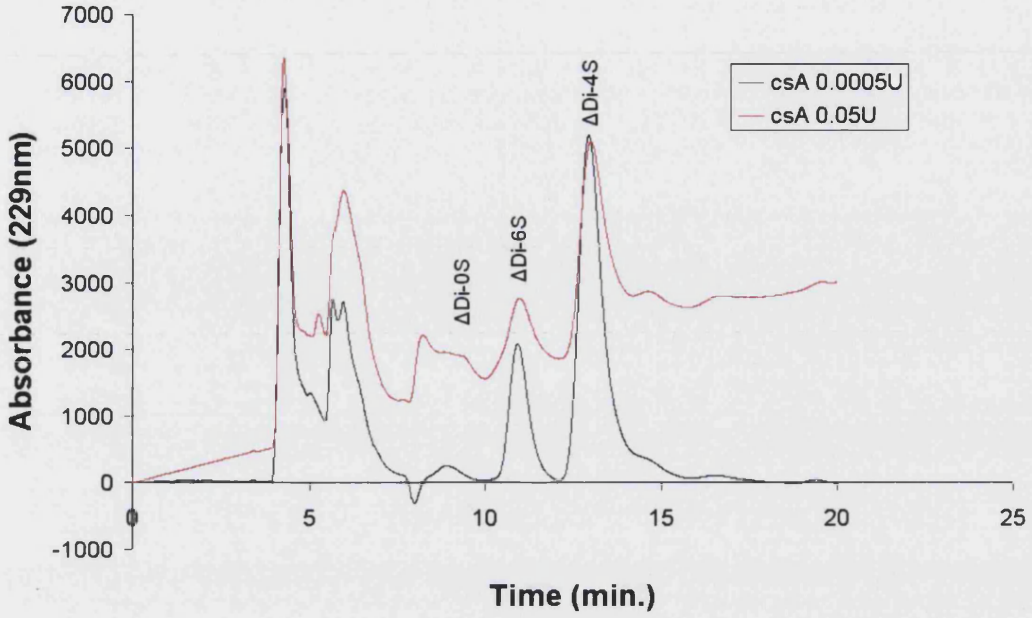

Figure 5-3 Chromatograms of chondroitin sulphate A digested with 0.05U and 0.0005U of chondroitinase ABC

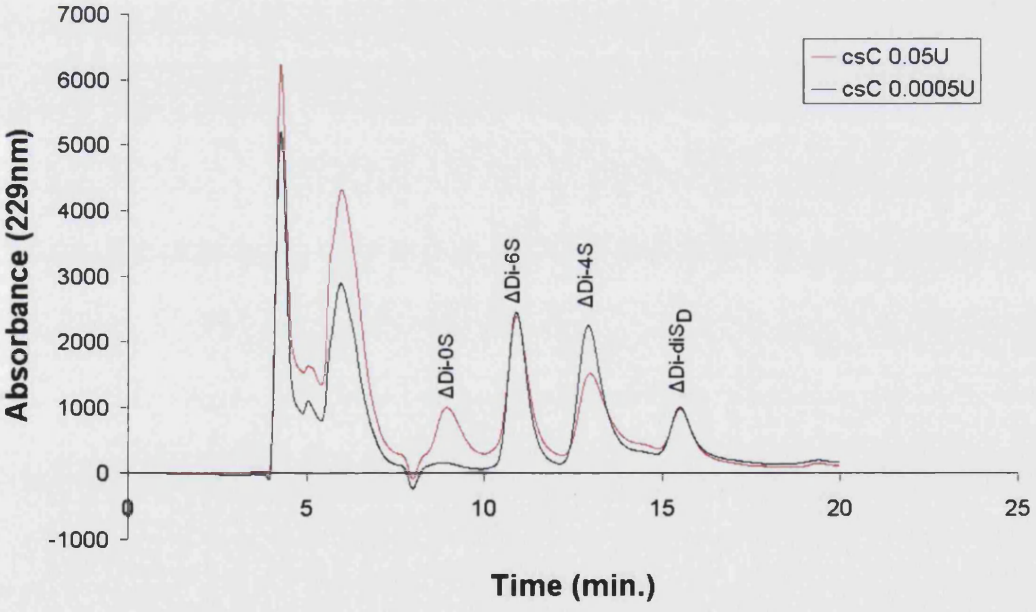

Figure 5-4 Chromatograms of chondroitin sulphate C digested with 0.05U and 0.0005U of chondroitinase ABC

The experiment was repeated with chondroitin sulphate C, digested for 16 hours with 0.05U and 0.005U of chondroitinase ABC (Figure 5-4). This time the largest peak is the ΔDi-6S, the principal component of chondroitin sulphate C. Again the peaks appear to be different sizes with different quantities of enzyme. In this case it appears to be a shift from ΔDi-4S to ΔDi-0S with the change from 0.005U to 0.05U. This suggests that amount of enzyme affects the results of the digestion.

Finally, a set of commercial standards was run to confirm that the retention times of the disaccharides were repeatable (Figure 5-5). This showed that the retention times were very similar; the small differences are probably attributable to subtle differences between the runs (e.g. room temperature, variations between batches of mobile phase).

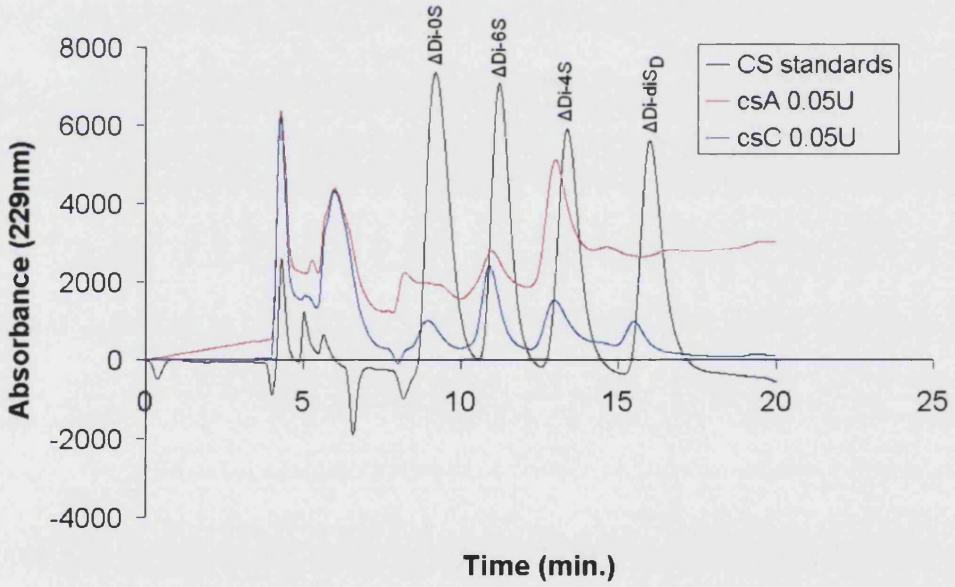

Figure 5-5 CS disaccharide standards compared to chondroitin sulphate A and chondroitin sulphate C runs

5.3.2 Optimisation of digestion protocol

As the first runs showed that changing the concentration of enzyme affected the size of the peaks, it was decided to investigate this phenomenon further. For these experiments 0.025U of enzyme were used with 40μg of glycosaminoglycan. The digestion buffer was varied between the 250μM

Tris-HCl (pH 8.0) used by Zebrower et al. (1991) and the 100μM Tris-acetate (pH8.0) used by Koshiishi et al (1998).

The results of digesting chondroitin sulphate C for 0.5, 1, 2, 4, and 16 hours in Tris-acetate buffer showed that there were strong peaks after 0.5 hours digestion (Figure 5-6a). These peaks strangely disappeared after 1 and 2 hour digestions (Figures 5.6b & c), only to reappear after 4 hours and remain at 16 hours (Figures 5.6d & e). The 0.5 hour peaks were the largest peaks.

A similar pattern occurs when digesting chondroitin sulphate C in Tris-HCl buffer. The peaks are present at 0.5 hours (Figure 5-7a), then disappear at 1 hour and 2 hours (Figures 5-7b & c). The peaks reappear after 4 hours diggestion (Figure 5-7d), and remain at 16 hours digestion (Figure 5-7e). The largest peaks occur at 0.5 hours, although the falling baseline caused difficulty in estimating the size of the peaks at 16 hours

The pattern changes subtely when hyaluronic acid is digested in Tris-acetate buffer. The peak for the appears after 0.5 hours digestion (Figure 5-8a), the peaks disappear at 1 and 2 hours digestion (Figure 5-8b), and remerge after 4 hours digestion. The peak remains at 16 hours (Figure 5-8c), although interference from the baseline (Figure 5-9) makes it difficult to determine the peak's exact area. Peaks from the digestion of chondroitin sulphate appear with the hyaluronic acid peaks (Figure 5-8).

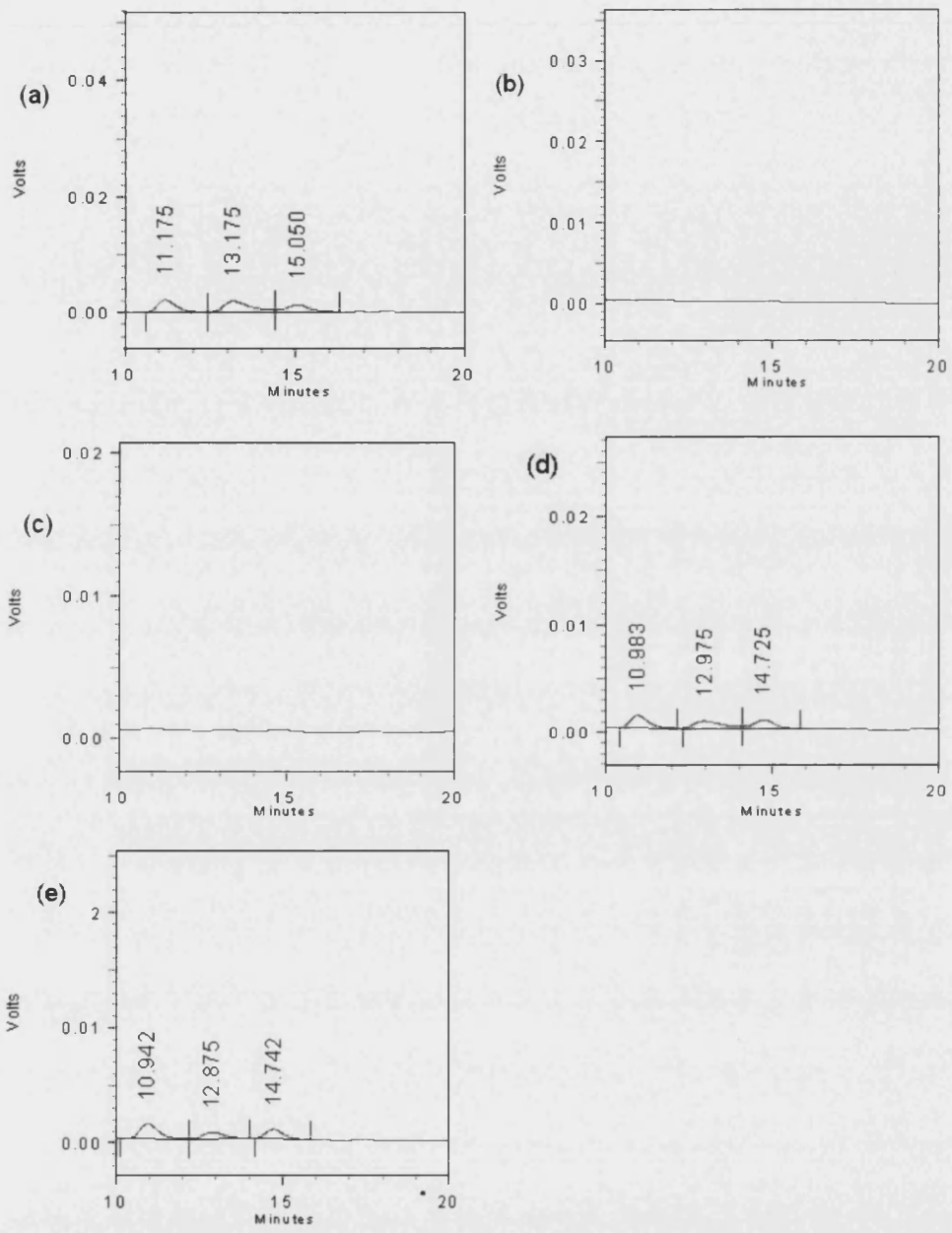

Figure 5-6 Chondroitin sulphate C digested in Tris-acetate buffer for: (a) 0.5 hours, (b) 1 hour, (c) 2 hours, (d) 4 hours, and (e) 16 hours.

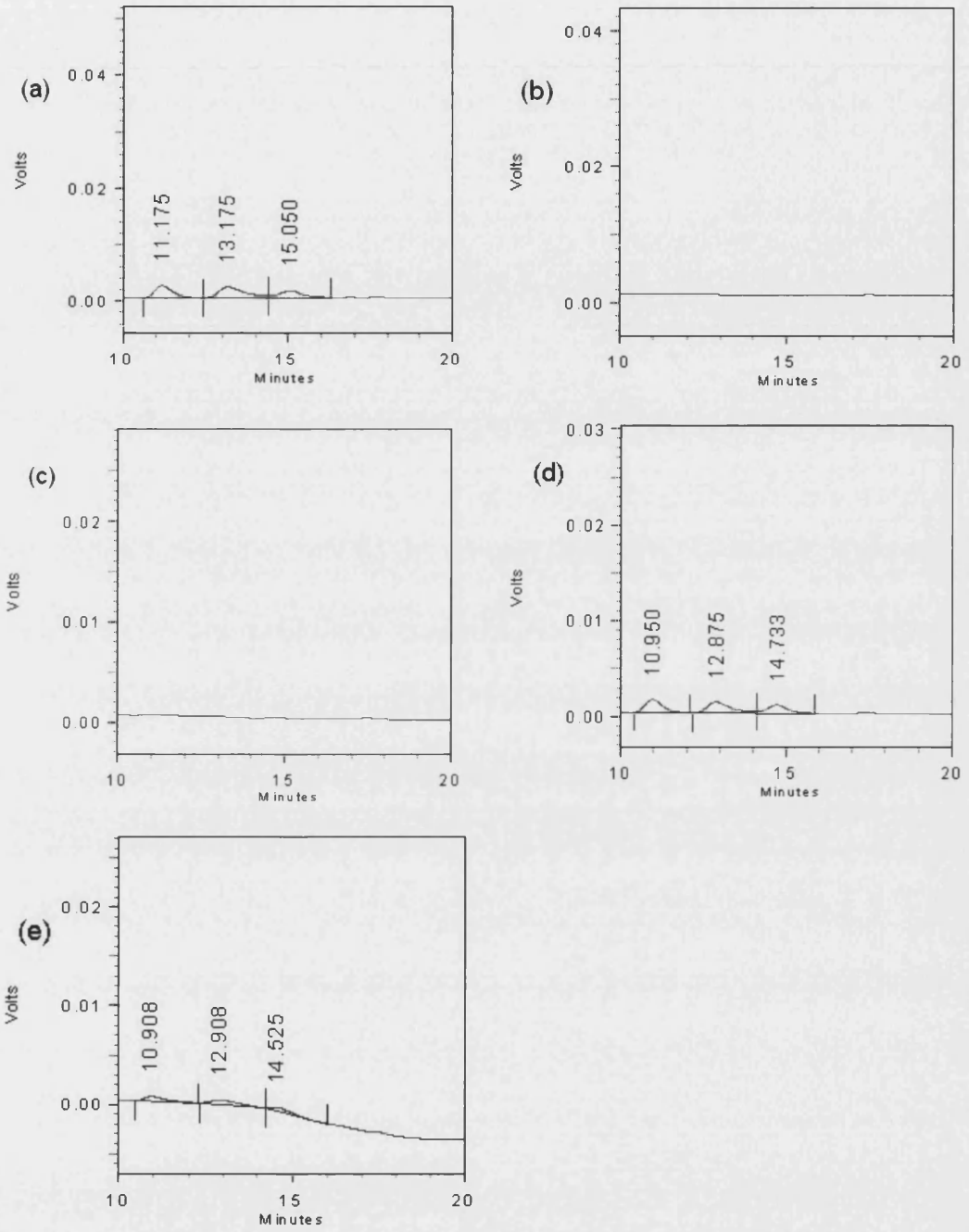

Figure 5-7 Chondroitin sulphate C digested in Tris-HCl buffer for: (a) 0.5 hours, (b) 1 hour, (c) 2 hours, (d) 4 hours, and (e) 16 hours.

Finally, the results from digesting hyaluronic acid in Tris-HCl buffer are slightly different to the previous results, prior to four hours digestion there are

no peaks from the digestion of hyaluronic acid, the only peaks present are chondroitin sulphate peaks at 0.5 hours (Figure 5-10a). After 4 hours digestion the only peak present is the peak from the digestion of hyaluronic acid (Figure 5-10c). This peak remains after 16 hours digestion and has a higher area (Figure 5-10d).

Correlating the results from digesting with Tris-actetate and Tris HCl reveals that the two digestions give similar, but not identical results (Figure 5-11).

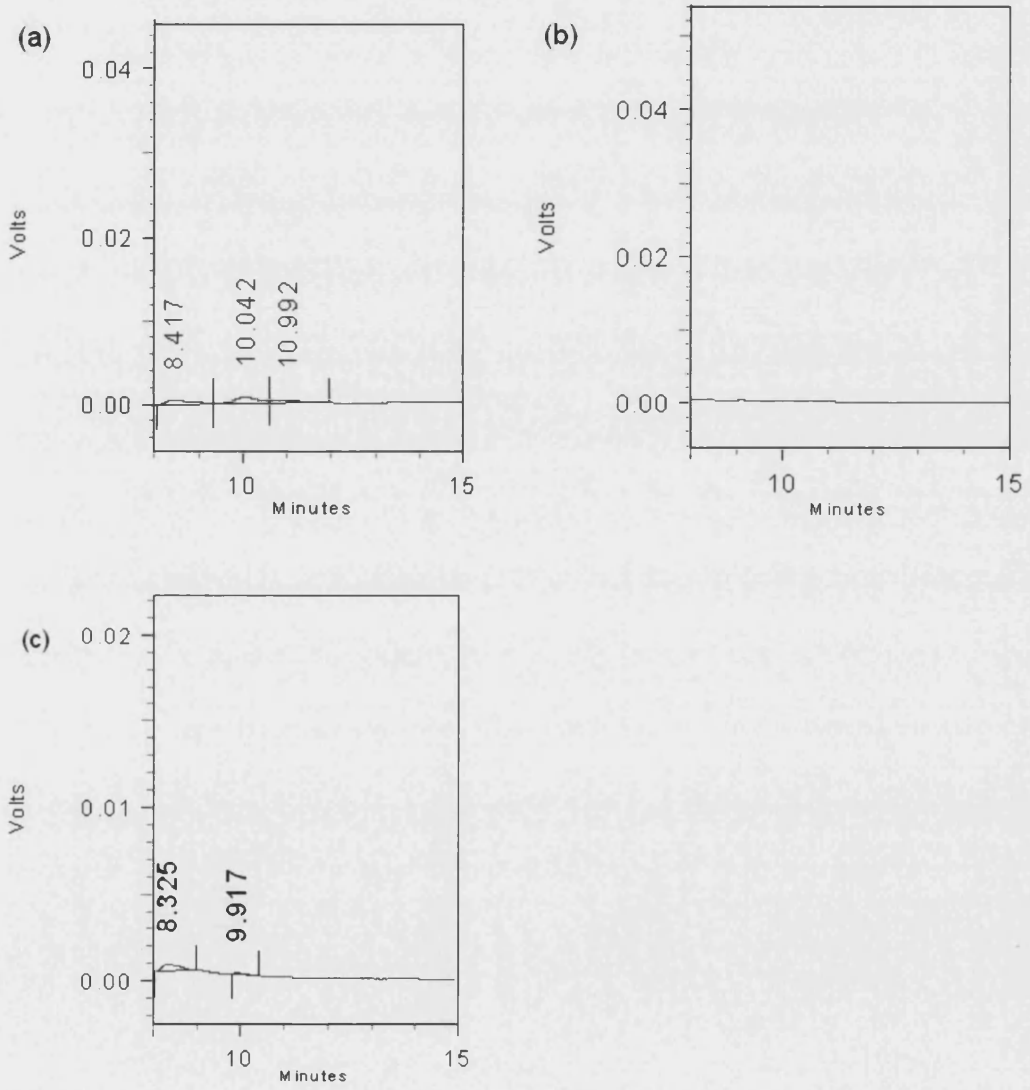

Figure 5-8 Digestion of hyaluronic acid in Tris-acetate buffer for (a) 0.5 hours, (b) 2 hours, and (c) 16 hours

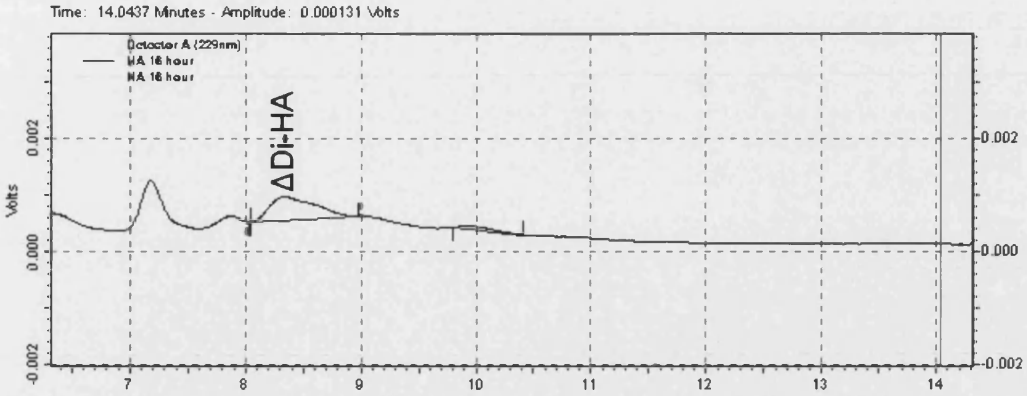

Figure 5-9 Detailed view of the ΔDi-HA peak produced by digesting hyaluronic acid in Tris-acetate buffer for 16 hours.

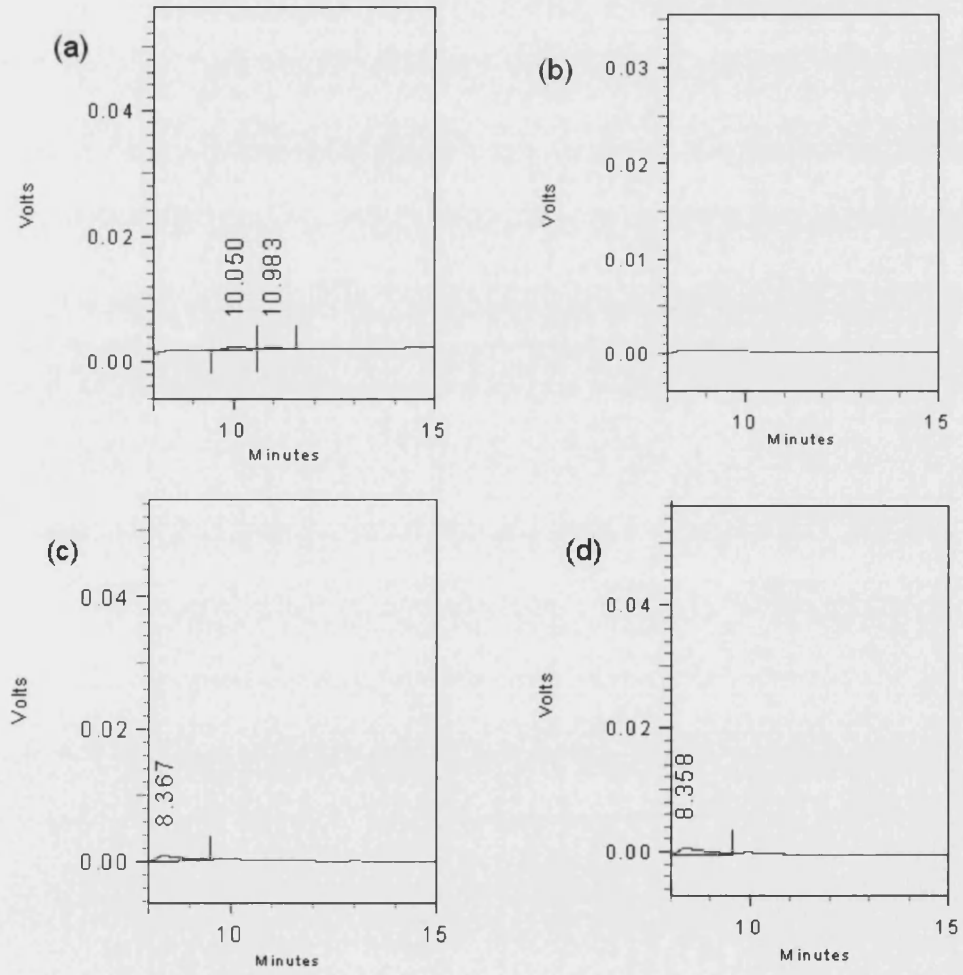

Figure 5-10 Digestion of hyaluronic acid in Tris-HCl buffer for (a) 0.5 hours, (b) 2 hours, (c) 4 hours, and (d) 16 hours

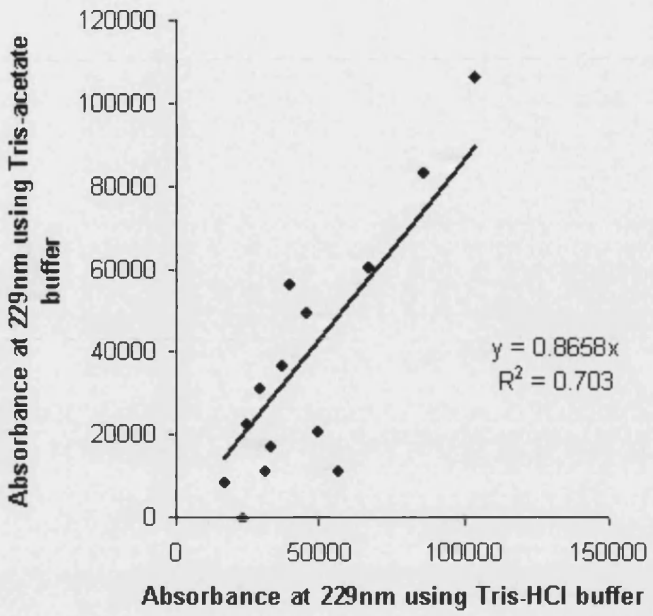

Figure 5-11 Comparison of the absorbance following digestion of hyaluronic acid and chondroitin sulphate for 0.5, 1, 2, 4 and 16 hours using Tris-acetate or Tris-HCl buffer

5.3.3 HPLC following papain digestion

The last question to be answered was whether digesting samples with papain would affect the analysis. To do this, blank papain digestions were run (i.e. papain digestion without a substrate) and then treated as a sample and digested with 0.025U of chondroitinase ABC in Tris-HCl buffer for 16 hours. The results showed that papain resulted in noise following the longer solvent front that would overlap with the disaccharides (Figure 5-12).

The solution to this problem was to run the disaccharide standards dissolved in the solution resulting from a blank papain digestion to create a set of standards that took account of the way that papain would elevate the reading for several of the disaccharides. Standards of ΔDi-HA, ΔDi-0S, ΔDi-6S, ΔDi-4S, ΔDi-diSD, ΔDi-diSB, ΔDi-diSE, and ΔDi-triS were made at concentrations of 1, 2, 4, and 8ng/µl by adding them to blank papain digestions processed with chondroitinase ABC. This approach resulted in high R^2 values for the standards, with all but one standard having R^2 values over 0.98, and the one exception being above 0.95 (Table 5-1 and Figure 5-13). The ΔDi-triS peak was not detected at the 1 and 2ng/µl levels.

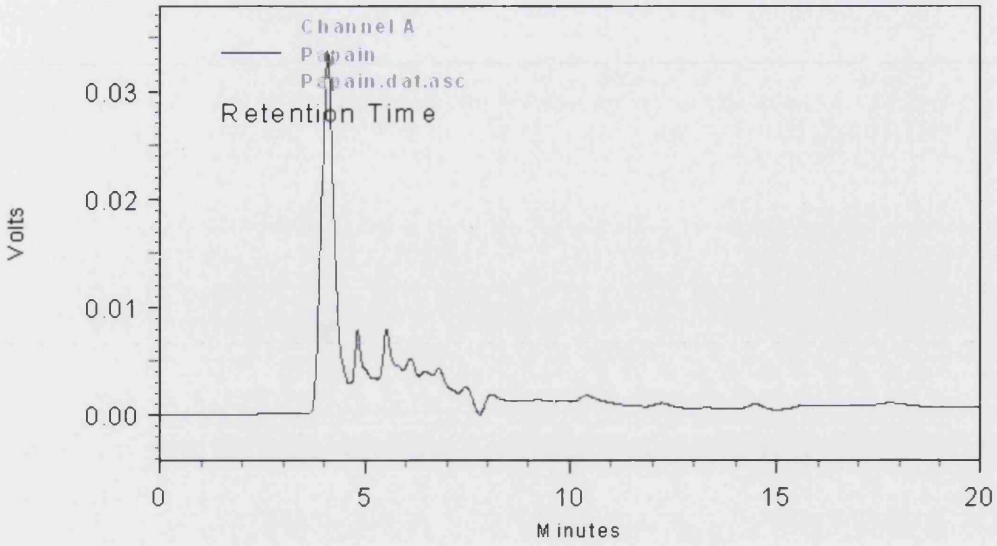

Figure 5-12 Sample chromatogram of blank papain digestion

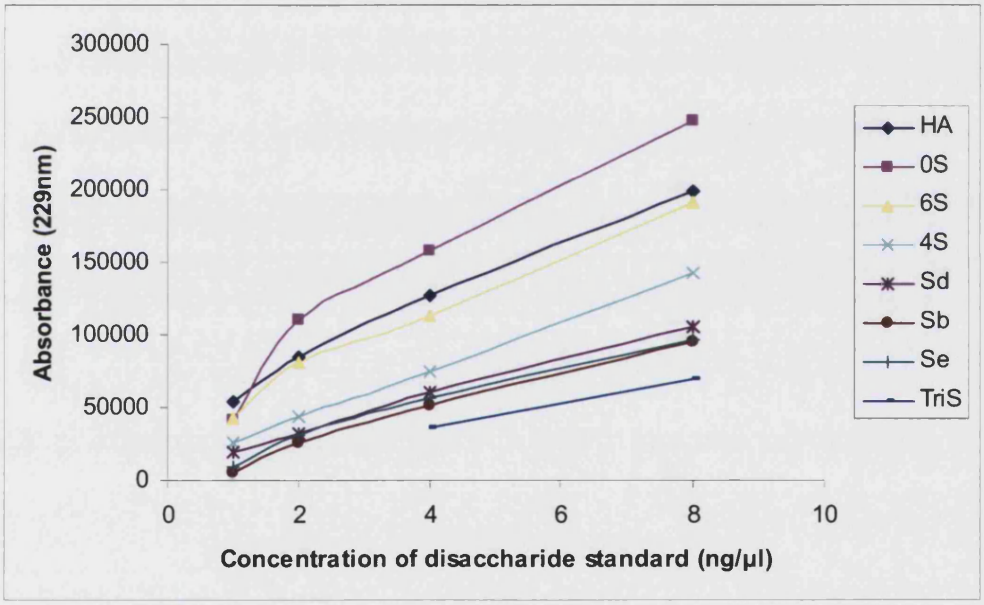

Figure 5-13 Relationship between concentration of disaccharide standards and absorbance at 229nm as measured by the area under the peak for each standard

Disaccharide	R^2
ΔDi-HA	0.991
ΔDi-0S	0.953
ΔDi-6S	0.986
ΔDi-4S	1
ΔDi-diS_D	0.997
ΔDi-diS_B	0.989
ΔDi-diS_E	0.982

Table 5-1 Correlation coefficients for disaccharide standards

5.4 Discussion

5.4.1 Sensitivity and repeatability

These results show that it is possible to modify the separation procedure used by Zebrower et al. (1991) to allow quantification of glycosaminoglycan disaccharides as an outcome measure for tissue engineering. Using a more up-to-date chromatography system appears to increase the sensitivity of the technique to the point where as little as 20ng of disaccharide can be detected on each injection (or 80ng for ΔDi-triS). This is almost an order of magnitude more sensitive than achieved by Zebrower et al. (1991). The retention times appear consistent from run to run, although they fluctuate slightly with temperature, and change slightly when the mobile phase is changed.

The main problems appear to be associated with the digestion protocol. Changing the concentration of enzyme changes the area of the disaccharide peaks. More surprisingly, the digestion time has a strange effect on the size of the peaks. Peaks are detectable after 0.5 hour digestions, but not 1 or 2 hours digestion under the same conditions. Then the peaks reappear after 4 hours digestion and remain after 16 hours digestion.

5.4.2 Issues with chondroitinase digestion

There is a possible explanation for the changes in the relative sizes of the peaks. The bacterium, *Proteus vulgaris,* which produces chondroitinase ABC also produces chondrosulphatases (Dodgson and Lloyd 1957). These are enzymes that remove the sulphate groups from chondroitin sulphate. If the chondroitinase ABC was contaminated by some residual chondrosulphatases then this would explain why there was a shift from the sulphated disaccharides to the non-sulphated disaccharides with more enzyme. More enzyme would result in more contaminating chondrosulphatases, resulting in the removal of more sulphate groups from the chondroitin sulphate disaccharides.

Another result that needs to be understood is the difference between the digestion of hyaluronic acid and the digestion of chondroitin sulphate. According to the literature, hyaluronic acid is degraded much slower than chondroitin sulphate (Yamagata et al. 1968). Unfortunately, there is little consensus as to the correct protocol for complete hyaluronic acid digestion: Yamagata et al (1968) reports complete digestion of hyaluronic acid after 5 hours digestion of 20µg with 0.008U of enzyme for two hours, followed by the addition of 0.15U for the last three hours (although the change of the slope of the curve suggests that the digestion was complete long before the three hours ended).Yamagata et al (1968) found that the initial rate of reaction for hyaluronic acid is 2% of that for chondroitin sulphate A or C. Koshiishi et al (1998) found complete digestion of 2 µg hyaluronic acid with 0.025U of enzyme in one hour. Imanari et al (1996), in their review of HPLC procedures for quantifying glycosaminoglycans, suggest that for up to 100µg of glycosaminoglycan 0.05U of chondroitinase ABC for three hours is sufficient.

The chondroitin sulphate peaks occurring in the hyaluronic acid digestion are presumably due to chondroitin sulphate being a contaminant of the commercial hyaluronic acid used.

The more disconcerting problem is that of the disappearance of the peaks at one and two hours. All the samples were prepared at the same time, using the same reagents so differences between reagents on the other runs are not a possible explanation. The most likely explanation is that another enzyme is contaminating the digestion. The most likely explanation is that it contains a β-glucuronidase, which is capable of digesting the disaccharides further. Such enzymes are known to be produced by other chondroitinase producing bacteria, such as *Aeromonas sp. 83* (Kitamikado and Lee 1975), and *Flavobacterium heparinum* (Suzuki et al. 1968), although this has not been reported for *Proteus vulgaris*. The strange disappearance and reappearance of the peaks might be explained if the β-glucuronidase was affected by product inhibition.

5.4.3 Papain digestion

The problem of the papain digestion adding noise to the HPLC analysis appears to be soluble by running the standards on top of a blank papain digestion. This approach might reduce the sensitivity of the assay, but this approach, combined with more modern chromatography equipment still results in a technique that is roughly an order of magnitude more sensitive to most disaccharides than the published technique of Zebrower et al. (1991).

5.4.4 Current solutions

The major problem appears to be the presence of contaminating enzymes. This appears to vary from batch to batch of the enzyme, the first batch of enzyme used behaved as if it were contaminated by a chondrosulphatase; the second batch behaved as if contaminated by a β-glucuronidase. As the influence of the putative β-glucuronidase appears to be limited at 16 hours with 0.025U of chondroitinase ABC with tris-HCl buffer, these digestion conditions will be used. As the samples will all undergo the same treatment by the same batch of enzyme, it should be possible to compare them. To control for the effects of chondrosulphatases, the data for the chondroitin sulphate disaccharides will be pooled. The principal downside to this

approach is a loss of sensitivity, which can be mitigated by using large sample sizes.

5.4.5 Possible future solutions

In order to get as much sensitivity as possible, the problems with the enzymes would be better by preventing these unwanted digestions. Two options are possible: the first is that enzymes could be inhibited by specific inhibitors, for instance chondrosulphatase activity can be inhibited with sodium fluoride without affecting the activity of chondroitinase ABC (Dodgson and Lloyd 1957). The other options would be to compare chondroitinases from different suppliers to identify one with minimal contamination, or to further purify the enzyme before use.

Once these problems have been solved, another problem is identifying the best protocol to isolate the glycosaminoglycans from the scaffold. Papain was chosen for this work as it is widely used, but perhaps other enzymes would work better in conjunction with this HPLC assay and not produce the peaks associated with blank papain digests. An alternative might be to use chaotropic agents to recover the ECM components, guanidine hydrochloride followed by guanidine thiocyanate had been tried with engineered cartilage, but it was necessary to use papain subsequently to digest all the glycosaminoglycans (Hoemann et al. 2002).

Finally, it might be possible to achieve greater sensitivity by using fluorescent probes if the equipment were available. This might also reduce the noise from the papain digest as fluorophores have been identified that respond with a much stronger emission in the presence of disaccharides than potential contaminants (Imanari et al. 1996).

5.5 Conclusions

In conclusion, it is possible to replicate the separation achieved by Zebrower et al (1991). With a more modern chromatography system this technique is

roughly an order of magnitude more sensitive, in spite of the need to run the standards on top of a blank papain digestion. The sensitivity is limited by the unwanted side effects of the enzymatic digestion. For this project, these side effects will be mitigated by using a large sample size, and pooling the chondroitin sulphate disaccharide results. In the future, it might be possible to eliminate these side effects by inhibiting them, or by identifying a better source of chondroitinase.

6 Control of Pore Structure from film-like to fibrous in Porous Silk Scaffolds

6.1 Introduction

6.1.1 Silk fibroin as a biomaterial for tissue engineering

Porous silk fibroin (SF) scaffolds are promising biomaterials for tissue engineering. Recent work has shown that they are a promising material for growing cartilage *in vitro* (Wang et al. 2005b), and bone *in vitro* and *in vivo* (Kim et al. 2005a; Meinel et al. 2006). One of the major advantages of silk over other biomaterials is that a lot more is understood about how the body reacts to silk due to the extensive use of silk sutures, allergy to silk is normally a response to sericin (Kurosaki et al. 1999), a protein that can be easily removed by thorough degumming (Altman et al. 2003). Allergy to the major remaining proteins is rare, but not unknown (this might be caused by sensitisation to sericin) (Kurosaki et al. 1999). The evidence from silk sutures is that silk causes a mild inflammation response, although suture structure might be playing a role (Altman et al. 2003). When implantation of SF films was compared to implantation of collagen and poly-lactic acid films, the SF films caused a milder inflammatory reaction than the other films (Meinel et al. 2005). As SF is a protein it will be broken down into peptides, which will be less problematic than the acids released by the hydrolysis of poly-lactic and poly-glycolic acids. Silk fibroin is also a very thermally stable protein, intramolecular and intermolecular hydrogen bonds are broken between 150 and 180°C, then the silk filament begins to gradually lose weight at 175 °C (Nakamura et al. 1994). These properties allow silk to be safely autoclaved.

6.1.2 Effects of pore size on tissue engineering

Three of the important variables in controlling the behaviour of cells grown upon scaffolds are pore size, pore structure, and porosity. When regenerating musculoskeletal tissue there appears to be a range of pore

sizes that are ideal for encouraging good tissue formation, although it is not clear whether differences in the optimal pore size range found in different experiments reflect differences in the behaviour of different types of connective tissue cell, differences between biomaterials or different experimental set ups. This section will focus on the effect of pore size in bone and cartilage engineering; the role of pore size in connective tissue engineering will be discussed further in Chapter 7.

When regenerating bone *in vivo* there is a recommendation for the pores to be at least 300μm to allow good vascularisation, below this pore size the new tissue becomes more fibrous (Hulbert et al. 1970; Karageorgiou and Kaplan 2005) (although pore size does not appear to be an important variable under non-load bearing conditions (Itala et al. 2001)). The effects of pore size on articular cartilage growth are less clear. Traditionally, it has been thought that small pores (~20μm) to limit nutrient supply and/or promote cell-cell contact were advantageous (Woodfield et al. 2005). Recently, positive results have been achieved by both: dynamic pore reduction, in which large pores (to promote cell seeding) are contracted by the cells to form small pores to encourage chondrogenesis, resulted in elevated levels of collagen II and a more chondrocytic morphology of the cells (Vickers et al. 2006). In contrast a very different scaffold with a gradient of pores designed to mimic the superficial, middle, and lower zones was given very large pores in the medial and deep zones, intended limit cell-cell contact and cell-matrix ratio, showed increased collagen II accumulation compared to superficial zone with smaller pore sizes (200μm) and cellular organisation reminiscent of the zones of immature cartilage (Woodfield et al. 2005).

6.1.3 Effects of porosity and pore structure on tissue engineering

Porosity has primarily been of interest due to its potential to control mass transfer of nutrients to cells. Higher porosity generally results in better bone formation *in vivo* presumably due to better vascularisation (Karageorgiou and Kaplan 2005); although some *in vitro* studies show increased osteogenesis with lower porosity, and better cell proliferation with higher porosity

(Karageorgiou and Kaplan 2005). For cartilage engineering, a multivariate study found that pore structure can be a very important variable. It was found that scaffold structure (mesh vs. sponge) was a more important determinant of chondrogenesis *in vitro* than scaffold material (benzylated hyaluronan vs. polyglycolic acid) when comparing highly porous (>90%) biomaterials grown in either Petri dishes or rotating wall bioreactors (Pei et al. 2002). A more recent study has shown that, surprisingly, a pore structure with less well connected pores appeared to maintain higher chondrocyte viability when implanted into osteochondral defects (Emans et al. 2006). It is striking that there has been very little work comparing the effect of two or more scaffold fabrication variables on tissue engineering outcomes despite the importance of this work for our ability to rationally develop better biomaterials.

6.1.4 Porous silk scaffolds

There have been four main methods used to make porous silk scaffolds, these methods have recently been reviewed (Wang et al. 2006). The first of these is silk hydrogels; these are typically made by changing the chemical environment of the silk in solution, for instance, by changing pH, or evaporating water. Hydrogels have been used to promote the healing of critical sized cancellous bone defects (Fini et al. 2005) and for cartilage tissue engineering (Kim et al. 2004). One limitation of this approach is that only hydrogels with relatively small pores can be prepared.

The second approach is to make non-woven mats of microfibres or nanofibres (Min et al. 2004; Unger et al. 2004). Microfibres are made by spinning silk solutions into a coagulant bath (Um et al. 2004), whereas nanofibres are made by electrospinning, where a silk solution is forced out through a charged syringe needle, and attracted to a metal plate carrying the opposite charge to the needle (Min et al. 2004). Nanofibres are of great interest to tissue engineering for their unique properties such as their very high specific surface area. However, currently there is limited control of the pore size in non-woven mats, and the process results in noticeably anisotropic materials. The third approach is a development of the second

approach, this approach is to weave silk fibres into 3D structures (Horan et al. 2005b). These are intentionally anisotropic to take advantage of silk's mechanical properties, but this approach results in scaffolds with limited porosity.

The final approach is to use techniques such as freeze drying, gas foaming and salt leaching to make 3D porous scaffolds (Kim et al. 2005b; Nazarov et al. 2004). These are made by adding a porogen to a silk solution, then evaporating the solvent and removing the porogen; in the case of freeze drying the formation of ice crystals in the solvent acts as the porogen. These methods have the advantages of creating scaffolds with high porosity and the allowing control of the pore size, especially when salt is used due to the availability of salt with a large range of particle sizes. The first methods to make silk scaffolds with these techniques used organic acids to dissolve regenerated SF, this allowed scaffolds to be with small or large pores, but the interconnectivity between the pores was limited (Nazarov et al. 2004). More recently, scaffolds have been made using water as the solvent, this increased the interconnectivity, but it was only possible to make scaffolds with large pores (over 500μm) (Kim et al. 2005b). A porous silk scaffold that combined well connected pores with smaller pore sizes would be potentially very useful for tissue engineering.

6.1.5 Outline of experimental work

This chapter will report the invention of porous silk scaffolds that allow control of both pore size and pore structure. The minimal pore size of the fibrous scaffolds with well connected pores is roughly half that achieved by Kim et al (2005b). These scaffolds will be characterised by a combination of SEM, FTIR and light microscopy to determine porosity. Changes in the fabrication process will be made in order to better understand how these scaffolds are formed. Finally, a variety of musculoskeletal cell types will be cultured on the new scaffolds to determine the scaffold's effects on cell viability.

6.2 Materials and methods

Cell culture methods for this chapter are described in Section 4.2.1; regenerated silk fibroin preparation in 4.2.2; procedures to determine the solubility of silk in various solvents in 4.2.3; fabrication of silk scaffolds is described in Section 4.2.4; and decorating the scaffolds with RGD in Section 4.2.5. The analytical methods used to characterise the scaffold are: SEM (4.3.1), FTIR (4.3.2) and light microscopy (4.3.3). To quantify cell number after cell culture on the scaffolds, Picogreen (4.3.4) was used.

6.3 Results

6.3.1 Solubility of silk in aqueous organic acid solutions

The starting point for this work was the hypothesis that the failure to form porous silk scaffolds with pore sizes of less than 500μm was due a combination of the high solubility of salt in water, and the larger specific surface area of the smaller salt particles resulting in the rapid precipitation of SF when small salt particles were used. Therefore it was decided to try to limit the solubility of salt in silk by dissolving the silk in an aqueous organic acid. The organic acid initially chosen was formic acid as silk dissolves readily in this organic acid (Um et al. 2004). SF was soluble in all tested mixtures of formic acid and water at 5% w/v, but only dissolved at 10%w/v in 20% v/v formic acid; it did not dissolve completely at 15% w/v in any of the solvents tested (Table 6-1).

Subsequently, HFIP and acetic acid were tested as solvents. HFIP as it is also a known solvent for SF (Zhao et al. 2003), and acetic acid was chosen due to its chemical similarity to formic acid. When 10% w/v SF was placed into aqueous HFIP or acetic acid, the SF formed a white gel at 10% w/v in 20% v/v HFIP, and in 20% v/v acetic acid, but it did not form a solution at any concentration of acetic acid or HFIP (Table 6-1). These solvents were unsuitable for further use for fabricating porous silk scaffolds as the white gel was did not flow.

Table 6-1 Solubility of regenerated SF in formic acid, acetic acid and hexafluoroisopropanol

Organic Acid	% w/v of SF	% v/v Organic Acid			
		20%	40%	60%	80%
Formic Acid	5%	✓	✓	✓	✓
	10%	✓	x	x	x
	15%	x	x	x	x
Acetic Acid	10%	G	x	x	x
Hexafluoroisopropanol	10%	G	x	x	x

Key:

✓ - SF dissolves completely

x - SF does not dissolve completely

G - SF forms a gel

6.3.2 Preparation of silk fibroin scaffolds with aqueous formic acid

The next step was to test whether it was possible to make scaffolds using 10% w/v SF dissolved in 20% v/v formic acid; these first scaffolds were made by pouring the silk solution into the mould, followed by salt. At first inspection by eye, this method appeared to make porous silk scaffolds. The top surfaces of these scaffolds were noticeably smoother than scaffolds made with 100% FA, almost appearing to be a single film, and contained a small dimple where the solution was pipetted in (cf. Figures 6-1a & b).

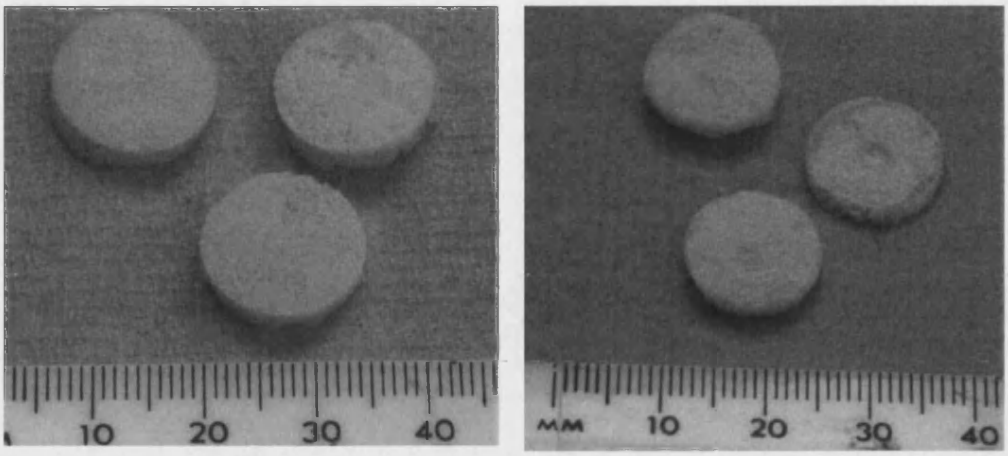

(a) (b)

Figure 6-1 Comparison of whole scaffolds: (a) Scaffolds made by salt leaching with 100% FA, and (b) Scaffolds made by salt leaching with 20% v/v FA. MeOH was used as a coagulant for all these scaffolds.

To understand how the solvent affected the pore structure, these scaffolds were examined further with SEM. Two types of scaffold were compared by using either 20% v/v FA or 100% FA as the solvent, both were made with 10% w/v silk. The scaffolds made with 100% formic acid had pores with a predominately film-like character (Figures 6-2a &b); whilst the scaffolds made with 20% FA had a more fibrous character (Figures 6-2c & d), with pores that were noticeably better connected than the scaffolds made with 100% FA.

The limitation of these new scaffolds was a marked heterogeneity between pores between different scaffolds upon visual inspection of SEM images. The difference between Figures 6-2c and d shows the difference between pores in two scaffolds made with 20% FA at the same time and with the same process.

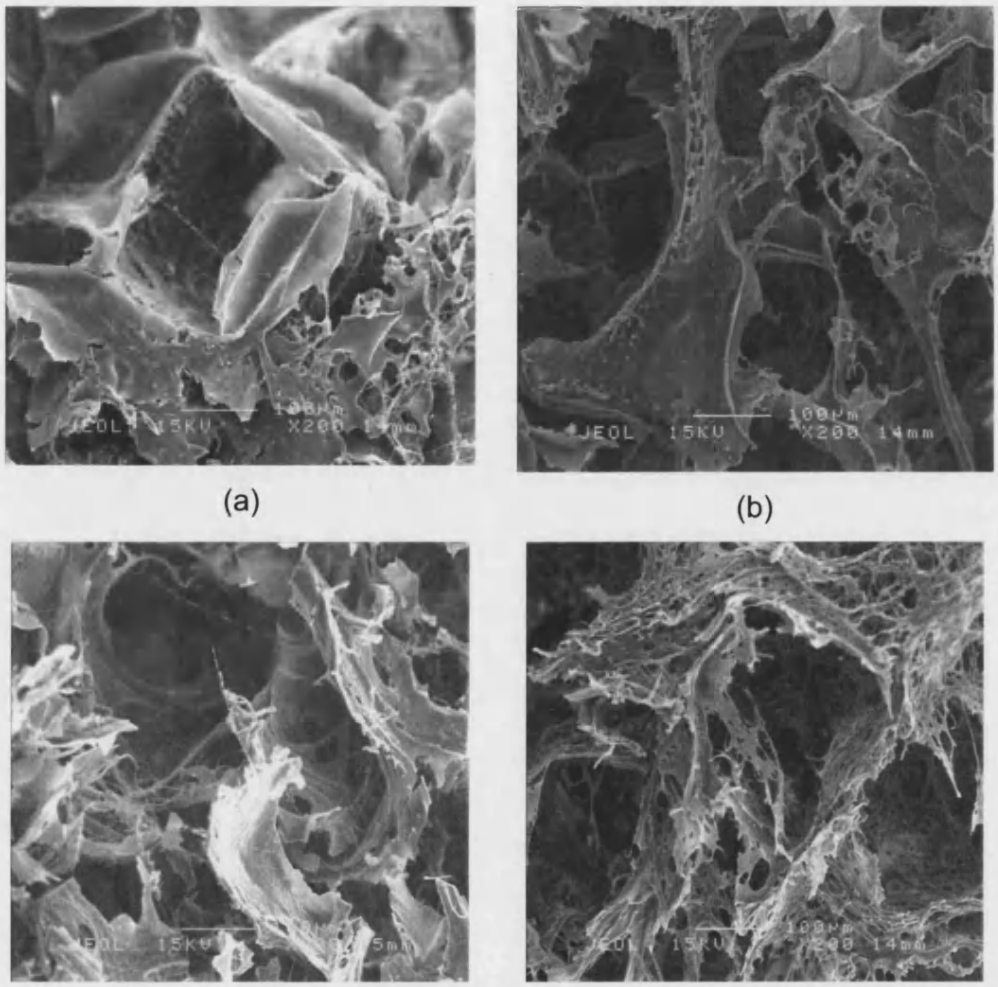

Figure 6-2 Pore structure of two scaffolds made using the initial process: (a) & (b) made with 100% formic acid, and (c) & (d) made with 20% v/v formic acid. Scale bars = 100µm.

To try and eliminate this heterogeneity a number of different variations on the original method (Method A) were tried, these methods are described in detail in Section 4.2.4:

- salt was put in the mould after the silk (Method B);
- the weight of salt was increased, keeping the ratio of silk : salt the same (Method C);
- the percentage of silk in the solvent was varied to 5% (Method D) and 7.5% (Method E) as well as 10%;
- a PTFE lid was placed onto some of the scaffolds (Method F).

Only one of these variations failed to produce scaffolds for SEM: Method D (5% w/v SF) resulted in very friable scaffolds that largely disintegrated during salt leaching. The other scaffolds were compared with SEM, and it was found that adding salt to the mould before silk was put in (Method B) resulted in a more homogenous pore structure. This result was clarified by the deeper scaffolds made with a greater amount salt (Method C), which showed these scaffolds were more film-like towards the top surface, and more fibrous towards the bottom surface (Figure 6-3), suggesting that there was more SF towards the top of the scaffold. Decreasing the percentage of silk to 7.5% w/v (Method E) had the interesting effect of making the scaffold more fibrous (Figure 6-4a), whereas using a Teflon lid made the scaffold more film like (Figure 6-4b). It was decided to investigate the contrast between scaffolds made with 7.5% w/v and 10% w/v SF further.

To confirm that scaffolds could be made with small pore sizes with 20% FA as the solvent and either 7.5% and 10% w/v silk dissolved in it. Salt was sifted to give salt particles of between 125 and 250μm. Scaffolds were successfully made with these small particles and both 7.5% w/v and 10% w/v SF dissolved in aqueous formic acid (Figures 6-5a & b).

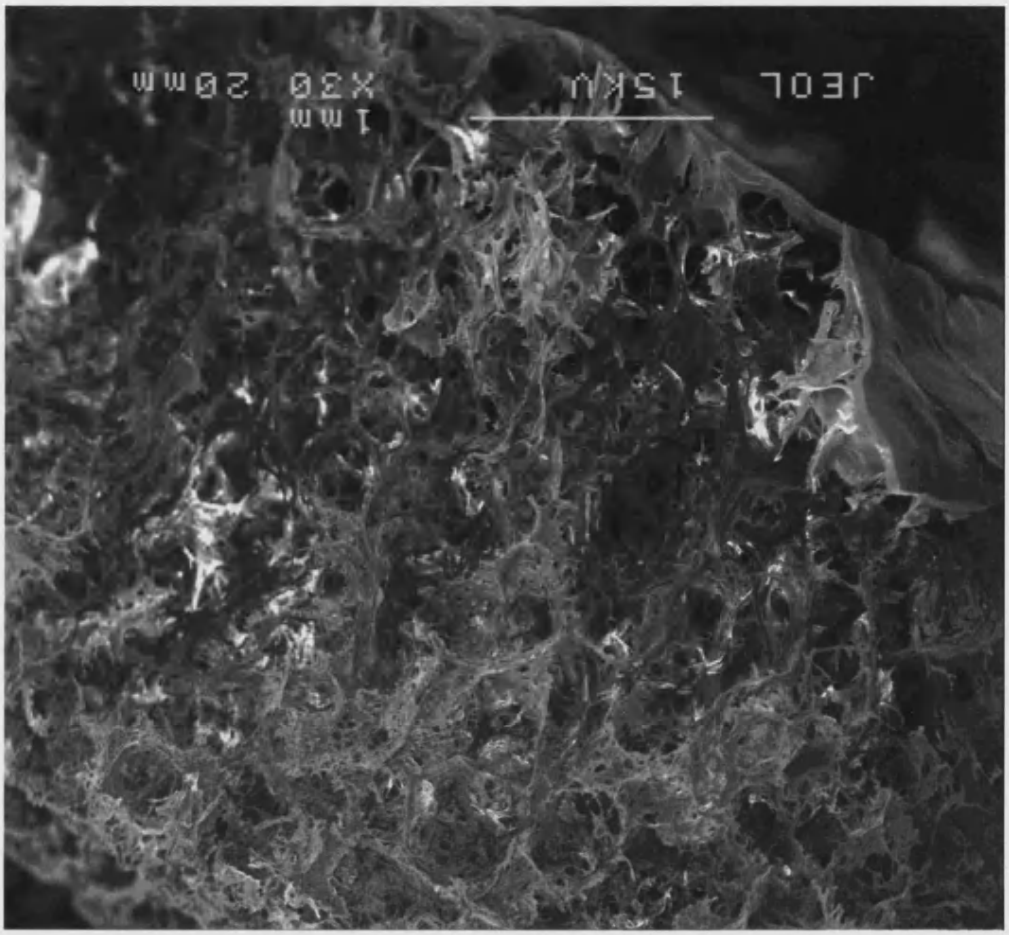

Figure 6-3 Scaffold made with 10%w/v silk dissolved in 20% v/v formic acid added to 1g salt (Method C); film at top of picture is the top surface of the scaffold (scale bar = 1mm)

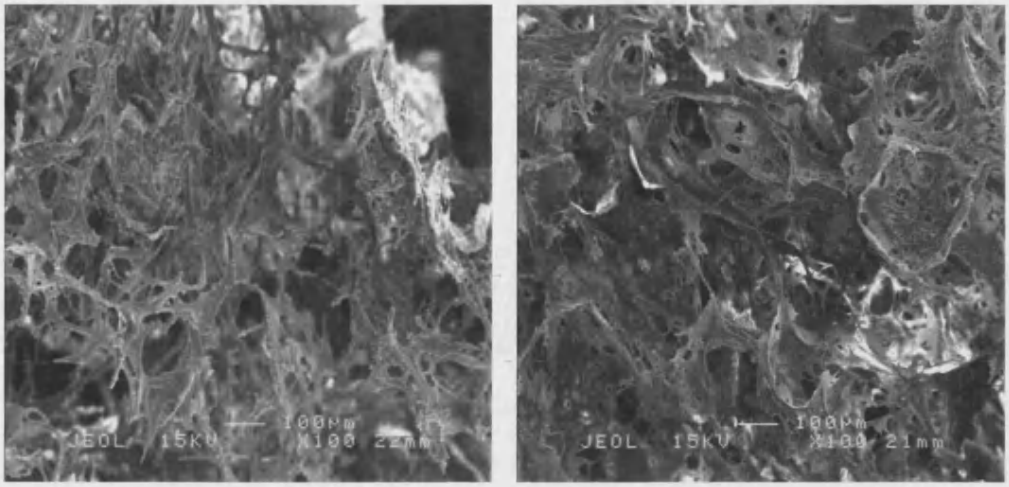

(a) (b)

Figure 6-4 (a) scaffold made with 7.5% w/v silk dissolved in 20% v/v formic acid pipetted onto 0.6g salt (Method E); and (b) scaffold made with 0.6g of salt added to 10% w/v silk dissolved in 20% v/v formic acid and covered with a Teflon cap (Method F). (Scale bars = 100µm)

6.3.3 Scaffolds made with aqueous formic acid saturated with salt

To better understand the effect that salt has on the formation of these scaffolds, scaffold formation with saturated salt solutions was studied. First, the solubility of SF in aqueous formic solutions was determined by dissolving 10% w/v silk in 10-90% aqueous formic solutions. Silk dissolved fully in 40%, 80%, and 90% FA solutions saturated with salt (Table 6-2). The 40% solution required brief mixing with a vortex mixer to dissolve it completely.

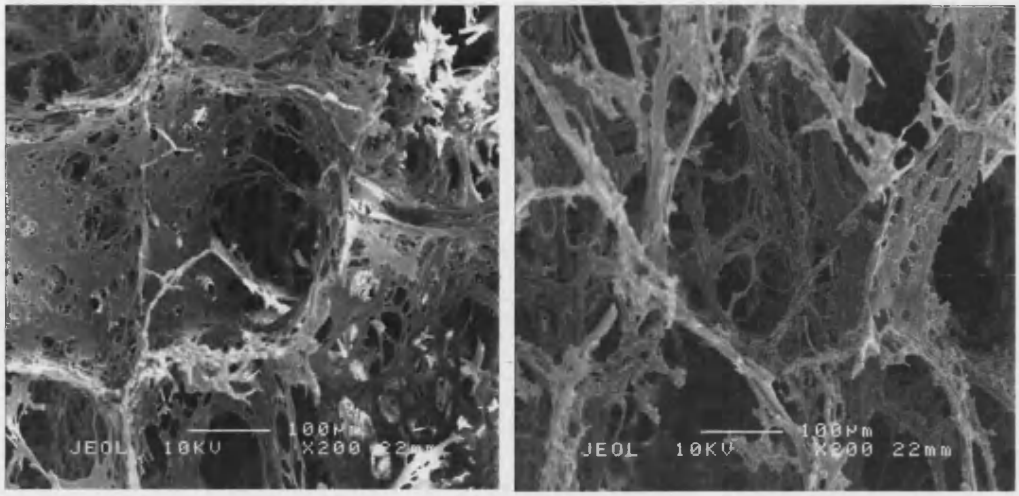

(a) (b)

Figure 6-5 Pore structure of a scaffold made with: (a) 10% w/v silk dissolved in 20% v/v formic acid added salt with particles of 125-250µm, and (b) 7.5% w/v silk dissolved in 20% v/v formic acid added to salt with particles of 125-250µm (x200). Scale bars = 100µm

The 40% and 80% FA solutions saturated with salt were investigated further to see how they would influence pore structure. The scaffolds made with 40% FA saturated with salt appeared to consist of interconnected sheets of SF, towards the ends of the sheets there were fibrous SF structures (Figure 6-6a). In contrast to the 100% FA scaffolds (Figures 6-2a & b), where it appears that entire salt particles were coated with SF, with 40% FA saturated with salt it appears that many of the surfaces of the salt particles do not result in SF sheets, resulting in a much more interconnected scaffold structure (Figure 6-6a). The scaffolds made with 80% FA saturated with salt (Figure 6-6b) appear much more similar to those made with 100% FA (Figures 6-2a &b) than those made with 40% FA saturated with salt (Figure 6-6a).

Table 6-2 Solubility of silk in aqueous formic acid solutions saturated with salt

% Formic Acid	10	20	30	40	50	60	70	80	90
Dissolves 10% w/v silk?	x	x	x	✓*	x	x	x	✓	✓

(* - required brief vortexing to dissolve the silk)

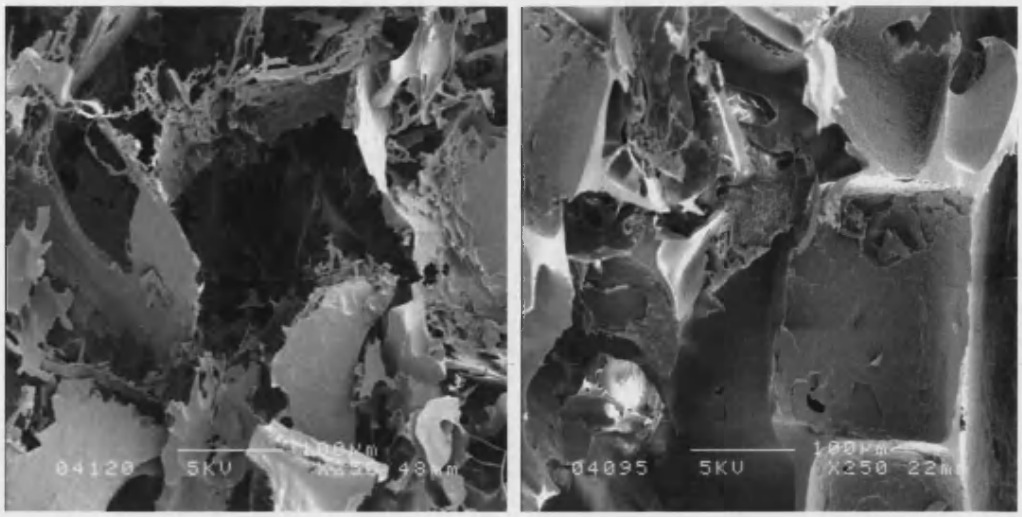

(a) (b)

Figure 6-6 SEM of pore structure of silk scaffolds made with aqueous formic acid solutions saturated with salt: (a) 40% v/v formic acid and (b) 80% v/v formic acid. Both at x 250.

6.3.4 Fourier transform infrared spectra of silk scaffolds

SF exists in at least three crystalline forms: silk II is the form of natural silk fibres; silk I and random coil silk can be produced by chemical processing of these fibres. The process of regenerating SF changes its crystalline structure from silk II to random coil. Fourier transform infrared spectroscopy (FTIR) is commonly used to determine whether silk is in its silk II form or not. The position of the peaks of the amide I (C=O stretching), II (secondary NH bending), and III (C-N stretching) vibrational bands is determined by presence or absence of hydrogen bonding therefore whether or not the silk is in silk II form (Ha et al. 2005). Peaks at 1630cm^{-1} (amide I), 1520cm-1 (amide II) and 1270cm^{-1} (amide II) correspond to the silk II form; peaks at 1650cm^{-1} (amide I), 1540cm^{-1} (amide II) and 1230cm^{-1} (amide II) correspond to the silk I or random coils forms (Asakura et al. 1985). The FTIR spectra were compared for silk scaffolds treated with methanol prior to salt leaching with scaffolds left untreated prior to salt leaching. The results obtained were

almost identical for all scaffolds and show that the silk was in the silk II form (Figure 6-7).

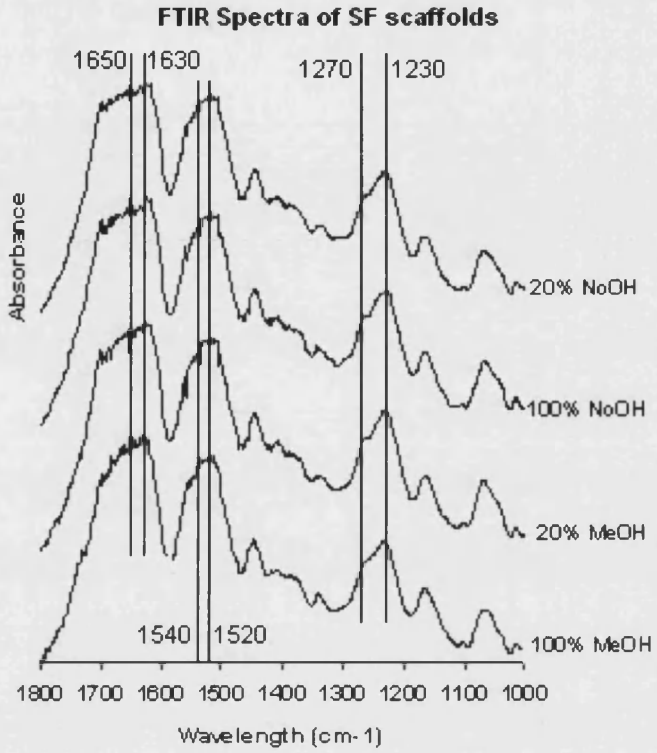

Figure 6-7 FTIR Spectra of SF scaffolds: percentage refers to the percentage FA in the solvent, NoOH indicates no coagulant and MeOH indicates methanol as a coagulant

6.3.5 Porosity

Scaffolds were made with 10% w/v SF with formic acid, and 7.5% and 10% w/v SF with aqueous formic acid. The scaffolds were cut to 2mm height to remove the more film-like top of the scaffold. It was found to be necessary to soak the scaffolds in methanol prior to cutting to prevent them from splitting whilst being cut. FTIR had shown that this treatment had no effect on the crystalline structure (Figure 6-5). The porosity for the scaffolds was: 0.964 +/- 0.009 for 10% silk dissolved in formic acid; 0.971 +/- 0.005 for 10% silk in aqueous formic acid; and 0.964 +/- 0.005 for 7.5% silk in aqueous formic acid (Figure 6-8). The differences between the scaffold types were not significant, $F(2,8)=1.16$ $p>0.05$. This shows that these scaffolds can be used to examine the effects of pore size and structure without differences in porosity affecting the results.

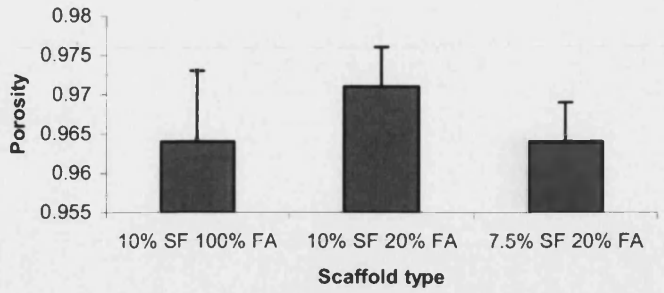

Figure 6-8 Effect of scaffold type on porosity (Error bars are +/- 1 s.d.)

6.3.6 Cell proliferation & attachment

In order to confirm that cells survive on these scaffolds, they were seeded with ligament fibroblasts and DNA content was quantified after 24 hours (to determine cell attachment) and 7 days (to confirm cell survival). The cell attachment study was also used to determine whether decorating the scaffolds with a peptide containing RGD would improve cell attachment with these silk scaffolds as it does to other porous silk scaffolds (Sofia et al. 2001).

To quantify cell attachment twelve scaffolds were made with each of these solvent/solute combinations: 7.5% w/v SF 20% FA, 10% w/v SF 20% FA, and 10% w/v SF 100% FA. From each of these conditions four scaffolds were decorated with GRGDS peptide using EDC:NHS, four scaffolds were reacted with EDC:NHS alone to control for any effect the crosslinking process had on the SF, and four scaffolds were soaked in PBS with no EDC:NHS (Table 6-3).

Table 6-3 Outline of experimental design for cell attachment experiment

		Scaffold type		
		7.5% w/v SF 20% FA	**10% w/v SF 20% FA**	**10% w/v SF 100% FA**
Decoration conditions	**EDC/NHS + RGD**	4 x EDC/NHS + RGD 7.5% w/v SF 20% FA	4 x EDC/NHS + RGD 10% w/v SF 20% FA	4 x EDC/NHS + RGD 10% w/v SF 100% FA
	EDC/NHS	4 x EDC/NHS (no RGD) 7.5% w/v SF 20% FA	4 x EDC/NHS (no RGD) 10% w/v SF 20% FA	4 x EDC/NHS (no RGD) 10% w/v SF 100% FA
	None	4 x no EDC/NHS 7.5% w/v SF 20% FA	4 x no EDC/NHS 10% w/v SF 20% FA	4 x no EDC/NHS 10% w/v SF 100% FA

The results are shown graphically in Figure 6-9. It appears from the graph that there is no consistent improvement in attachment for either of the EDC:NHS groups, there might be an effect of scaffold structure with the 10% SF 100% FA scaffolds increasing cell attachment. Two-way ANOVA effectively pools the results across single independent variables to determine if that independent variable has an effect. This analysis showed that there was no effect of reacting the scaffolds with either the EDC:NHS and the GRGDS peptide or EDC:NHS in the absence of the peptide ($F(2,35)=1.83$, $p>0.05$; Figure 6-10a). However there was an effect of scaffold structure ($F(2,35)=9.43$, $p<0.01$; Figure 6-10b). The Tukey HSD procedure revealed the cells attached significantly better to scaffolds made with formic acid than to scaffolds made with aqueous formic acid and either 7.5% w/v SF ($p<0.05$) or 10% w/v SF ($p<0.01$) (see Figure 6-10b). No interaction between decoration and scaffold structure was found ($F(4,35)=1.44$, $p>0.05$; Figure 6-9).

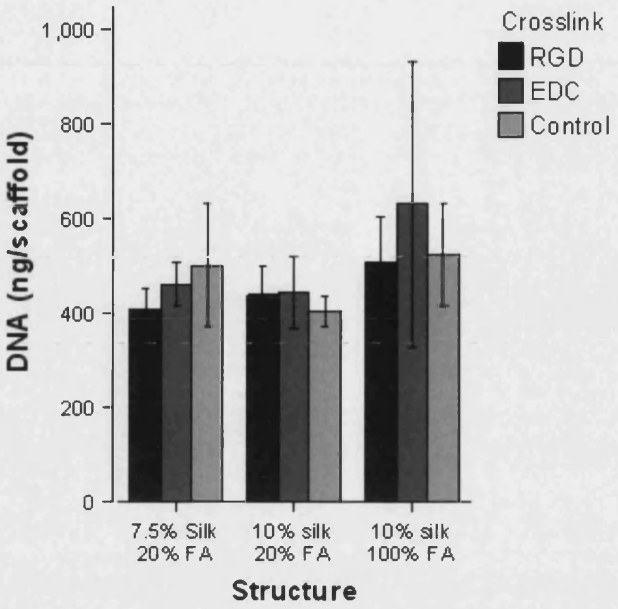

Figure 6-9 DNA content of scaffolds following 1 day attachment, error bars show 95% confidence intervals.

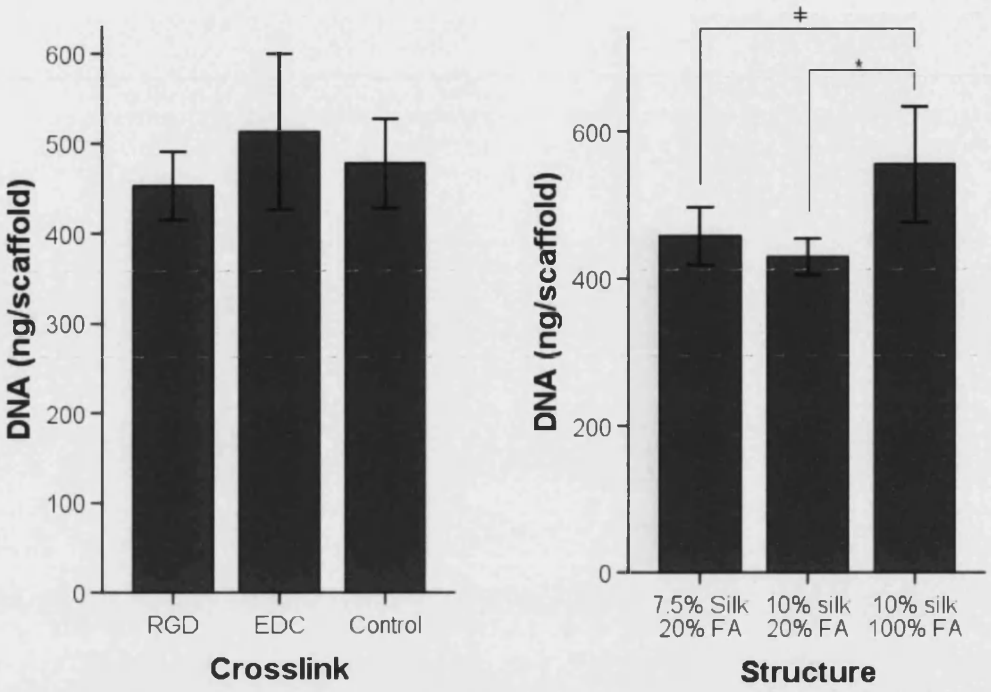

(a) (b)

Figure 6-10 DNA content of scaffolds following 1 day attachment: (a) by decoration type, and (b) by scaffold structure; * p<0.01, ‡ p<0.05 by Tukey HSD, error bars show 95% confidence intervals.

Scaffold structure showed a similar effect on cell proliferation after 7 days as it did on attachment. For this experiment, six of each type of scaffold (7.5% w/v SF 20% FA, 10% w/v SF 20% FA, and 10% w/v SF 100% FA) were seeded with ligament fibroblasts and cultured for 7 days. There was a significant difference between DNA content of the scaffolds ($F(2,17)=3.805$, $p<0.05$); post-hoc Tukey HSD tests revealed that there was a significant difference in DNA content between cells grown on scaffolds made with 10% w/v SF and 100% FA, and cells grown on scaffolds made with 10% w/v SF and 20% FA ($p<0.05$). There was no significant difference between scaffolds made with 7.5% SF and aqueous formic acid and either of the other two types of scaffold (Figure 6-11), this might be due to the smaller sample size and / or use of one way ANOVA instead of two way ANOVA.

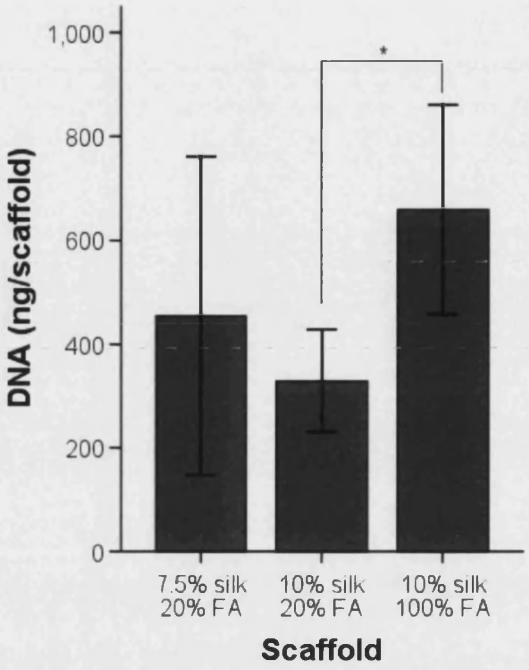

Figure 6-11 DNA content of scaffolds following 7 days proliferation: * p<0.05 by Tukey HSD, error bars show + 1 standard deviation.

This experiment was repeated with human osteoblast (MG63; n=3) and murine chondrocyte (ATDC-5; n=3) cell lines to confirm the viability of using these scaffolds for osteochondral engineering. A similar pattern was obtained to the results of ligament fibroblasts. Two way ANOVA revealed a significant effect of scaffold type: $F(2,10) = 10.98$, $p<0.005$, and cell type: $F(1,12) = 97.45$ $p<0.00001$, but no interaction: $F(2,10)=2.77$ $P>0.05$. Post-hoc tests showed that the effect of scaffold type was due to greater proliferation on 100% FA scaffolds than the 7.5% SF 20% FA scaffolds (Figure 6-12). The effect of cell type shows that the osteoblast cell line proliferates better on these scaffolds at 7 days than the chondrocytes cell line.

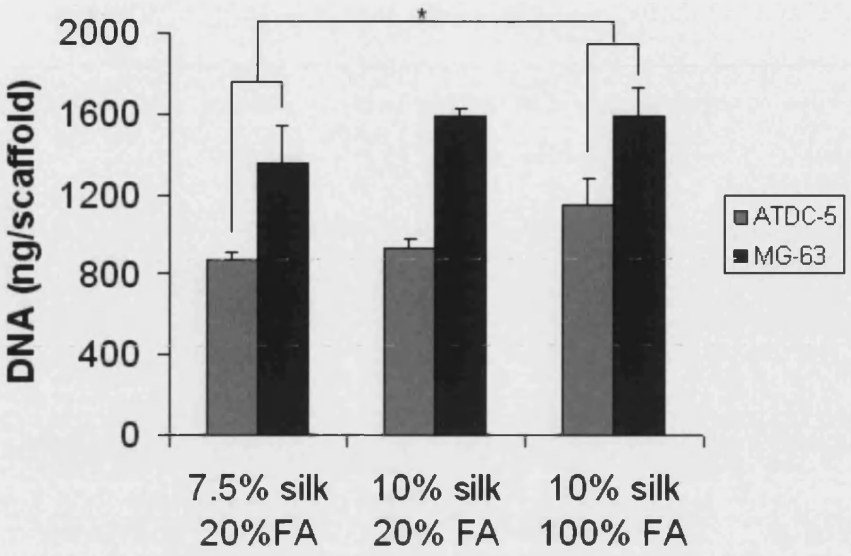

Figure 6-12 Results of osteochondral proliferation for 7 days: * $p<0.05$ by Tukey HSD, error bars show + 1 standard deviation.

6.4 Discussion

6.4.1 Scaffold fabrication

Silk scaffolds with a pore structure that varies from fibrous to film-like have been successfully developed by using aqueous formic acid solutions, and a variety of musculoskeletal cells cultured upon them. The principal initial problem was that there was a great deal of heterogeneity between scaffold samples; this problem was solved by adding the silk solution to the salt rather than salt to silk solution. The SEM results from this change suggested that the SF was precipitating soon after contact with the salt (Figure 6-3), potentially explaining the heterogeneity found when salt was added to silk solution in the mould: the initial salt crystals would receive a more substantial SF coating than later particles, but the distribution of these particles would be somewhat random within the scaffolds, producing the heterogeneity.

The new process produced scaffold structures that were anisotropic. On visual inspection this anisotropy was visible as a film like layer on top of the scaffolds, for cell culture and porosity studies this top layer was removed to leave the more fibrous bottom layer. Comparisons between the porosity of the scaffolds made with 100% FA (which are close to isotropy), and those made with 20% FA suggest that removing this layer does not affect the porosity significantly. The fibrous structure of these scaffolds remains to be explained. Some clues come from observation of the fabrication process. Whereas scaffolds made with 100% FA remain rather malleable until the FA is evaporated, scaffolds made with 20% FA quickly form a solid upper crust that becomes the film described above. This suggests that the silk's crystalline form changes from soluble to insoluble once the silk solution is added to the salt. In the case of the SF dissolved in water, it seems to be that interaction with the salt causes the formation of a silk hydrogel, and a change to insoluble silk II (Kim et al. 2005b), a similar process is possible with silk dissolved in 20% FA. Although it is unclear how this alone would account for the structures observed with 20% FA (Figure 6-3) as scaffolds made with 40% FA saturated with salt have markedly different structures (Figure 6-6a). Comparing made with 40% FA saturated with salt with scaffolds made with 80% FA saturated with salt (Figure 6-6) suggests that increasing the amount of salt dissolved by aqueous formic acid reduces the number of sides of each salt crystal that form silk sheets, but the increased amount of salt dissolved in 40% FA does not appear to result in a more fibrous structure than scaffolds made with 100% FA, similar fibrous structures can be seen in both types of scaffolds (cf. Figures 6-2b and 6-6a).

Trying to make scaffolds with pores smaller than those reported here results in a high failure rate, producing scaffolds with a dense top film and a very fragile bottom. It appears possible to make scaffolds with smaller pore sizes reliably by cooling the mould, the salt, and the silk solution to 4°C. This fits with the idea that the silk is precipitating soon after contact with salt particles, and that this precipitation is driven by the salt that dissolves in the silk solution from the salt particles, changing the silk into its insoluble silk II form. There are two possible causes of this increased precipitation: first, the

smaller the particles are the greater their surface area, increasing the rate at which silk dissolves; second, to get sufficient salt with small particle sizes to make a number of scaffolds it was necessary to use a different source of salt, as the mass of sub-180μm particles in the original salt was vanishingly small. This new salt was from a different source and appeared to carry some contaminating salts: scaffolds made with it have a bluish tinge, suggesting the presence of copper. There is increasing evidence that copper plays an important role in the transition of silk from its soluble forms to insoluble silk II (Zhou et al. 2006; Zhou et al. 2003; Zong et al. 2004), with increased copper ii content can trigger the transition to silk II at low concentrations (0.02M). It should be noted that the copper content within the silkworm is roughly 1000 times smaller. According to the certificate of analysis (Appendix C), the new salt contains at most 5mg/kg copper; if all the copper in the salt crystals dissolved in the solvent this would be enough copper to form a copper solution stronger than 0.015M, clearly there is the possibility that slight contamination with copper could dramatically affect the results.

That it is possible to slow this process with cooling indicates that it might be possible to get scaffolds closer to isotropy by changing the process in other ways. Adding the silk solution to the salt by centrifugation could accelerate the speed at which the solution penetrates the salt, reducing the amount of precipitation. Various metal ions have also been shown to impact upon the process of silk crystallisation (Zhou et al. 2003; Zhou et al. 2004), and by changing the concentrations of these ions, it might be possible to slow the process down, and create more regular scaffolds.

6.4.2 FTIR

The FTIR results strongly suggest that the solvent is having no effect on the eventual silk structure. In the case of pure formic acid, this is thought to be because the silk is partially dissolved in formic acid as the silk II form, and then the rest of the SF is rearranged into silk II form as it dries (Ha et al. 2005). As suggested above, it appears that SF dissolved in 20% FA undergoes the transition to silk II as salt dissolves in the solvent. This result

indicates that the chemistry of the SF scaffolds made with formic acid and aqueous formic acid is identical, allowing investigation of the effects of pore size and pore structure without different scaffold chemistry complicating the results.

6.4.3 Cell attachment and proliferation

The results from growing cells on scaffolds modified with RGD contradict the published reports of the effect of linking an RGD containing peptide to silk scaffolds (Sofia et al. 2001). The most likely explanation for this is that the precise molecular structure of biomaterials appears to be important in determining the effect of RGD on cells. Work on hydrogels and membranes shows that RGD works best when it is separated from the bulk of the hydrogel or surface by a short (~0.5-3.5kDa) spacer molecule (De Bartolo et al. 2005; De Bartolo et al. 2006; Hern and Hubbell 1998; Park et al. 2005). An alternative hypothesis for the absence of an effect of RGD is highlighted by the fact that when compared to fibronectin RGD enables sub-optimal attachment (Mardilovich et al. 2006). It could be that silk processed with formic acid allows better adsorption of fibronectin from FCS, eliminating the effect of RGD. Recently a new peptide containing two sequences from fibronectin, RGD and PHSRN, has been synthesised that increases cell attachment to levels indistinguishable from fibronectin (Mardilovich et al. 2006); with this new peptide it might be possible to enhance cell attachment to silk.

The cell attachment and proliferation results taken together show that varying pore structure whilst keeping pore size, scaffold chemistry and porosity constant can change the way that cells behave on a scaffold. Mathematical modelling appears to suggest a trade off between some of the scaffold parameters that are important for mass transfer such as porosity and specific surface area which is important for cell attachment (Lemon et al. 2006). Whilst no model is yet sophisticated enough to explain the data in this chapter, a trade off between mass transfer and cell attachment would explain these attachment results. Some of the theoretical models of permeation

though porous materials also suggests a trade off between permeability and specific surface area (Sander and Nauman 2003). Given that cell attachment is a good predictor of subsequent proliferation (Bigerelle and Anselme 2005), the cell proliferation results might be explained largely by the initial cell attachment. These are unexpected results, the objective of developing these scaffolds with better connected pores was to improve mass transfer and thereby improve tissue engineering outcomes. This appears to be somewhat different to the results found by Pei et al with chondrocytes (Pei et al. 2002), who found that HYAFF-II® mesh performed significantly better than the HYAFF-11® sponge in a bioreactor. This suggests that the optimal biomaterial design may well be a function of other parameters such as the fluid flow conditions.

Multivariate analysis of scaffold parameters is a useful tool to analyse how different biomaterial parameters affect tissue engineering. Some questions can only be answered with multivariate experiments, for instance, if there is an interaction between pore size and pore structure. Currently, the numbers of these experiments that have been carried out have been limited by the complexity of biomaterials; this complexity makes it difficult to keep one parameter constant without affecting other parameters. The new silk scaffolds allow the independent control of pore size and pore structure. This will allow new questions to be asked. Chapter 7 uses these scaffolds to understand what the optimal pore size and pore structure for the initiation of ligament engineering is.

6.5 Conclusions

This chapter reports the invention of porous silk scaffolds that allow the control of pore structure from fibrous to film-like by using 20% v/v formic acid to make fibrous scaffolds, and 100% formic acid to make film-like scaffolds. By reducing the silk content in the solvent from 10% w/v to 7.5% w/v the scaffolds can be made more fibrous. Fibrous scaffolds with pores smaller than 250μm can be made with thee new methods; this is roughly half the

pore size of the scaffolds with well connected pores made by Kim et al (2005b). SEM characterisation revealed an anisotropic structure that might be the result of a liquid-liquid separation during scaffold formation caused by sodium chloride dissolving in the silk solvent. Saturating the silk solvent with sodium chloride resulted in markedly different scaffold structures supporting this suggestion. FTIR results showed identical chemistry when comparing the fibrous and film-like scaffolds. No significant differences were found between the porosity of the fibrous and film like scaffolds. Decorating the scaffolds with RGD does not appear to improve attachment of ligament fibroblast, but ligament fibroblasts do appear to attach better to the film-like scaffolds. The improved attachment appears to improve cell proliferation of ligament fibroblasts at 7 days. In addition to the successful culture of ligament fibroblasts, human osteoblast and murine chondrocyte cell lines have been successfully cultured on the scaffolds for 7 days, again the cells appeared to proliferate better on the film-like scaffolds.

7 Effect of Pore Size, Pore Structure, and Animal on Ligament Fibroblasts in Porous Silk Scaffolds

7.1 Introduction

7.1.1 Initiation of ligament engineering

There is growing evidence that ligament regeneration *in vitro* is a multi-stage process. This evidence comes from work looking at the differentiation of bone marrow stromal cells towards a ligament fibroblast like phenotype. Two different lines of evidence are available: differentiating BMSCs with growth factors, and differentiating BMSCs with mechanical stress.

When the differentiation of BMSCs with growth factors in 2D culture was attempted it was found that treating them with epidermal growth factor (EGF) for a week followed by TGF-β for a week gave the best results in terms of collagen type I and III expression, cell morphology, and proteoglycan expression, when compared to TGF-β, insulin-like growth factor II, insulin, bFGF, or insulin + TGF-β for two weeks or bFGF for one week followed by TGF-β for one week (Moreau et al. 2005a). Similar results were found in 3D culture: when BMSCs were seeded onto bundles of twisted silk fibres and cultured in petri dishes and treated with either bFGF, EGF, or nothing for five days, followed by TGF-β1 or nothing for nine days, it was found that bFGF followed by TGF-β1 resulted in the greatest cell metabolic activity, and collagen I production at the end of the culture period (Moreau et al. 2005b). Taken together these results suggest that there are at least two different phases to ligament engineering *in vitro*, a first phase lasting around about a week when mitogens such as EGF or bFGF have a positive impact on the outcome, then a second phase where TGF-β has a positive impact on the outcome.

A second line of evidence comes from the mechanical differentiation of BMSCs in 3d culture. The BMSCs were seeded onto bundles of twisted silk fibres and cultured in Petri dishes for 1, 3, or 9 days and then transferred to a

bioreactor for mechanical stimulation for 6 days. Transferring the cells after 1 or 3 days caused a large drop cell metabolic activity. In contrast, after 9 days of Petri dish culture, mechanical loading increased cell metabolism significantly. The experiment also measured mRNA levels of fibronectin, integrins α2, α5 and β1, collagen type I and heat shock protein 70 (HSP-70) on day 1, 3, 5, 9, 11 and15 of Petri dish culture. Transcript levels of the integrins, fibronectin and collagen type I, peaked at or around day 9. HSP-70 was highest on day 1, possibly correlating with the large decline in cell metabolism when cells were mechanically stimulated after 1 day. Levels of all the integrins were low at three days, possibly partially explaining the poor cell metabolism triggered by mechanical stimulation after 3 days of Petri dish culture. Similarly, fibronectin levels were low at days 1 and 3 which might also be connected with the poor cell metabolism (Chen et al. 2006). This paper suggests again that there are two stages to ligament engineering, in the first stage the cells lay down ECM components such as fibronectin and express cell surface receptors such as the integrins to enable the cells to detect mechanical stimulation. A successful first stage can greatly improve the cellular response to subsequent mechanical stimulation.

These two approaches are connected by the fact that TGF-β1 is a key mediator of the response of ligament fibroblasts to cyclical tensile strain (Hsieh et al. 2000; Kim et al. 2002). Taken together this work suggests that the conditions needed for the first stage of ligament engineering are different from those when cyclical tensile strain or TGF-β is applied. This chapter will investigate whether biomaterial structure can enhance the initiation of ligament engineering.

7.1.2 Effect of pore size and scaffold structure on connective tissue engineering

Very little work has been done on optimising pore size and scaffold structure for connective tissue engineering. Surprisingly, the consensus that fibrous tissue needs small pores of around a 100μm comes from work on implanting scaffolds to promote bone repair. It was found that scaffolds with pores larger

than 100μm promoted the formation of bone (Hulbert et al. 1970). However, this was in an osteogenic environment, and in an environment that promotes fibrous tissue formation a different pore size might be optimal. It is revealing that the optimal pore size for bone tissue engineering is thought to be over 300 μm to promote vascularisation (Karageorgiou and Kaplan 2005).

Work has been done with collagen-glycosaminoglycan scaffolds grafted onto mice to regenerate skin (Yannas et al. 1989). In this case the outcome variables considered were how well the scaffold resisted contraction of the wound, and how normal the regenerated tissue was, judged by histology. It was found that scaffolds with pore sizes of 20 -125μm were ideal for resisting wound contraction, and that these scaffolds promoted partial regeneration of skin with a less fibrotic character than scar tissue. Further work showed that cells attached better to scaffolds with smaller pore sizes and higher specific surface areas (O'Brien et al. 2005). More recently, work has been done on *in vitro* connective tissue engineering with PEGT/PBT scaffolds that were seeded with adipose tissue fibroblasts (Wang et al. 2005a). This suggested that by using a bioreactor pores of up to 273μm might be filled and that scaffolds of 1.5-1.6mm in depth could be completely bridged by connective tissue within two weeks of culture; with larger pores of up to 401μm cells could still bridge the gap between fibres, but the result was a more loosely organised ECM. This work has also shown that scaffolds with average interconnected pore sizes of 160μm produced homogenous tissue, scaffolds with higher or lower interconnectivity did not (Wang et al. 2005a). It should be noted that speed of tissue bridging in these results may well be connected to the great number of mesenchymal stem cells in adipose tissue (Strem and Hedrick 2005).

There has been no quantitative investigation of the impact of pore size and structure on matrix synthesis for connective tissue engineering. It is conceivable that the looser tissue found in the larger pores by Wang et al (2005) was indicative of hyaluronic acid being synthesised to fill the void space. Therefore when the initiation of ligament tissue engineering is being considered, and high intial levels of hyaluronic acid are desired, larger pores

might be superior to smaller pores. Larger pores should also promote mass transfer, possibly aiding cell survival and penetration of the scaffold.

7.1.3 Advantages of novel porous silk scaffolds

A number of attempts to develop engineered ligaments have focused on developing biomaterials that mimic the mechanical properties of ligament (Altman et al. 2002a; Murray and Macnicol 2004; Sahoo et al. 2006). When this approach uses biodegradable biomaterials, the idea of these scaffolds is that the cells should synthesise ECM at the same rate as the material degrades to maintain constant mechanical properties.

The major limitation of this approach is that achieving sufficient mechanical strength requires a lot of biomaterial, limiting the porosity. Porosity is very important is determining the mass transfer properties of a tissue engineering scaffold. For instance, for porosities below 0.8 the following equation provides a good approximation of the intrinsic permeability (Equation 7-1; where k = intrinsic permeability, ψ = porosity, So = Specific Surface Area, and K = Kozeny constant (this includes tortuosity and a shape factor)).

$$k = \frac{\psi^3}{(1-\psi)^2 S_o^2 K}$$

Equation 7-1 Estimation of permeability from material properties (Sander and Nauman 2003).

Clearly, lower porosities result in much lower permeabilities; this will result in much less efficient mass transfer, especially in a bioreactor. This limited mass transfer might limit cell metabolism and ECM production, especially towards the centre of scaffolds. This effect is most clearly shown in the work of Moreau et al (2006) who cultured BMSCs seeded on bundles of twisted silk fibres in Petri dishes for 28 days under stimulation by various growth factors. In all cases the BMSCs form a dense ECM on the surface of the scaffold, but not inside the scaffold. This suggests that there might be an

advantage to increasing porosity and mass transfer at the expense of mechanical strength.

The second problem will be matching the degradation rate of the scaffold to the rate at which the cells produce ECM. The experience with the Leeds-Keio non-degradable artificial ligament in which all patients show signs of knee degeneration in the long term (Murray and Macnicol 2004), suggests that any replacement ligament will need to be biodegradable. If the scaffold degrades too quickly then the construct risks mechanical failure; on the other hand if the scaffold degrades too slowly then this might adversely affect subsequent ECM production. To take an extreme example, histological examination of Leeds-Keio artificial ligaments several years after implantation reveals evidence of a sustained foreign body reaction, and extensive remodelling continuing for years after implantation (Nomura et al. 2005). Closely matching scaffold degradation with ECM production will be a major challenge.

The third major problem with strong biomaterials is that they might result in the cells receiving sub-optimal mechanical stimulation. There is growing evidence that some tendinopathies do not heal as the injured part of the tendon is shielded from stress (Maganaris et al. 2004; Rees et al. 2006). A scaffold composed of strong fibres is likely to transmit the majority of the stress via the fibres, limiting the mechanical stimulation that the cells receive, particularly if the cells are not directly attached to the scaffold. A related issue is that cells in tendons *in vivo* are primarily exposed to shear stress, not tensile stress (Screen et al. 2004); whereas cells attached to long fibres running from end to end of a scaffold will be exposed to much more tensile stress than *in vivo*.

On the other hand, some notable successes have been achieved with weak biomaterials. Mechanically stimulated MSC seeded collagen gels appear to be capable of approaching the normal mechanical properties of tendon after 12 weeks when used to repair full length patellar tendon defects in rabbits (Juncosa-Melvin et al. 2006). Calve et al (2004) managed to make tendon

with similar mechanical properties to embryonic tendon, by enabling cells to self assemble themselves without a scaffold into a cylinder suspended between two posts.

The novel silk scaffolds reported in Chapter 6 will be used for this investigation of the initiation of ligament tissue engineering as they allow independent control of pore size and pore structure, two variables that have not been considered for ligament tissue engineering. These scaffolds should allow collagen fibrils to form and interact with minimal interference from the scaffold itself due to the high porosity of the scaffolds. In addition, these scaffolds can be autoclaved to sterilise them, which simplifies their handling.

7.1.4 Predictions

The work studying collagen fibrillogenesis in tendons suggests several predictions that should be met, if ligament engineering follows a similar path to collagen fibrillogenesis *in vivo*:

1. The percentage of glycosaminoglycan that is hyaluronic acid should be high initially and then drop (Parry et al. 1982).
2. The percentage of glycosaminoglycan that is chondroitin and dermatan sulphate (the two will not be distinguished in this experiment) should increase with time (Parry et al. 1982).
3. The amount of chondroitin sulphate should tend to drop over the course of the experiment (Scott et al. 1981).
4. The amount of hydroxyproline (an amino acid unique to collagen) should increase over the course of the experiment (Scott et al. 1981).
5. The ratio of glycosaminoglycan : hydroxyproline should drop rapidly (Scott et al. 1981).

In addition, work on ligament engineering *in vitro* suggests that cell number should fluctuate over the course of the experiment (Moreau et al. 2006). The main objective of this work is to identify a combination of pore size and pore structure that maximises the number of predictions met.

7.2 *Materials and Methods*

Methods for cell culture are detailed in Section 4.2.1; methods for regenerating silk fibroin and preparing scaffolds are in 4.2.2 and 4.2.4. DNA quantification is in Section 4.3.4 The method for papain digestion is described in Section 4.3.5. The method for hydroxyproline analysis is in Section 4.3.6, and HPLC analysis of glycosaminoglycans is detailed in Section 4.3.7.

7.3 *Results*

7.3.1 Overview of experimental design

For each time point of this experiment, 54 scaffolds were sacrificed. These 54 scaffolds consisted of 6 sets of the 9 combinations of different scaffold types arising from 3 pore sizes and 3 pore structures (Table 7-1); each set was seeded with cells from one sheep, and a different sheep supplied the cells for each set. Thus, the 54 scaffolds were made of the combinations of 3 pore sizes x 3 pore structures x 6 sheep. Scaffolds were sacrificed after one day, one week, two weeks and three weeks. The same 6 sheep were used to supply cells at each time point, so that the effect of individual differences between animals could be investigated.

Table 7-1 The nine different combinations of pore size and pore structure

180-250μm 7.5% silk 20% FA (Highly fibrous)	180-250μm 10% silk 20% FA (Fibrous)	180-250μm 10% silk 100%FA (Film like)
300-355μm 7.5% silk 20% FA (Highly fibrous)	300-355μm 10% silk 20% FA (Fibrous)	300-355μm 10% silk 100%FA (Film like)
425-500μm 7.5% silk 20% FA (Highly fibrous)	425-500μm 10% silk 20% FA (Fibrous)	425-500μm 10% silk 100%FA (Film like)

On the first day only DNA was quantified; DNA, hydroxyproline, and GAGs (hyaluronic acid and chondroitin sulphate) were determined at the subsequent time points. This gives a total of four dependent variables; analysing each dependent variable with a factorial ANOVA would increase the chance of a type I error to almost 20%, so the alpha level needs to be corrected to 0.0125 instead of 0.05, using the Bonferroni correction. As it is difficult to hypothesise what effects this experiment will detect, the data will be analysed using exploratory ANOVA of all main effects, and two-way and three-way interactions to determine the important effects. Then the significant results will be plotted and subjected to a post-hoc analysis where appropriate.

The following sections will describe the results of ANOVA following DNA, hydroxyproline, chondroitin sulphate, and hyaluronic acid quantification. Then correlations between the outcome variables will be examined.

7.3.2 DNA

Three main effects are found to have a significant impact on the amount of DNA within the scaffolds (Table 7-2): Time, pore size and animal. Three two way interactions are significant: time x pore size, time x animal, and pore size x animal. The only significant three way interaction is time x pore size x animal. Of these effects, the most important variable is time x animal, explaining 36% of the variance in the population alone. Time accounts for 16% of the variance. Time x pore size x animal and animal each account for a further 8%. The last three significant effects account for less than 10% of the variance together: time x pore size for 3%, pore size x animal accounts for 3%, and pore size accounts for 1%. In total, these variables account for 75% of the variance in the population.

The effect of time is a significant reduction in DNA at day 21, compared to days 1, 7 and 14 (Figure 7-1). Post-hoc tests do not reveal what the effect of pore size is, but the graph suggests that the smallest pore size limits cell number (Figure 7-2). This failure to identify a difference with post hoc tests is consistent with the very small effect size.

Table 7-2 Exploratory ANOVA of DNA quantification. (Probability is left blank where data is not significant, F-vales and effect size rounded to 2 decimal places, probability rounded to 2 significant figures)

Variable / Interaction	F value	Probability	Effect size
Time	F(3,60) = 43.05	5.7E-15	0.16
Pore structure	F(2,60) = 1.91		
Pore size	F(2,60) = 4.93	0.010	0.01
Animal	F(5,60) = 14.28	3.4E-09	0.08
Time x Pore structure	F(6,60) = 0.74		
Time x Pore size	F(6,60) = 4.68	0.00058	0.03
Time x Animal	F(15,60) = 20.74	2.7E-18	0.36
Pore structure x Pore size	F(4,60) = 1.63		
Pore structure x Animal	F(10,60) = 0.98		
Pore size x Animal	F(10,60) = 3.81	0.00050	0.03
Time x Pore structure x Pore size	F(12,60) = 1.01		
Time x Pore structure x Animal	F(30,60) = 0.51		
Time x Pore size x Animal	F(30,60) = 3.18	6.7E-05	0.08
Pore structure x Pore size x Animal	F(20,60) = 0.86		

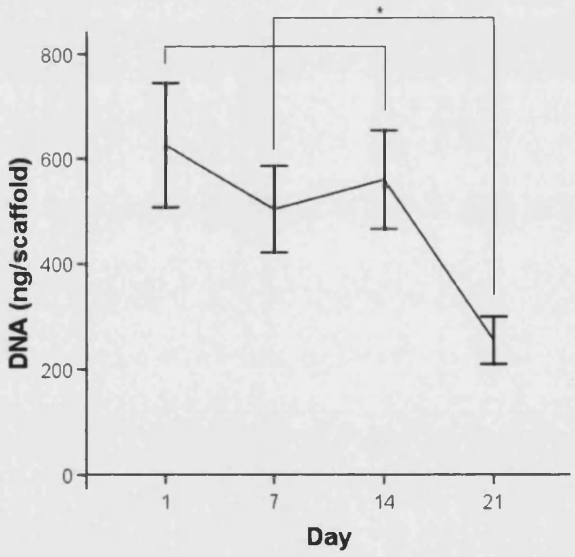

Figure 7-1 DNA content of scaffolds on different days (Error bars show 95% confidence intervals, * P<0.001 by Games-Howell post-hoc test)

Cells from animal 4 appears to have a consistently higher cell number than cells from animals 1, 2, & 3 (Figure 7-3).

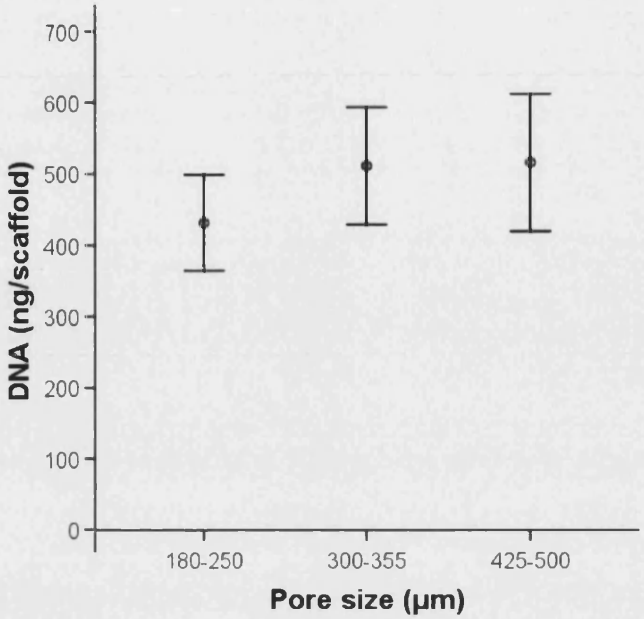

Figure 7-2 DNA content of scaffolds with respect to pore size (Error bars show 95% confidence intervals)

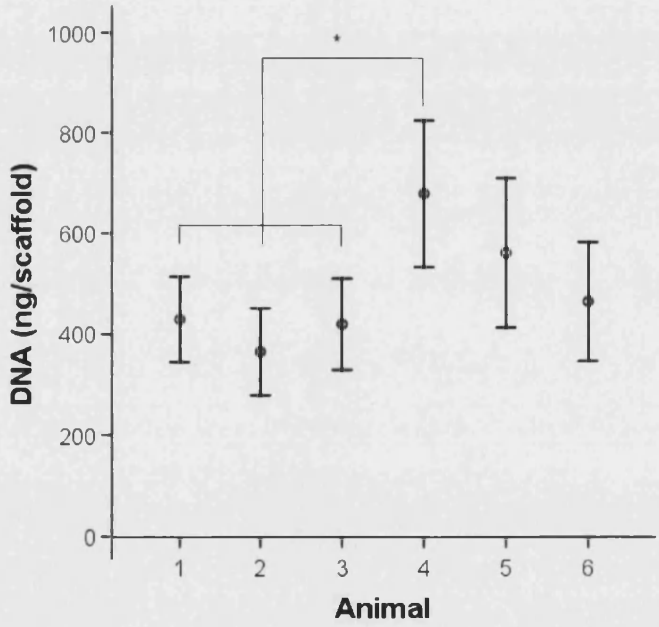

Figure 7-3 DNA content of scaffolds with respect to animal (Error bars show 95% confidence intervals, * P<0.05 by Games-Howell post-hoc test)

Simple effects analysis shows that the interaction between time and pore size is related to significant differences between scaffolds with different pore sizes (Table 7-3). Pairwise comparison shows that the scaffolds with 425-

500μm pores have most DNA on day 1, and scaffolds with either 300-355μm or 425-500μm pores have more DNA than scaffolds with 180-250μm pores on day 14 (Figure 7-4).

Table 7-3 Simple effects analysis of the effect of pore size within time on scaffold DNA content. (Based on the linearly independent pairwise comparisons among the estimated marginal means).

Variable	F value	Probability
Pore size within day 1	F(2,72) = 8.18	0.001
Pore size within day 7	F(2,72) = 3.11	
Pore size within day 14	F(2,72) = 7.00	0.002
Pore size within day 21	F(2,72) = 0.66	

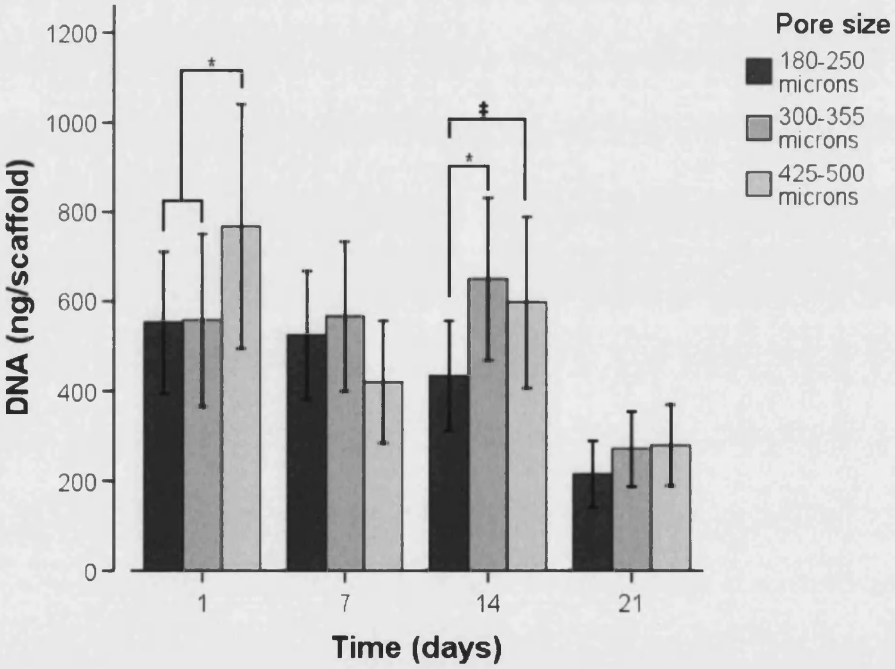

Figure 7-4 DNA content of scaffolds showing the interaction between pore size and time (Error bars show 95% confidence intervals; * P<0.005 and ‡ P<0.05 by pairwise comparison with Sidak correction)

There are significant differences between DNA content with respect to animal at all four time points studied (Table 7-4). On day 1, DNA content of the cells from the first three animals is significantly different from that of the cells from the last three; in addition, the DNA content of the cells from animal 5 is significantly different to that of cells from animals 4 and 6. On day 7, the

each of the first three animals is again significantly different to the last three. By day 14 the pattern has changed: DNA content of cells from animal 6 is significantly lower than from the first four, and the DNA content of cells from animal 5 is significantly lower than from cells of animals 1, 3 and 4. On day 21, pairwise comparison reveals no significant differences; the difference found in the simple effects analysis reflects pooled differences (Figure 7-5).

Table 7-4 Simple effects analysis of the effect of animal within time on scaffold DNA content. (Based on the linearly independent pairwise comparisons among the estimated marginal means).

Variable	F value	Probability
Animal within day 1	F(5,72) = 41.00	9.6E-20
Animal within day 7	F(5,72) = 18.83	6.4E-12
Animal within day 14	F(5,72) = 13.21	4.0E-009
Animal within day 21	F(5,72) = 3.368	0.009

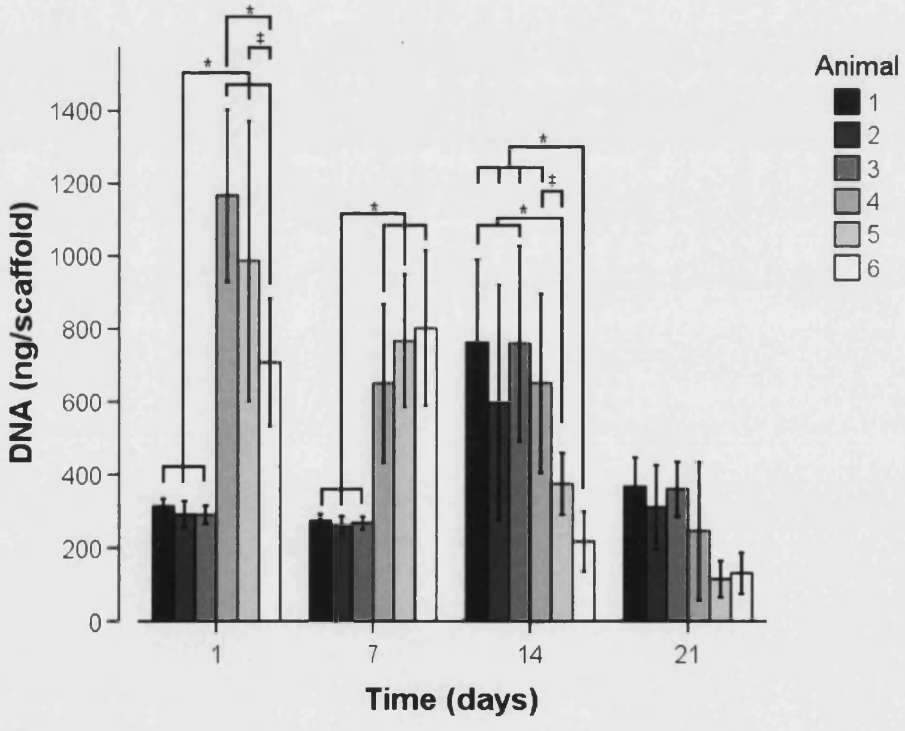

Figure 7-5 DNA content of scaffolds showing the interaction between animal and time (Error bars show 95% confidence intervals; * P<0.001 and ‡ P<0.05 by pairwise comparison with Sidak correction)

For half the cells from the animals the interaction with pore size has no significant effect (Table 7-5). For the cells from animal 2 it the largest pore size increases cell number, for animal 3 300-355µm pores result in a higher cell number than 425-500µm pores, and for the cells from animal 4 it the two largest pore sizes increase cell number. (Figure 7-6)

Table 7-5 Simple effects analysis of the effect of pore size within animal on scaffold DNA content. (Based on the linearly independent pairwise comparisons among the estimated marginal means).

Variable	F value	Probability
Pore size within animal 1	F(2,72) = 0.60	
Pore size within animal 2	F(2,72) = 7.25	0.001
Pore size within animal 3	F(2,72) = 5.21	0.008
Pore size within animal 4	F(2,72) = 7.012	0.002
Pore size within animal 5	F(2,72) =2.96	
Pore size within animal 6	F(2,72) =0.97	

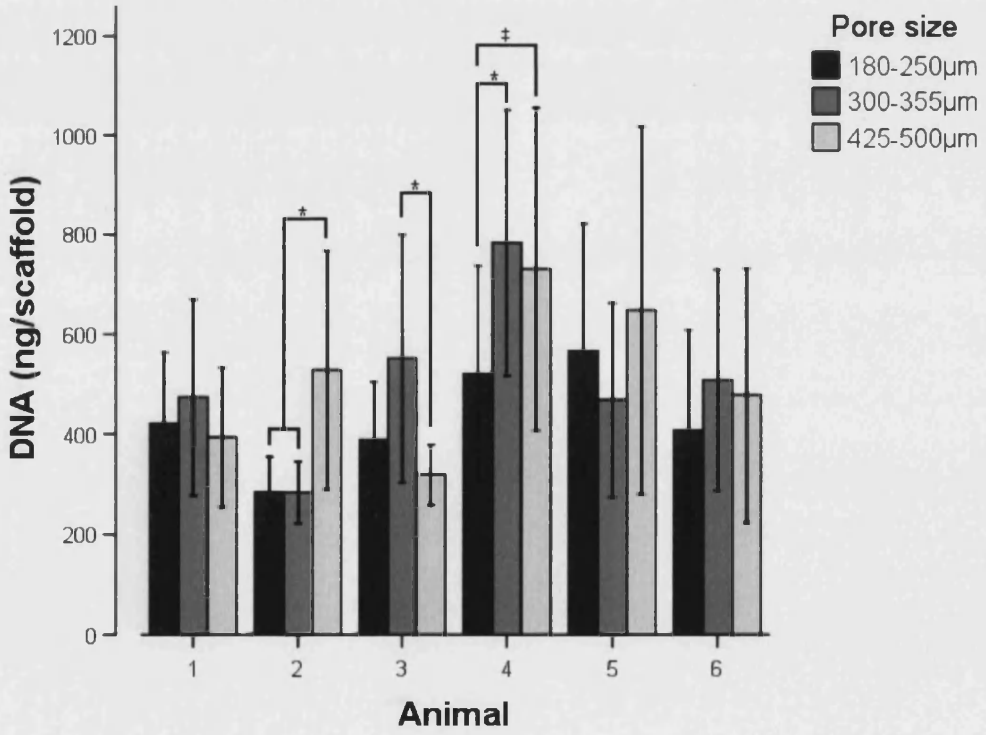

Figure 7-6 DNA content of scaffolds showing the interaction between pore size and animal (Error bars show 95% confidence intervals; * P<0.01 and ‡ P<0.05 by pairwise comparison with Sidak correction)

Finally, the three way interaction between pore size, time and animal, is related to different behaviour in response to different pore sizes for cells from animals 4 and 5 on days 1 and 7, and cells from animals 2, 3, and 4 on day 14 (Table 7-6). On day 1 cells from animal 4 attach better to the scaffolds with the largest pores than to scaffolds with the smallest pores; cells from animal 5 attach least well to scaffoids with the middle pore size, and attach best to scaffolds with the largest pores. The pattern is different on day 7, DNA content is higher in scaffolds with the middle pore size than the largest pore size for cells from animal 4; for cells from animal 5, DNA content is lower for scaffolds with the largest pores than the other two. On day 14, scaffolds with the largest pores result in most DNA for cells from animal 2, for cells from animal 3 scaffolds with the middle sized pores perform best, and the largest pores result in more DNA than the smallest pores (Figure 7-7).

Table 7-6 Simple effects analysis of the effect of pore size within animal within time on scaffold DNA content. (Based on the linearly independent pairwise comparisons among the estimated marginal means).

Variable	F value	Probability
Pore size within animal 1 within day 1	F(2,72) = 0.05	
Pore size within animal 2 within day 1	F(2,72) = 0.23	
Pore size within animal 3 within day 1	F(2,72) = 0.06	
Pore size within animal 4 within day 1	F(2,72) = 5.69	0.005
Pore size within animal 5 within day 1	F(2,72) = 26.00	3.2E-9
Pore size within animal 6 within day 1	F(2,72) =2.09	
Pore size within animal 1 within day 7	F(2,72) = 0.05	
Pore size within animal 2 within day 7	F(2,72) = 0.02	
Pore size within animal 3 within day 7	F(2,72) = 0.002	
Pore size within animal 4 within day 7	F(2,72) = 6.17	0.003
Pore size within animal 5 within day 7	F(2,72) = 4.26	0.018
Pore size within animal 6 within day 7	F(2,72) = 0.35	
Pore size within animal 1 within day 14	F(2,72) = 2.47	
Pore size within animal 2 within day 14	F(2,72) = 16.40	1.4E-6
Pore size within animal 3 within day 14	F(2,72) = 13.48	1.1E-5
Pore size within animal 4 within day 14	F(2,72) = 4.17	0.019
Pore size within animal 5 within day 14	F(2,72) = 0.26	
Pore size within animal 6 within day 14	F(2,72) = 0.54	
Pore size within animal 1 within day 21	F(2,72) = 0.05	

Pore size within animal 2 within day 21	F(2,72) = 1.03	
Pore size within animal 3 within day 21	F(2,72) = 0.42	
Pore size within animal 4 within day 21	F(2,72) = 1.87	
Pore size within animal 5 within day 21	F(2,72) = 0.023	
Pore size within animal 6 within day 21	F(2,72) = 0.022	

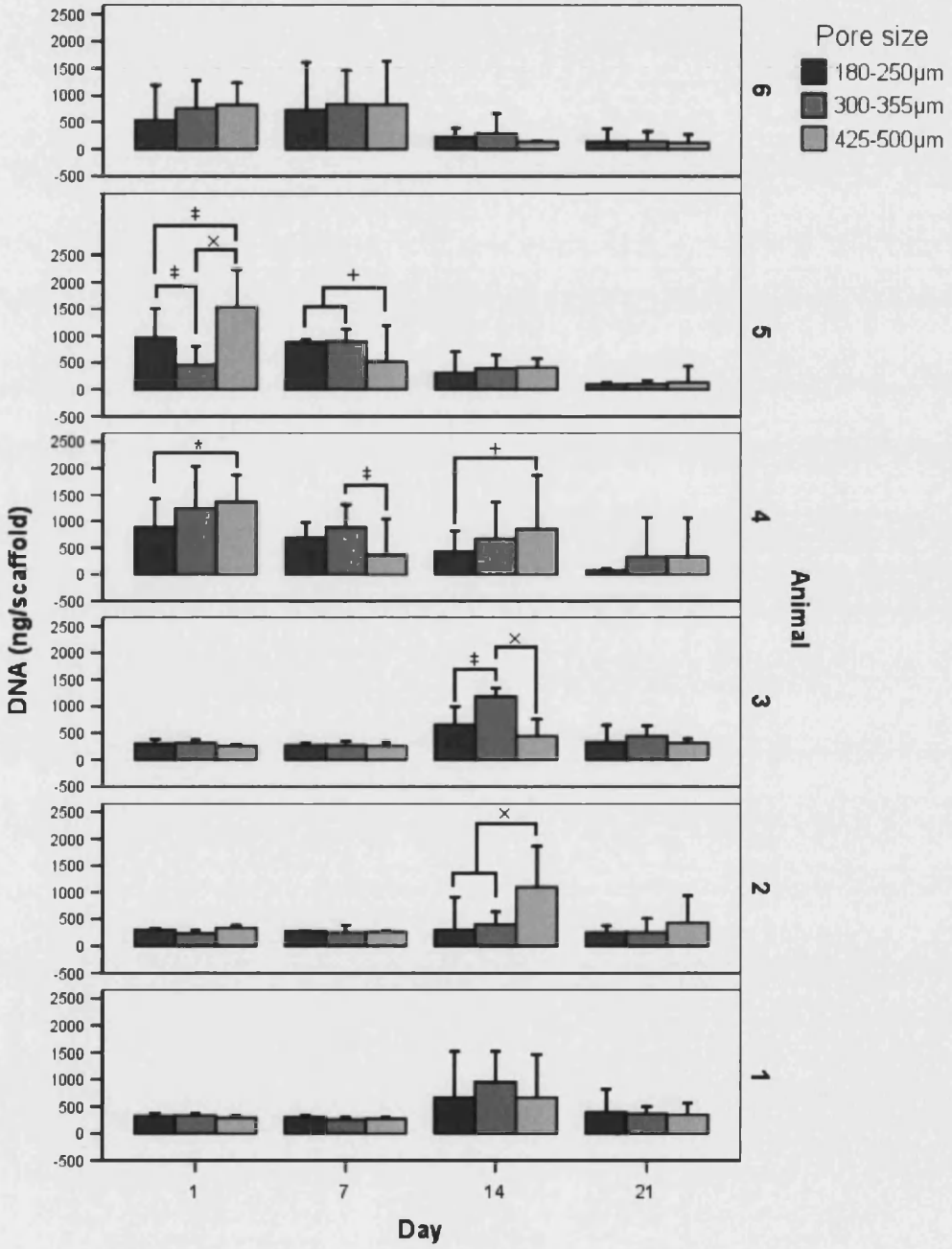

Figure 7-7 Bar chart of DNA content in scaffolds showing the interaction between pore size, animal and time (Error bars show 95% confidence intervals; + P<0.05, * P<0.01, ‡ P<0.005 and x P<0.001 by pairwise comparison with Sidak correction)

Overall, there appears to be divergent cell attachment, accounted for by differences between cells from different animals (Figure 7-5), with cells from the last three animals attaching better than the first three; most of these differences remain significant at day 7; by day 14 this pattern appears to be somewhat reversed. Cell number at day 21 is significantly lower than at the first three time points (Figure 7-1). Averaged across the experiment, cells from animal 4 have a higher cell number than cells from animals 1, 2 and 3 (Figure 7-3). There are also complex differences in the way cells from different animals respond to different pore sizes at different time points (Figure 7-7). For those cells from animals who respond differently to different pore sizes, either the middle or largest pores result in the highest cell number (Figures 7-4 and 7-7).

At day 7 conditions that produced high cell numbers at day 1 tend to result in a reduction of cell number, conditions that allowed fewer cells to attach tend to maintain a similar cell number, although in a couple of cases cell number increases (Figure 7-8). At day 14 the trend for conditions that attached better to decline in cell number continues, whereas conditions that resulted in lower cell numbers at day 7 tend to have higher cell numbers at day 14, this is particularly noticeable in some animals with one or more of the larger pore sizes (Figure 7-8). At day 21 the various conditions seem to converge (Figure 7-8).

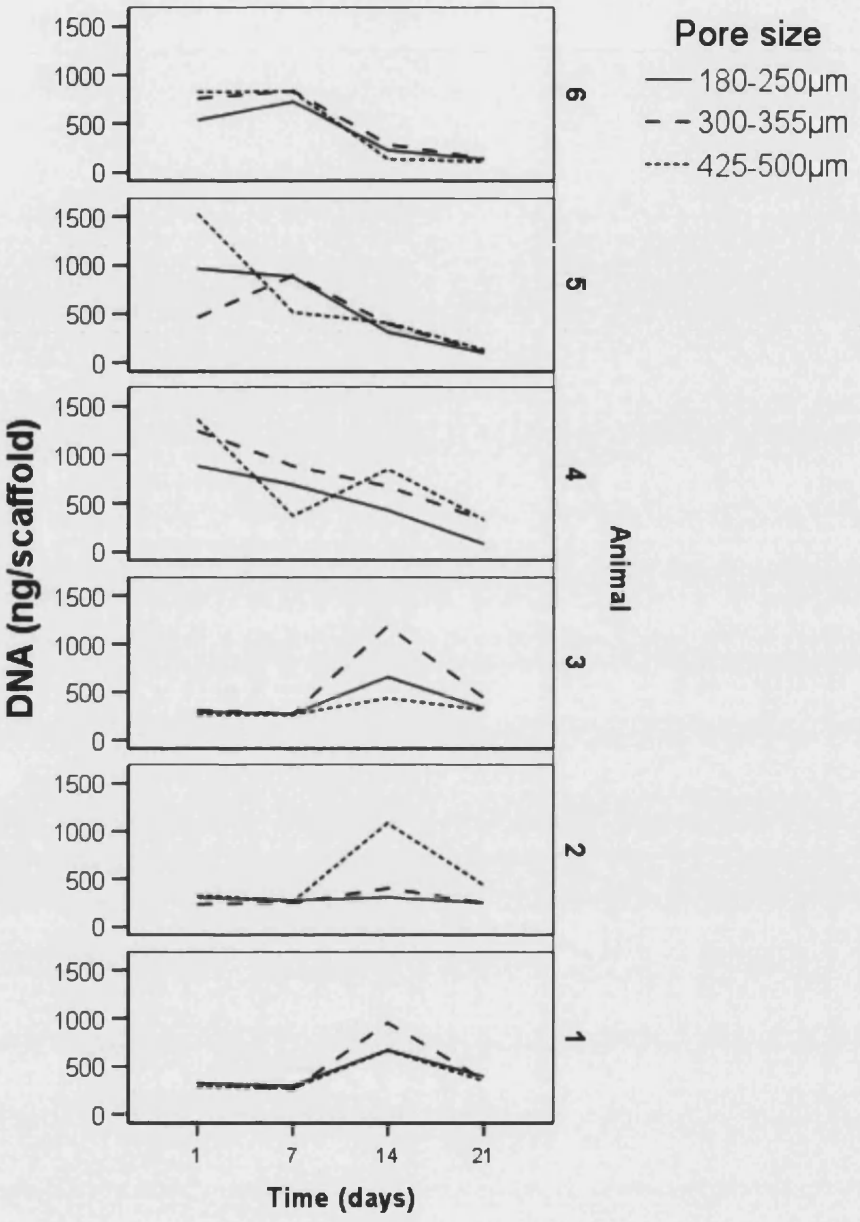

Figure 7-8 Line chart of DNA content in scaffolds showing the interaction between pore size, animal and time

7.3.3 Hydroxyproline

Fewer variables and interactions have an impact on hydroxyproline levels (Table 7-7). The most important effect is time, accounting for over 20% of the variance in the population. This is because hydroxyproline levels are higher at day 21, than days 7 and 14 (Figure 7-9). The second most

important effect is the animal, accounting for 11% of the variance. Cells from animal 6 produce significantly less hydroxyproline than cells from animals 1, 2, and 3; whilst cells from animal 5 produce less hydroxyproline than cells from animal 3 (Figure 7-10).

Table 7-7 Exploratory ANOVA of hydroxyproline results. (Probability is left blank where data is not significant, F-vales and effect size rounded to 2 decimal places, probability rounded to 2 significant figures)

Variable / Interaction	F value	Probability	Effect size
Time	F(2,40) = 28.58	2.0E-08	0.21
Pore structure	F(2,40) = 1.48		
Pore size	F(2,40) = 0.69		
Animal	F(5,40) = 6.8	0.00011	0.11
Time x Pore structure	F(4,40) = 0.49		
Time x Pore size	F(4,40) = 1.08		
Time x Animal	F(10,40) = 3.05	0.0058	0.08
Pore structure x Pore size	F(4,40) = 0.29		
Pore structure x Animal	F(10,40) = 0.993		
Pore size x Animal	F(10,40) = 1.02		
Time x Pore structure x Pore size	F(8,40) = 0.52		
Time x Pore structure x Animal	F(20,40) = 0.88		
Time x Pore size x Animal	F(20,40) = 1.34		
Pore structure x Pore size x Animal	F(20,40) = 0.883		

The last significant effect: time x animal, accounts for 8% of the variance. This interaction seems to be caused by the cells from first three animals producing more hydroxyproline at day 7, and cells from animal 6 producing less hydroxyproline at day 21 than cells from animals 1, 3 and 4, and in addition, cells from animal 4 producing more hydroxyproline than cells from animals 2 and 5 as well as more than cells from animal 6 (Table 7-8 and Figure 7-14).

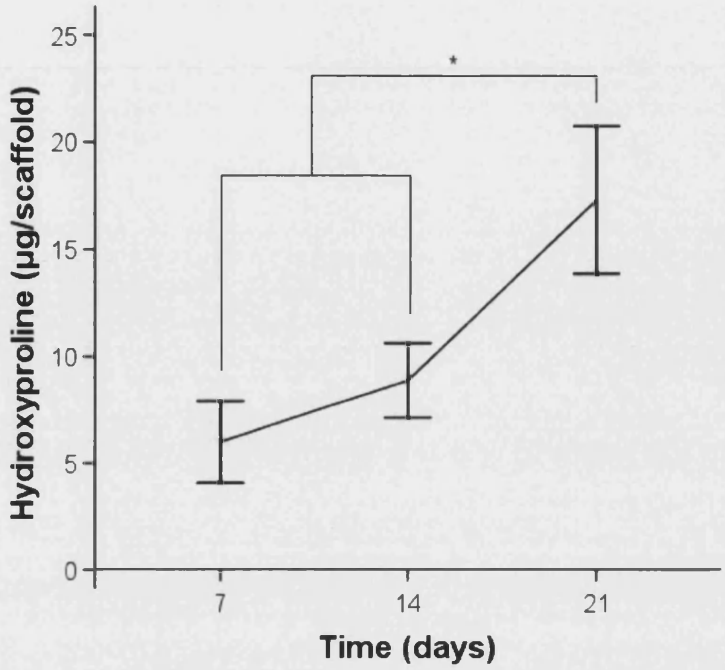

Figure 7-9 Hydroxyproline content of scaffolds on different days (Error bars show 95% confidence intervals, * P<0.001 by Games-Howell post-hoc test)

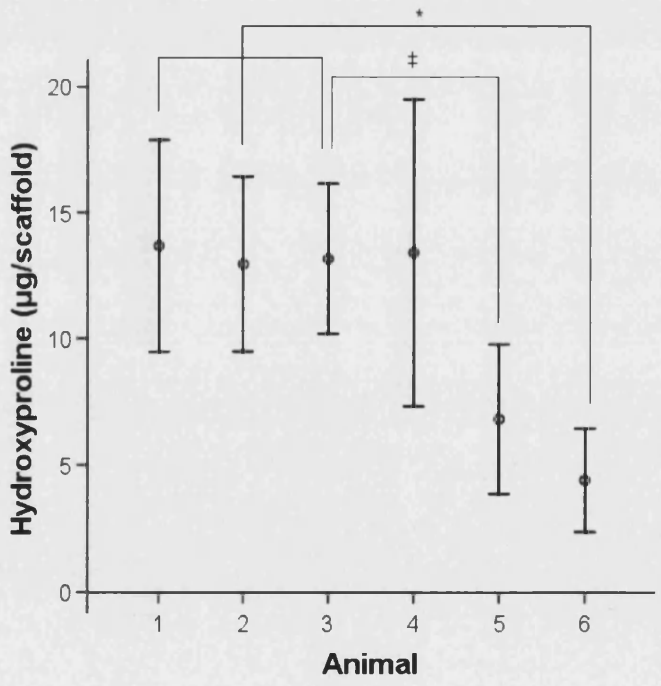

Figure 7-10 Hydroxyproline content of scaffolds with respect to different animals averaged over all three time points (Error bars show 95% confidence intervals, * P<0.005 and ‡ P<0.05 by Games-Howell post-hoc test)

Table 7-8 Simple effects analysis of the effect of animal within time on scaffold hydroxyproline content. (Based on the linearly independent pairwise comparisons among the estimated marginal means).

Variable	F value	Probability
Animal within day 7	F(5,48) = 5.56	0.00041
Animal within day 14	F(5,48) = 1.36	
Animal within day 21	F(5,48) = 7.11	4.8E-5

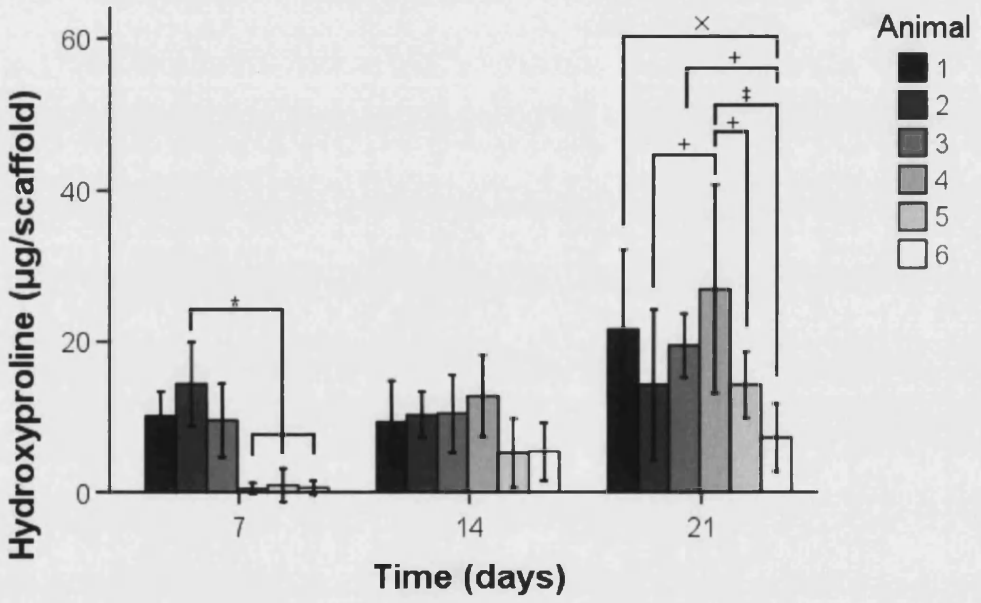

Figure 7-11 Hydroxyproline content of scaffolds showing the interaction between animal and time (Error bars show 95% confidence intervals; +, P<0.05, * P<0.01, x P<0.005 and ‡ P<0.001 by pairwise comparison with Sidak correction)

Overall, the largest effect is that hydroxyproline levels increase at day 21. There are also significant differences in the amount of hydroxyproline cells from different animals produce (Figure 7-10), and the relative performance of cells from different animals changes with time (Figure 7-11).

7.3.4 Chondroitin sulphate

The same three effects that were significant in explaining the variance in hydroxyproline levels are those that are important in explaining chondroitin sulphate levels. Again, time is the most important variable (Table 7-9)

explaining 36% of the variance in the population; although with chondroitin sulphate there is a significant drop at days 14 and 21 compared to day 7 (Figure 7-12). The second most important effect is the differences between the animals, explaining 9% of the variance. Post-hoc comparisons reveal that cells from animal 1 produce significantly more chondroitin sulphate than cells from animal 6 (Figure 7-13). In should be noted that in some cases chondroitin sulphate was not detectable.

Table 7-9 Exploratory ANOVA of chondroitin sulphate results. (Probability is left blank where data is not significant, F-vales rounded to 2 decimal places, probability and effect size rounded to 2 significant figures)

Variable / Interaction	F value	Probability	Effect size
Time	F(2,40) = 62.39	5.05E-13	0.36
Pore structure	F(2,40) = 2.28		
Pore size	F(2,40) = 1.10		
Animal	F(5,40) = 7.22	6.74E-05	0.09
Time x Pore structure	F(4,40) = 1.29		
Time x Pore size	F(4,40) = 0.24		
Time x Animal	F(10,40) = 3.82	0.0011	0.08
Pore structure x Pore size	F(4,40) = 1.64		
Pore structure x Animal	F(10,40) = 2.00		
Pore size x Animal	F(10,40) = 0.58		
Time x Pore structure x Pore size	F(8,40) = 1.64		
Time x Pore structure x Animal	F(20,40) = 1.07		
Time x Pore size x Animal	F(20,40) = 0.32		
Pore structure x Pore size x Animal	F(20,40) = 0.965		

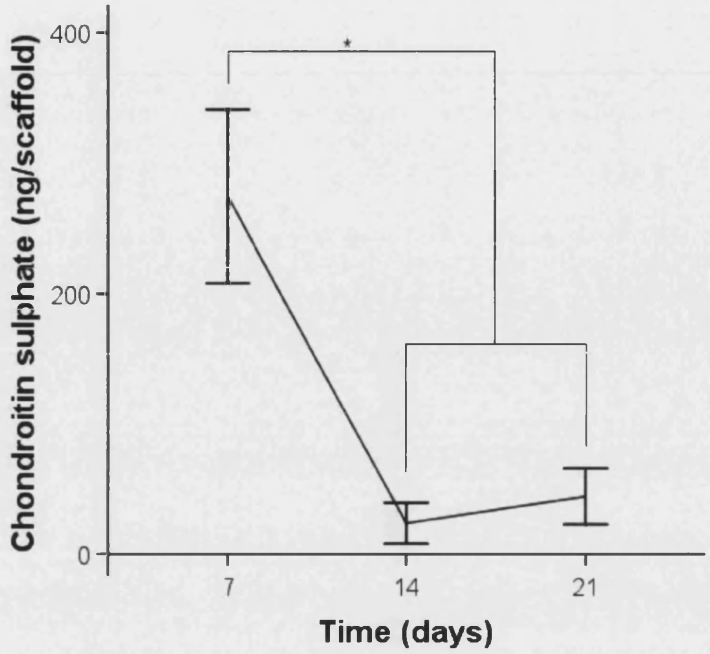

Figure 7-12 Chondroitin sulphate content of scaffolds on different days (Error bars show 95% confidence intervals, * P<0.001 by Games-Howell post-hoc test)

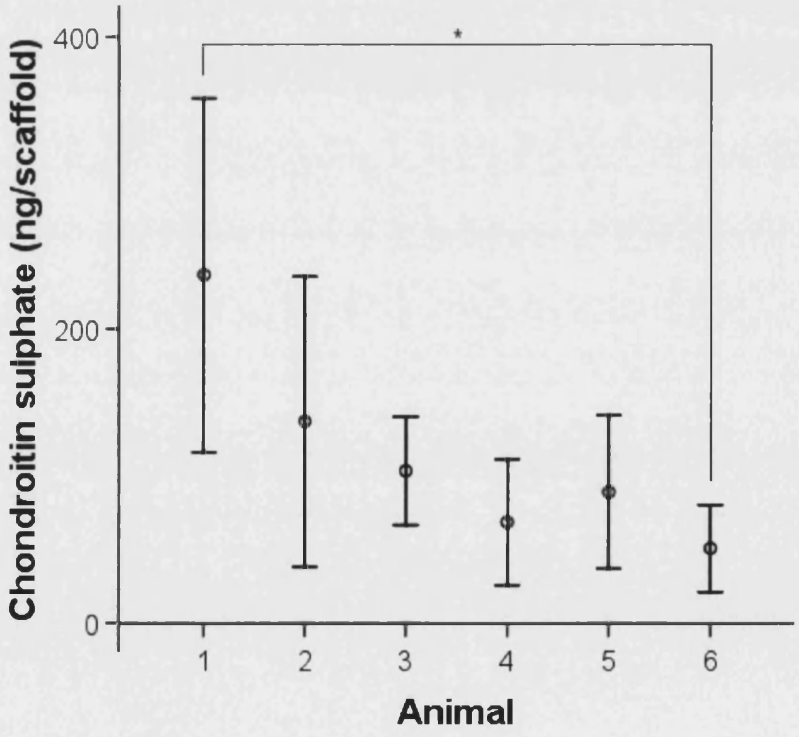

Figure 7-13 Chondroitin sulphate content of scaffolds with respect to different animals averaged over all three time points (Error bars show 95% confidence intervals, * P<0.05 by Games-Howell post-hoc test)

The interaction between time and animal explains almost as much variance (8%) as the main effect for animal. This interaction appears to be due to elevated chondroitin sulphate produced by cells from animal 1 relative to cells from animals 3, 4, 5 and 6 at day 1, and by cells from animal 2 relative to cells from animals 3 and 6 (Figure 7-14). No significant differences were found after day 7 (Table 7-10).

Table 7-10 Simple effects analysis of the effect of animal within time on scaffold chondroitin sulphate content. (Based on the linearly independent pairwise comparisons among the estimated marginal means).

Variable	F value	Probability
Animal within day 7	F(5,48) = 11.79	1.8E-7
Animal within day 14	F(5,48) = 0.635	
Animal within day 21	F(5,48) = 1.004	

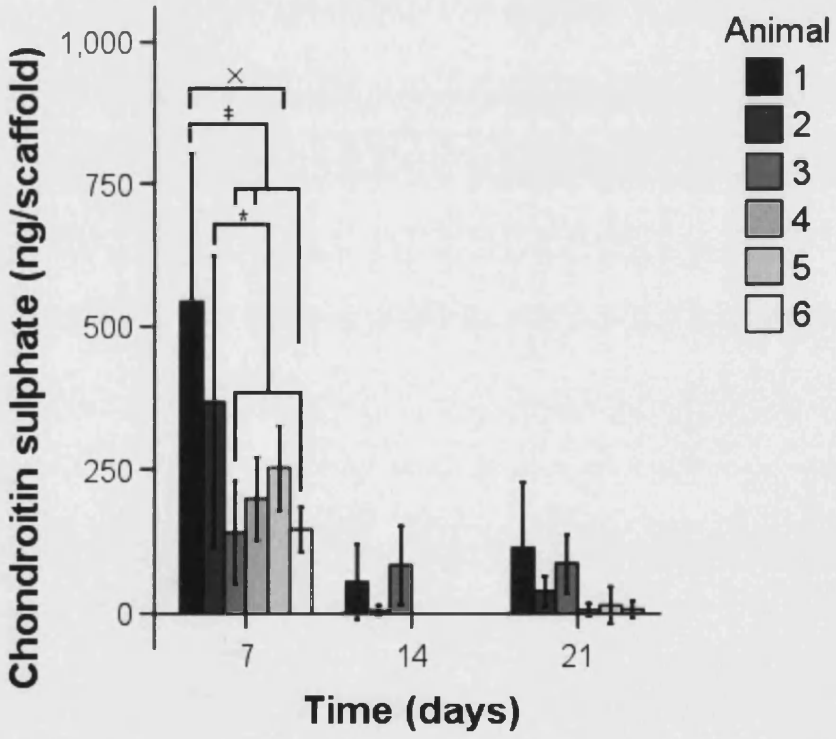

Figure 7-14 Chondroitin sulphate content of scaffolds showing the interaction between time and animal (Error bars show 95% confidence intervals; * P<0.05, x P<0.005, and ‡ P<0.001 by pairwise comparison with Sidak correction)

In summary, the most important effect is that of time, there are high chondroitin sulphate levels at day 7, which drop at day 14 and remain low at day 21 (Figure 7-12). Cells from animal 1 produce more chondroitin sulphate than cells from animal 6 (Figure 7-13), and cells from some animals produce significantly more chondroitin sulphate on day 7.

7.3.5 Hyaluronic acid

Very little hyaluronic acid was detected, in most cases the level of hyaluronic acid was below the limit of detection, the errors bars in Figure 7-18, combined with the very low levels indicate this fact. This limited detection resulted in no significant differences being found (Table 7-5).

Table 7-11 Exploratory ANOVA of Hyaluronic Acid results. (No significant differences were found).

Variable / Interaction	F value
Time	F(2,40) = 3.35
Pore structure	F(2,40) = 0.13
Pore size	F(2,40) = 1.88
Animal	F(5,40) = 1.19
Time x Pore structure	F(4,40) = 0.134
Time x Pore size	F(4,40) = 1.88
Time x Animal	F(10,40) = 1.19
Pore structure x Pore size	F(4,40) = 0.45
Pore structure x Animal	F(10,40) = 1.09
Pore size x Animal	F(10,40) = 0.90
Time x Pore structure x Pore size	F(8,40) = 0.46
Time x Pore structure x Animal	F(20,40) = 1.09
Time x Pore size x Animal	F(20,40) = 0.90
Pore structure x Pore size x Animal	F(20,40) = 1

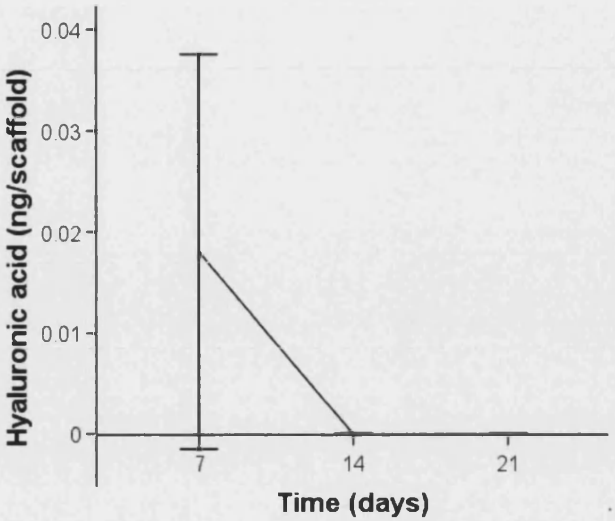

Figure 7-15 Hyaluronic acid content of scaffolds on different days (Error bars show 95% confidence intervals)

7.3.6 Correlations between data

Another way of investigating the relationships is to correlate the results from the different measurements from different days, hyaluronic acid results were excluded due to limited detection (Table 7-12). It should be noted that as the results from different days are determined from different scaffolds, the correlations between results on different days will underestimate the correlations due to intra-individual variability.

The DNA results show that DNA levels on day 1 have a moderate correlation of 0.437 with DNA on day 7, and a small, negative correlation of -0.291 with DNA on day 21. It is also negatively correlated with chondroitin sulphate on day 14 (-0.308) and day 21 (-0.305), and hydroxyproline on day 7 (-0.608). DNA on day 7 is negatively correlated with DNA on day 14 (-0.458) and day 21 (-0.585). It has similar relationships to chondroitin sulphate and hydroxyproline as DNA on day 1, but the correlations appear marginally stronger.

DNA on day 14 strongly predicts DNA on day 21 (0.772), and is also correlated positively with chondroitin sulphate on day 21 (0.300), and hydroxyproline on days 7 (0.313) and 21 (0.384). DNA on day 21 is

correlated with chondroitin sulphate on day 7 (0.281), and day 21 (0.383) and hydroxyproline on days 7 (0.430) and 21 (0.399).

The correlations between the productions of different matrix components are as follows. Chondroitin sulphate at day 7 is correlated with chondroitin sulphate at day 21 (0.461), and hydroxyproline at day 21 (0.443). Chondroitin sulphate at day 14 is only correlated with chondroitin sulphate at day 21 (0.461). On day 21 chondroitin sulphate is correlated with hydroxyproline at days 14 (0.378) and 21 (0.365). No further correlations exist.

Table 7-12 Correlations between DNA, chondroitin sulphate (CS), and hydroxyproline at days 7, 14, and 21 (* P<0.05, ** P< 0.01)

		DNA1	DNA7	DNA14	DNA21	CS7	CS14	CS21	Hy7	Hy14	Hy21
DNA1	Pearson Correlation	1	.437**	-.141	-.291*	-.259	-.308*	-.305*	-.608**	-.030	.059
	Sig. (2-tailed)		.001	.308	.033	.058	.024	.025	.000	.827	.674
	N	54	54	54	54	54	54	54	54	54	54
DNA7	Pearson Correlation	.437**	1	-.458**	-.585**	-.237	-.314*	-.362**	-.620**	-.165	-.123
	Sig. (2-tailed)	.001		.001	.000	.084	.021	.007	.000	.234	.376
	N	54	54	54	54	54	54	54	54	54	54
DNA14	Pearson Correlation	-.141	-.458**	1	.772**	.254	.039	.300*	.313*	.148	.384**
	Sig. (2-tailed)	.308	.001		.000	.063	.782	.027	.021	.287	.004
	N	54	54	54	54	54	54	54	54	54	54
DNA21	Pearson Correlation	-.291*	-.585**	.772**	1	.281*	.141	.386**	.430**	.099	.399**
	Sig. (2-tailed)	.033	.000	.000		.040	.311	.004	.001	.478	.003
	N	54	54	54	54	54	54	54	54	54	54
CS7	Pearson Correlation	-.259	-.237	.254	.281*	1	.032	.383**	.255	.200	.443**
	Sig. (2-tailed)	.058	.084	.063	.040		.820	.004	.062	.147	.001
	N	54	54	54	54	54	54	54	54	54	54
CS14	Pearson Correlation	-.308*	-.314*	.039	.141	.032	1	.461**	.110	.248	.129
	Sig. (2-tailed)	.024	.021	.782	.311	.820		.000	.430	.070	.351
	N	54	54	54	54	54	54	54	54	54	54
CS21	Pearson Correlation	-.305*	-.362**	.300*	.386**	.383**	.461**	1	.151	.378**	.365**
	Sig. (2-tailed)	.025	.007	.027	.004	.004	.000		.276	.005	.007
	N	54	54	54	54	54	54	54	54	54	54
Hy7	Pearson Correlation	-.608**	-.620**	.313*	.430**	.255	.110	.151	1	.028	-.016
	Sig. (2-tailed)	.000	.000	.021	.001	.062	.430	.276		.842	.911
	N	54	54	54	54	54	54	54	54	54	54
Hy14	Pearson Correlation	-.030	-.165	.148	.099	.200	.248	.378**	.028	1	.223
	Sig. (2-tailed)	.827	.234	.287	.478	.147	.070	.005	.842		.104
	N	54	54	54	54	54	54	54	54	54	54
Hy21	Pearson Correlation	.059	-.123	.384**	.399**	.443**	.129	.365**	-.016	.223	1
	Sig. (2-tailed)	.674	.376	.004	.003	.001	.351	.007	.911	.104	
	N	54	54	54	54	54	54	54	54	54	54

7.3.7 Summary of quantitative data

A similar pattern is found across DNA, hydroxyproline and chondroitin sulphate levels. Consistently, time, animal and the interaction between time and animal are the most important parameters (Figure 7-16). DNA levels are also affected by pore size and the interactions: time x pore size, pore size x animal and time x pore size x animal. One prediction is implied to be accurate by the data, but has not been demonstrated explicitly. That prediction is that the glycosaminoglycan : hydroxyproline ratio should fall sharply as the construct ages. This pattern is confirmed by Figure 7-17.

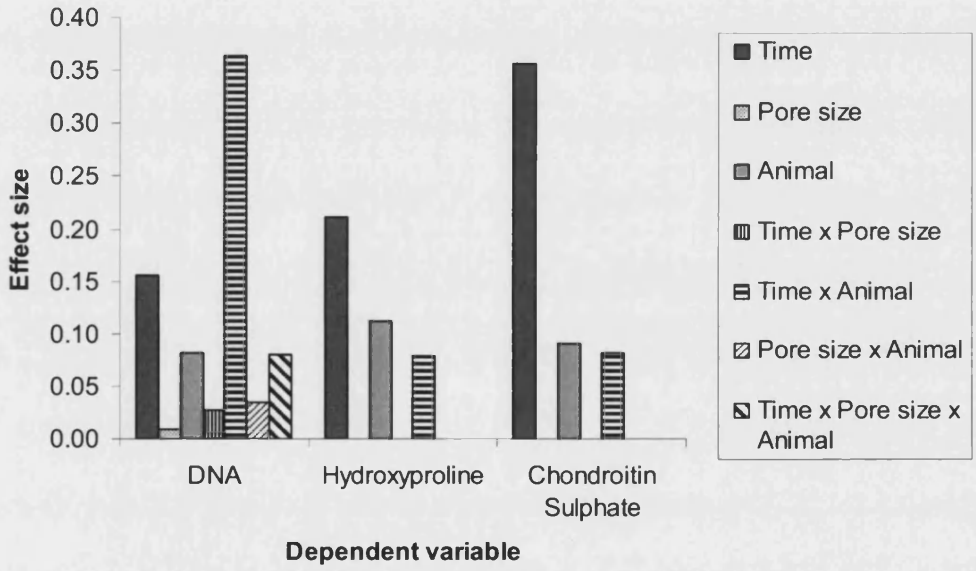

Figure 7-16 Effect sizes of significant independent variables

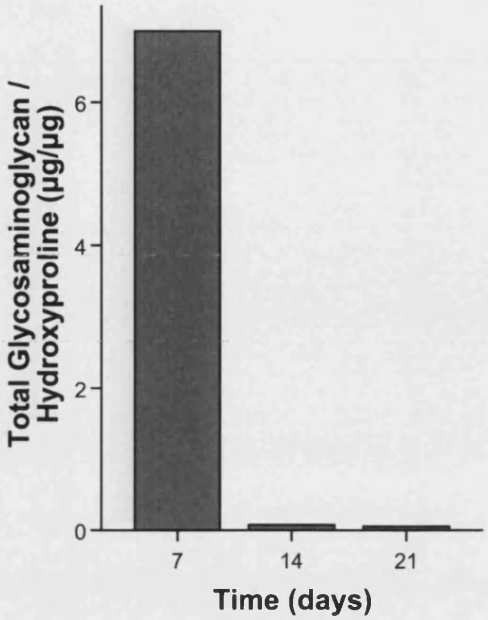

Figure 7-17 Glycosaminoglycan : hydroxyproline ratio

7.4 Discussion

7.4.1 DNA

The amount of DNA is a direct indicator of the cell number. Cell attachment at day 1 appears to be an important determinant of subsequent cell number. In those combinations of pore size and animal that promote high attachment at day 1 cell number gradually drops to below 500ng of DNA per scaffold. It appears that the 300-355µm pores might accelerate this process, but this acceleration might also be accounted for by a slightly higher initial cell number causing a greater drop. However for a majority of the combinations that promote cell attachment, the drop is sharpest between day 7 and 14 (Figure 7-8).

For those combinations that limit cell attachment, cell number appears to be maintained at day 7, at day 14 some of these combinations (typically with larger pore sizes) promote dramatic increase in cell number, whilst some combinations maintain cell number. By day 21 the different combinations appear to converge at a similar level of DNA (Figure 7-8).

This pattern is borne out by the correlations between DNA levels on different days, there is a positive correlation between DNA on day 1 and 7, fitting with cell number being maintained. Then a negative correlation between DNA on day 7 and 14 fits with the sharp drops seen in many of the combinations that promote cell attachment and sharp increases in some of the combinations with limited cell attachment. Levels on day 21 are strongly correlated with levels on day 14, but negatively correlated with levels on days 1 and 7. This could be a remaining effect of factors that promoted cell loss, although as the media was changed regularly perhaps the remaining cells remain inhibited by the high initial cell number in some way. Another factor is that DNA on days 14 and 21 correlates with hydroxyproline on day 7 (Table 7-12), perhaps the greater amount of collagen enables greater cell attachment.

One rule appears to emerge from the patterns described above: above roughly 500ng of DNA cell number drops, below this level cell number is maintained or increased. Larger pore sizes appear to increase the chance of a dramatic increase, although this appears to interact with the animal that the cells came from (Figure 7-7). Collagen levels at day 7 also seem to increase cell number (Table 7-14).

Fluctuations have been described in other systems measuring cell number or cell viability, for instance, Moreau et al (2006), looking at bundles of twisted silk fibres seeded with BMSCs found fluctuations in cell metabolism, and fluctuation, which were also found with BMSCs seeded in collagen gels (Orban et al. 2004). The exact time course of these fluctuations is unclear; it may well be shorter than 7 days, Orban et al (2004) measured cell metabolism more frequently and there does not appear to be a set period for those fluctuations. Moreau et al. (2006) assessed cell metabolism every three days after the first five for 28 days, and their results suggest that the length of the fluctuations increases as the experiment progresses. If these fluctuations take less than 7 days, then the pattern observed in Figure 7-8 which suggests that for some combinations of conditions cell number drops

continually over the three weeks might be misleading, as cell number might have risen on an unobserved day.

It is unclear exactly what these fluctuations indicate in this system. When the scaffolds were checked for signs of infection during the culture period there were normally a large number of cell floating in the media outside the scaffold. Therefore drops in cell number retained within the scaffold might reflect changes in cell attachment, rather than cell death. In 2d culture ligament fibroblasts detach for the surface in order to divide, this is particularly noticeable when the cells are expanding most rapidly following passaging. Two ways of preventing this loss of cells have been investigated for ligament tissue engineering: one is to increase the specific surface area by adding electrospun nanofibres to scaffolds (Sahoo et al. 2006), this appeared to increase cell proliferation, and expression of collagen I, decorin and biglycan; the other approach is to use a physical barrier to prevent the cells from escaping: for instance, wrapping a PGA scaffold seeded with tenocytes with intestinal submucosa and implanting the construct into a tendon defect resulted in a tendon that reached 83% of the breaking strength of normal tendon after 14 weeks implantation (Cao et al. 2002). Either of these approaches might help to support cell retention and thus proliferation if this system were developed further. Another problem might be that the absorption of FCS proteins to silk could be unstable causing cells to detach from the silk as the absorption fails.

One way of disambiguating these fluctuations would be to quantify DNA in the media, and to quantify cell death within the scaffold and in the media (possibly by quantifying lactate dehydrogenase activity by quantifying conversion of a substrate for lactate dehydrogenase that cannot cross an intact cell membrane, allowing indirect quantification of the number of cells with permeable membranes that can be assumed to be dead). If cells are dying then this should apparent, and effort should be focused on preventing cell death, perhaps by increasing mass transfer with a bioreactor; if many viable cells are being lost from the scaffold, then the strategies to limit cell loss are important.

7.4.2 Hydroxyproline

The pattern for hydroxyproline production is much simpler than that for DNA. The most important result is that hydroxyproline levels increase significantly from day 14 to day 21 (Figure 7-9). The second most important result is that cells from some animals synthesise less hydroxyproline than others (Figure 7-10). Finally, different animals appear to respond differently to the effect of time. Cells from animal 4 produce little hydroxyproline initially, but this rapidly increases so that it appears to produce the highest level of hydroxyproline at day 21. Cells from the first three animals produce a lot of hydroxyproline on day 7, and then gradually produce more hydroxyproline. Cells from animals 5 and 6 produce very little hydroxyproline on day 7 and then gradually produce more (Figure 7-11).

The significant increase in hydroxyproline between day 14 and day 21 could be the response of cells responding to mechanical stimulation by fluid shear stress induced by the orbital shaker. The principal reason to suggest this, is that it is known that it takes BMSCs 14 days to upregulate collagen mRNA in response to cyclical tensile strain (Altman et al. 2002b), so a similar period might be necessary for response to other mechanical stresses, including fluid shear stress. That work measured collagen mRNA, whereas in this experiment, hydroxyproline was measured, and the impact of up-regulation in collagen genes might not be apparent until several days had passed to allow sufficient collagen to be synthesised for the change to be detectable. The only result to corroborate this suggestion is the finding of Chen et al (2006) that BMSCs subjected to fluid flow synthesise produce as much mRNA for collagen as BMSCs subjected to fluid flow and cyclical tension.

DNA on days 1 and 7 is negatively correlated with hydroxyproline on day 7 (Table 7-12). Cells from some animals lay down collagen prior to day 7 whilst not proliferating, and then proliferate on subsequent days. If the higher cell number for cells from animals 4, 5 and 6 reflects greater proliferation (with many cells being lost to the media) then this would explain their lower

collagen synthesis. In bone tissue engineering there is thought to be a tension between proliferation and matrix synthesis, a similar tension might exist in ligament engineering, this has been reported for tenocytes at high cell densities (Zayas and Schwarz 1992). After day 7 this trend is reversed and hydroxyproline on day 7 correlates positively with DNA on day 14 and day 21, perhaps the additional collagen for cells from the first three animals allows better attachment to the scaffolds, increasing cell number. The lack of correlations between hydroxyproline on day 14 and DNA might be explained by the lack of significant differences between cells from different animals on day 14 (Figure 7-11). Hydroxyproline on day 21 is positively correlated with DNA on days 14 and 21, suggesting that by this stage cell number has a positive impact on collagen synthesis.

The other striking correlation is that of chondroitin sulphate at 7 days with hydroxyproline at 21 days; this is in contrast to the lack of correlation between hydroxyproline at days 7 or 14 with day 21. This is further evidence that there at least two stages to ligament regeneration. Chondroitin sulphate might be useful biomarker for this first stage, possibly in conjunction with other putative biomarkers for the first stage suggested by the work by Chen et al (2006), such as mRNA for integrins, and heat shock protein 70. Further work might be able to identify how non-destructive assays might be used to predict the ligament engineering process and account for some of the individual differences between cells from different animals. This result also raises questions about the utility of many short term studies of ligament and tendon cell biology, where the principal outcome measure is collagen production; if it were confirmed that collagen content in the first two weeks was a poor predictor of subsequent collagen content in other systems then measuring collagen would be of limited importance for the first two weeks, and cell biology studies that wanted to study collagen production would have to run for longer than two weeks.

7.4.3 Chondroitin sulphate

In some respects the pattern of the chondroitin sulphate content of the matrices is the opposite of that of hydroxyproline. In particular, chondroitin sulphate levels are significantly higher at day 7 than days 14 and 21 (Figure 7-12). Cells from animal 1 produce significantly more chondroitin sulphate than cells from animal 6 (Figure 7-13). On day 7, cells from animal 1 appear to produce more chondroitin sulphate than cells from animals 3, 4, 5, and 6; and cells from animal 2 produce more than cells from animals 3 and 6 (Figure 7-14). Then overall trend is for chondroitin sulphate levels to drop over the course of the experiment.

DNA at day 7 and at day 14 is negatively correlated with chondroitin sulphate at days 14 and 21 (Table 7-12). This might be the result of cells synthesising chondroitinases to remove chondroitin sulphate after day 7, which would fit with the sharp drop. DNA at days 14 and 21 is positively correlated with chondroitin sulphate at day 21, which might indicate that after day 14 cells begin to synthesise more chondroitin sulphate at higher cell numbers. Chondroitin sulphate at day 21 is correlated with hydroxyproline levels at days 14 and 21, suggesting that more collagen might be result in more chondroitin sulphate, possibly as the chondroitin sulphate containing proteoglycans have more collagen to bind to. Chondroitin sulphate at day 21 is also correlated with chondroitin sulphate at days 7 and 14. Given the absence of a correlation between chondroitin sulphate at days 7 and 14, this suggests that levels of chondroitin sulphate at day 21 is a combination of two processes, for instance, retention of chondroitin sulphate from day 14, and synthesis of new chondroitin sulphate, reflecting the correlation with day 7.

Chondroitin sulphate at day 7 is an interesting predictor of the outcome variables at day 21 (Table 7-12). Of the outcome variables prior to day 21, it alone is correlated with DNA, chondroitin sulphate and hydroxyproline levels at day 21. There are a number of possible explanations for these correlations:

- It is possible that higher initial levels of chondroitin sulphate improve the assembly of the extracellular matrix as glycosaminoglycans, they are a couple of possible mechanisms known for this: glycosaminoglycans self-aggregate (Scott 1992), more chondroitin sulphate might provide more binding sites for this self-aggregation to encourage matrix assembly; it is also known that the quantity of some polysaccharides such as alginate or hyaluronic acid alters the self assembly of collagen fibrils (Tsai et al. 2006).
- More chondroitin sulphate might indicate greater levels of the small proteoglycans that bind TGF-β1 (Hildebrand et al. 1994), this might result in alteration of the TGF- β1 signal, changing cell behaviour.
- It could indicate other differences between proteoglycans such as a change in the biglycan to decorin ratio, as biglycan binds two chondroitin sulphate chains (Young et al. 2002), and decorin only one (Iozzo 1998)
- Alternatively, the correlation might not be a cause of the improved properties at 21 days, and instead be due to some other property that results in elevated chondroitin sulphate levels.

Chondroitin sulphate merits further investigation as a possible outcome marker for the initiation of ligament engineering, and a way of predicting something of the individual differences.

7.4.4 Hyaluronic acid

The striking result from the analysis of hyaluronic acid production is the very low levels of hyaluronic acid produced. This might be a limitation of the sensitivity of the HPLC assay, but much more chondroitin sulphate was detected suggesting that hyaluronic acid production was, in fact, much lower. This result shows that this process for ligament engineering produces results dissimilar to those that might be expected for embryonic ligament. This might be because it is not the ligament fibroblasts that are laying down hyaluronic acid in the embryo. Hyaluronic acid is laid down early in development, in part to facilitate to cell migration (Nathanson 1990). It is known that in other

mesodermic tissues, primitive mesenchymal cells lose the ability to synthesise hyaluronic acid (Toole et al. 1989).

If ligament fibroblasts do lose most of their ability to synthesise hyaluronic acid then there is possibly a paradox if fibrotic tissue is associated with elevated levels of hyaluronic acid (Riley et al. 1994) and this is not produced by ligament fibroblasts. The obvious alternative is that hyaluronic acid is produced by other cells. Mesenchymal stem cells migrating to the wound site would be one option, but these seem only to migrate to the surface of tendons (Zavahir et al. 2001). Alternatively, the same study identified a new class of cells in the tendon that respond to injury by sending out lots of cytoplasmic processes that appear to force the collagen fibrils apart. These cells may well be producing hyaluronic acid to force the fibrils apart. Another possibility is that this system could be missing the growth factors required to produce hyaluronic acid. Macrophages appear to produce growth factors the stimulate hyaluronic acid production by synovial fibroblasts (Pulkki 1986; Wells et al. 1992); TGF-β1, interleukin-1, and tumour necrosis factor α appear to be important mediators of this stimulation (Haubeck et al. 1995; Konttinen et al. 1991).

7.4.5 Hydroxyproline : glycosaminoglycan ratio

These results show a partial confirmation of the prediction that the glycosaminoglycan : hydroxyproline ratio should drop rapidly, although in absolute terms the ratio of glycosaminoglycan : hydroxyproline is higher than in the published reports (Scott et al. 1981). There are several possible explanations for this: the Scott et al (1981) paper only measures this ratio following birth, and the initiation of tissue engineering should perhaps be analogous to embryonic tissue when it would be anticipated that chondroitin sulphate levels would be higher; the higher level could be indicative of fibrotic development, as tendonitis results in elevated levels of glycosaminoglycans (Riley et al. 1994); or the synthesis of ECM might be appropriate, but chondroitin sulphate might be adsorbed better onto the scaffold. To distinguish these possibilities it would be helpful to have more than three

weeks' data, and have measurements for other indicators of fibrosis such as fibril diameter.

7.4.6 Possible improvements to experimental design

It should be noted that statistics are all based on mathematical models, and make a number of simplifications and assumptions about the data and the experiment, they are only as useful as the experimental design, and should not be taken as a definitive model of how a particular experiment works. To quote one introduction to statistics: "all statistical models are wrong" (Crawley 2005). In this case, more information about the animals that provided the cells would be useful (gender, age, location of farm, breed, farming methodology, etc.) to see if these differences could explain the difference seen between cells from different animals.

With the benefit of hindsight, the results of this experiment might have been clearer if more time had been spent optimising the cell number with which to seed the scaffolds. A lower cell number should have promoted a growth phase so the kinetics of cell growth on the scaffolds more closely resembled the textbook examples.

A third area for improvement would have been to identify additional useful assays, such as quantifying lactate dehydrogenase to quantify cell death. This would help to explain why cell number fluctuates: were the cells dying, or just de-attaching from the scaffold? Assays of fibrosis such as collagen type III : type I ratio would be useful in further quantifying what sort of matrix the ligament fibroblasts were producing.

Finally, given that cell number over long durations appears to fluctuate, these fluctuations would be better characterised by more frequent sampling. As this would require a large number of scaffolds to be sacrificed, a better solution would be to adapt a non-destructive test of cell viability to work with 3d scaffolds, allowing the fluctuations to be tracked better without sacrificing a large number of scaffolds.

7.5 Conclusions

Overall, the combination of large sample size with factorial ANOVA and correlations enabled a large amount of useful information to be gained about the initiation of ligament engineering. By considering several independent variables it is possible to determine which are the most important, and also how the variables interact. By using a large sample size it is possible to correlate the outcomes, which gives new information about how ligament engineering works. Of the six initial predictions about the outcome (Section 7.1.4), four have been met at least partially. The level of chondroitin sulphate dropped; the level of hydroxyproline increased; the ratio of glycosaminoglycan to hydroxyproline fell rapidly, and for some combinations of conditions, the cell number fluctuated. The two results that were not predicted were that for some combinations of animal and pore size cell number would appear to drop; and that almost no hyaluronic acid was detected.

The results show that the differences between cells from different animals are important in determining both proliferation and matrix synthesis of ligament fibroblasts. The effect of differences between animals varies with time. Pore size, and the two and three way interactions between pore size, animal and time only affect proliferation, not matrix synthesis. Pore structure has no detectable effect in this study.

8 Conclusions and Future Work

8.1 Introduction

This thesis has reported a new porous silk scaffold that allows independent control of pore size and pore structure, and the use of this scaffold to better understand the role of pore size and structure in ligament regeneration. The main findings of this work are summarised below, followed by discussions of how this work fits into the wider picture, and how this work could be taken forward.

8.2 Conclusions

8.2.1 Control of pore structure from film-like to fibrous in porous silk scaffolds

The solubility of regenerated silk fibroin in aqueous formic acid, acetic acid and hexafluoroisopropanol solutions was investigated. It was found that silk was only soluble in 20% (v/v) aqueous formic acid.

Porous scaffolds were prepared using aqueous formic acid by using salt leaching. Initially there were problems with variability in scaffold structure within batches. By varying the process used to make the scaffolds, it was discovered that by adding the silk fibroin solution to the salt, rather than salt to the silk fibroin, repeatable scaffold structures were obtainable, and that the pore structure of these scaffolds became more fibrous as the percentage of silk in the solvent was reduced.

To further understand the role of salt in the scaffold fabrication process, scaffolds were made with silk fibroin solutions saturated with salt. Aqueous formic acid solutions saturated with salt were tested to see if silk fibroin would dissolve in them. Silk fibroin dissolved in two concentrations of formic acid: 40% and 80%. In contrast to the fibrous pore structure of scaffolds made with 20% formic acid, scaffolds made with both solutions had rather

"cubic" pore structures, reflecting the particle structure of the salt crystals that the solution was added to. The difference between the 40% and 80% formic acid solutions was that the scaffolds made with 40% formic acid had a number of faces missing reflecting the greater solubility of salt in 40% formic acid.

FTIR was used to characterise the crystalline structure of the silk in the scaffolds. Peaks at $1630cm^{-1}$, $1520cm^{-1}$, and $1270cm^{-1}$ indicate that the silk was in the silk ii form. Spectra from scaffolds made with 20% formic acid appear identical to scaffolds made with 100% formic acid.

Porosity was investigated by sectioning scaffolds, then using image analysis to quantify the percentage of images of the stained sections that was silk. The scaffolds compared were made with: 7.5% w/v silk fibroin in 20% formic acid, 10% w/v silk fibroin in 20% formic acid, and 10% w/v silk fibroin in 100% formic acid. The porosity for the scaffolds was: 0.964 +/- 0.009 for 10% silk dissolved in formic acid; 0.971 +/- 0.005 for 10% silk in 20% formic acid; and 0.964 +/- 0.005 for 7.5% silk in 20% formic acid. The differences between the scaffold types were not significant.

To confirm that these scaffolds were suitable for tissue engineering, cell attachment and proliferation were assessed. Twelve scaffolds were made with each of: 7.5% w/v silk fibroin in 20% formic acid, 10% w/v silk fibroin in 20% formic acid, and 10% w/v silk fibroin in 100% formic acid. To investigate the effect of linking a peptide containing the RGD sequence, the twelve scaffolds with each structure were divided into three equal groups, one group was decorated with RGD using EDC:NHS, one was reacted with EDC:NHS alone and one was not reacted. The results showed that at 24 hours attachment was greatest to scaffolds made with 10% silk in 100% formic acid. Scaffold decoration made no significant difference.

Cell attachment was investigated with ligament fibroblasts and osteoblast and chondrocyte cell lines after 7 days proliferation on the scaffolds made with: 7.5% w/v silk fibroin in 20% formic acid, 10% w/v silk fibroin in 20%

formic acid, and 10% w/v silk fibroin in 100% formic acid. Ligament fibroblasts proliferated better on scaffolds made with 10% silk in 100% formic acid than scaffolds made with 10% silk in 20% formic acid. Osteoblast and chondrocyte cell lines grew better on scaffolds made with 10% silk in 100% formic acid than scaffolds made with 7.5% in 20% formic acid.

8.2.2 Implementation of HPLC GAG analysis

In order to quantify GAG produced by ligament fibroblasts, a published HPLC protocol was adapted for use as a tissue engineering analysis protocol. In order, to do this first some of the results of the paper were observing the retention times of chondroitin sulphate disaccharides produced by enzymatic digestion relative to purchased GAG disaccharide standards. The retention times were similar, but the quantity of enzyme appeared to affect the relative heights of the peaks.

In order to optimise the digestion protocol, hyaluronic acid, and chondroitin sulphates C were digested with 0.025U of chondroitinase ABC over half and hour to 16 hours. Surprisingly, peaks that were apparent after 0.5 hours digestion of chondroitin sulphate disappeared after 1 and 2 hours digestion, reappearing at 4 hours digestion. The hyaluronic acid peak showed a similar pattern, but the peak was largest after 16 hours digestion. It was therefore decided to use 16 hour digestions.

A final issue examined was how to digest the tissue engineered construct prior to GAG analysis. The solution resulting from a blank papain digestion (i.e. a papain digestion without a construct to digest) were analysed by HPLC, these revealed several peaks that might confound the HPLC analysis. By dissolving the standards in the blank papain digestion solution it was found that the assay could still be successfully calibrated using the GAG disaccharides.

8.2.3 Effect of pore size, pore structure, and animal on ligament fibroblasts in porous silk scaffolds

The scaffolds developed in Chapter 6 were used to examine the effect of pore size (180-250μm, 300-355μm, and 425-500μm) and pore structure (7.5% silk 20% formic acid, 10% silk 20% formic acid, and 10% silk 100% formic acid) on cell number (quantified as the amount of DNA present), and matrix synthesis: collagen (quantified as hydroxyproline), and glycosaminoglycans. Due to the number of primary cells needed, cells from 6 animals were used. DNA was quantified after 1, 7, 14 and 21 days. Glycosaminoglycans and hydroxyproline were quantified at 7, 14 and 21 days. Therefore in addition to pore size, pore structure, and animal, time was also analysed as an independent variable.

The results of quantifying DNA showed that time x animal interaction was the most important determinant of DNA levels, explaining 36% of the variance in the population, followed by time (16%), animal (8%), time x pore size x animal (8%), time x pore size (3%), pore size x animal (3%), and pore size (1%). Cells from different animals attached differently to the scaffolds, cells from the first three animals attached better, there was a trend for cell to attach better to cells with the largest pores, but this was limited to cells from a couple of animals. At day 7, the overall cell number was similar to day 1, those cells from animals with the best attachment on day 1, retained the highest cell number, although for the cells from animals for which the large pores had improved attachment, large pores now resulted in significantly lower cell number. On day 14, cell number was again similar. However, two of the cells from animals with the highest cell number on days 1 and 7, now had lower cell number than some, or, all of the other cells from four animals, and cell number for the cells from first three animals had increased. For cells from one animal, the middle pore size performed best; for another the largest pore size worked best, and for a third the largest pore size was better than the smallest. At day 21 the overall cell number decreased. There was a significant difference between the animals, but this could not be identified more precisely.

The largest effect on hydroxyproline levels is time, accounting for 21% of the variance in the population. Hydroxyproline levels are significantly higher at day 21 than day 14 or day 7. Animal is the second most important effect (11%), cells from animal 6 produced less hydroxyproline than cells from the first three, and cells from animal 5 produced less than cells from animal 3. The final significant effect is time x animal (8%), cells from animal 2 produced more hydroxyproline on day 7 than cells from the last three animals. On day 21, cells from animal 6 produced less than cells from animals 1, 3 and 4, and cells from animal 4 more than cells from animals 2, 5, and 6.

With chondroitin sulphate, time was again the largest effect (36%), CS was higher at day 7 than day 14 or 21. Animal was again the second most important effect (9%). Overall, cells from animal 1 produced more chondroitin sulphate than cells from animal 6. Time x animal accounted for 8% of the variance in the population. On day 7, cells from animal 1 produced more CS than cells from the last four animals, and cells from animal 2 more than cells from animals 2 and 6. Very little hyaluronic acid was produced, and no significant differences were found.

When the results from different days were correlated, it was found that DNA on day 1 positively correlated with DNA on day 7, and negatively with DNA on day 21, negatively with CS on day days 14 and 21, and negatively with hydroxyproline on day 7. in addition to the previous correlation, DNA on day 7 was also negatively correlated with DNA on day 14, and day 21, and with chondroitin sulphate on days 14 and 21, and hydroxyproline on day 7. DNA on day 14 was positively correlated with DNA on day 21, with CS on day 21 and with hydroxyproline on days 14 and 21. DNA on day 21 was positively correlated with CS on days 7, and 21, and hydroxyproline on days 7 and 21. CS on day 7 was correlated with CS on day 21 and hydroxyproline on day 21. CS on day 14 was positively correlated with CS on day 21. CS on day 21 was positively correlated with hydroxyproline on day 14 and day 21. The only

variable from the first three time points to be correlated with all three outcomes on day 21 was CS on day 7.

8.3 Relevance of this work to ligament engineering

Ligament engineering is attempting to repair ligaments *ex vivo*. In order to understand how this work fits into the wider picture it is useful to consider ligaments *in vivo* and how engineers might try to replicate the *in vivo* environment (Figure 7-1).

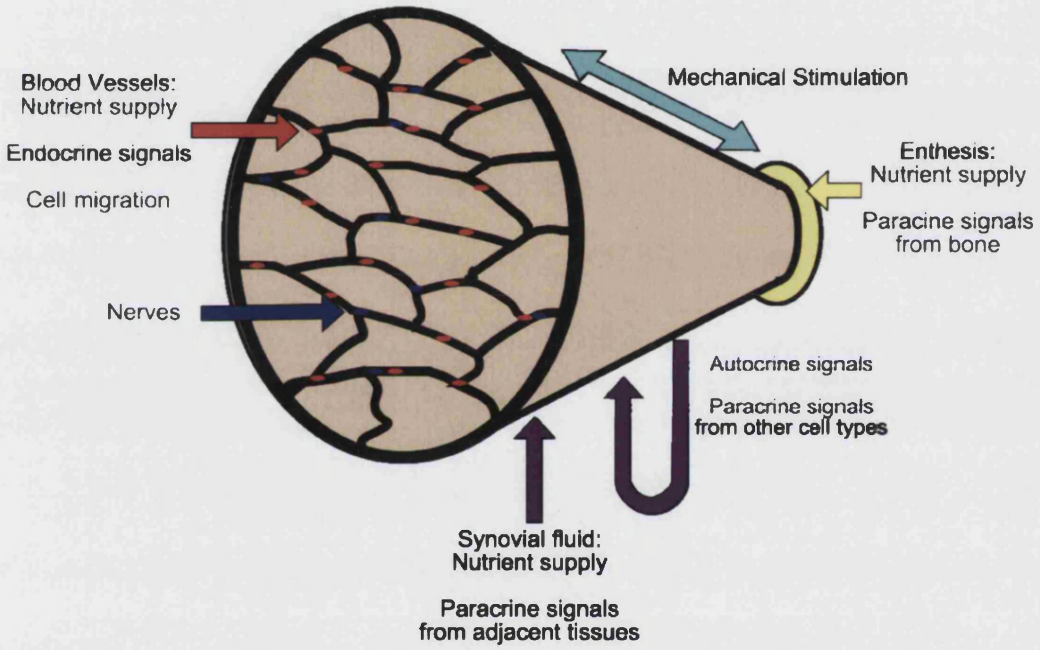

Figure 8-1 Overview of the ligament's environment *in vivo*

This thesis has focused on understanding the effects of pore size and pore structure on ligament engineering. This could be expected to alter nutrient supply by changing the mass transfer properties of the material, and cell response and autocrine signalling if the cells can detect differences in the materials. The results showed that pore size had a small effect on cell number, but not matrix synthesis. This absence of an effect might be due to the absence of some other factor that is present *in vivo*, in bone, mechanical stimulation is required for pore size to affect bone regeneration (Karageorgiou and Kaplan 2005). Instead, it was found that variation

between animals was consistently important in determining cell number and matrix synthesis, further, animal (along with time) interacted with pore size in determining cell number. This variation between cells from different animals might confound biomaterials experiments, a positive result in one experiment and negative result in an attempted replication might be the result of individual differences between animals.

The correlation results suggest a major issue for ligament cell biology as it is currently studied. If early collagen synthesis does not correlate with subsequent collagen synthesis, then the usefulness of short term (two week) cell biology experiments where collagen synthesis is the major outcome is questionable. These results also suggest that chondroitin sulphate levels might be more important in the early stages of ligament repair.

These results show the importance of determining how cells from different animals respond to different materials. After time, animal was the most important independent variable in determining ECM synthesis (Figure 7-19). The interaction between time and animal was also very important. As ligaments are predominately made out of collagen, collagen production is normally considered the most important outcome for ligament tissue engineering. In this system, the mean hydroxyproline level at day 21 differs by a factor of 4 depending on which animal the cells came from(Figure 7-14). This result has especially important implications for potential therapies where autologous cells might be used as a key problem will be predicting their behaviour. The problems this would pose are two fold: firstly logistical, without more knowledge it will be difficult to predict how long it will take to synthesise new tissue for any given patient, making it difficult to set a date for surgery; second, it will be difficult to design biomaterials that degrade at a similar rate to the synthesis of new ECM if the rate of ECM production varies so much. One possible solution to the second problem would be to use materials that allow the cells control the degradation rate. Silk degrades enzymatically (Horan et al. 2005a), but it is unclear which enzymes are responsible for this *in vivo*. Materials such as collagen and fibrin are degraded by well understood biochemical pathways, and it might be possible

to produce collagen or fibrin based biomaterials that respond to different levels of ECM synthesis by degrading at different rates.

This work suggests that pore size is of limited importance in determining the behaviour of ligament fibroblasts. Pore size has a very limited effect on cell number, and interacts with time and differences between cells from different animals to produce other small effects on cell number, but in this system, dramatic differences in response to pore size were not observed. Possibly, this is due to the absence of mechanical stimulation. Despite the extensive literature of pore size effects on osteogenesis *in vivo*, it has not been possible to identify such effects *in vivo* in the absence of mechanical loading (Itala et al. 2001). In this system the only loading is driven by the orbital shaker that the six well plates were incubated on. The fluid flow supplied by this system might be inadequate to drive pore size effects. No effect of pore structure was found, although it was found in the preliminary work on cell attachment and proliferation in Chapter 6. Two possibilities stand out: the scaffolds used in Chapter 6 had a larger diameter than the scaffolds used in this study. It is possible that pore structure effects are dependent on the scale of the ligament engineering system, with different pore structures having different influences at different scales, and these differences being undetectable at small scale. Otherwise, it could be that the wider range of salt particle sizes used in Chapter 6 (125-425μm) enabled pore structure to have an effect.

8.4 Future work

There are many aspects of the ligament *in vivo* not addressed by this work. Perhaps the most important are the paracrine signals from adjacent tissue, muscle-tendon crosstalk is known to be important to tendon development (Rodriguez-Guzman et al. 2007), bone-ligament crosstalk is probably important to ligament development; and mechanical stimulation which was discussed in Section 2.3. This section will consider how this work might be extended to see if mechanical stimulation is necessary for pore size to affect ligament repair, and to what extent this generalises to other materials.

8.4.1 Bioreactor design

Fluid flow to enhance mass transfer, and cyclical mechanical tensile strain are the two parameters that have been shown to be important for ligament engineering (Altman et al. 2002b; Chen et al. 2006). Less is known about the ideal characteristics of cyclical mechanical tensile strain to best stimulate regeneration. Low tensile strain (2-8% strain) decreases levels of inflammation markers in osteoblast-like periodontal ligament cells, whereas higher levels of strain (>12.5% strain) increase inflammation markers (Agarwal et al. 2003). Currently, 10% strain is typically used for ligament engineering, but it seems prudent to investigate multiple strains, on the basis of Agarwal et al. (2003), 6 and 12% with an unstrained control seem like sensible starting parameters.

8.4.2 Biomaterials

Silk scaffolds with variable pore size have been described in this paper, but an important question is whether these results are generalisable to other materials. In order to answer this question, scaffolds made from alternative materials should be tested. Scaffolds can be made with salt leaching using poly-lactic-co-glycolic acid (Suh et al. 2002), suggesting an useful contrast between the two materials. During this work the cell attachment and retention processes could be studying further in order to optimise attachment and retention of the cells.

8.4.3 Experimental design

Once the component systems had been optimised, this new study would resemble this study, five independent variables would be considered: time, biomaterial, mechanical regime, pore size and animal/subject. Ideally, human cells would be used so as to maximise clinical relevance. Instead of the time points used in this study, matrix synthesis would be studied at one, three and six weeks. This would demonstrate to what extent the results from one and three weeks correlated with the results at six weeks. It would be useful to

extend the matrix synthesis outcome measures to quantify the collagen I : III ratio, to measure levels of CS proteoglycans, and to examine histological measures of fibrosis such as fibril diameter. These additional measurements would help to either eliminate or confirm some of the main hypothesises generated in this work.

References

Agarwal S, Long P, Seyedain A, Piesco N, Shree A, Gassner R. 2003. A central role for the nuclear factor-kappaB pathway in anti-inflammatory and proinflammatory actions of mechanical strain. *FASEB J* 17(8):899-901.

Altman GH, Diaz F, Jakuba C, Calabro T, Horan RL, Chen J, Lu H, Richmond J, Kaplan DL. 2003. Silk-based biomaterials. *Biomaterials* 24(3):401-16.

Altman GH, Horan RL, Lu HH, Moreau J, Martin I, Richmond JC, Kaplan DL. 2002a. Silk matrix for tissue engineered anterior cruciate ligaments. *Biomaterials* 23(20):4131-41.

Altman GH, Horan RL, Martin I, Farhadi J, Stark PR, Volloch V, Richmond JC, Vunjak-Novakovic G, Kaplan DL. 2002b. Cell differentiation by mechanical stress. *FASEB J* 16(2):270-2.

Altman GH, Lu HH, Horan RL, Calabro T, Ryder D, Kaplan DL, Stark P, Martin I, Richmond JC, Vunjak-Novakovic G. 2002c. Advanced bioreactor with controlled application of multi-dimensional strain for tissue engineering. *J Biomech Eng* 124(6):742-9.

Amiel D, Frank C, Harwood F, Fronek J, Akeson W. 1984. Tendons and ligaments: a morphological and biochemical comparison. *J Orthop Res* 1(3):257-65.

Amiel D, Kleiner JB, Roux RD, Harwood FL, Akeson WH. 1986. The phenomenon of "ligamentization": anterior cruciate ligament reconstruction with autogenous patellar tendon. *J Orthop Res* 4(2):162-72.

Anderson AF, Dome DC, Gautam S, Awh MH, Rennirt GW. 2001. Correlation of anthropometric measurements, strength, anterior cruciate ligament size, and intercondylar notch characteristics to sex differences in anterior cruciate ligament tear rates. *Am J Sports Med* 29(1):58-66.

Archambault JM, Elfervig-Wall MK, Tsuzaki M, Herzog W, Banes AJ. 2002. Rabbit tendon cells produce MMP-3 in response to fluid flow without significant calcium transients. *J Biomech* 35(3):303-9.

Asakura T, Kuzuhara A, Tabeta R, Saito H. 1985. Conformation Characterization of Bombyx mori Silk Fibroin in the Solid State by High-Frequency 13C Cross Polarization-Magic Angle Spinning NMR, X-ray Diffraction, and Infrared Spectroscopy,. *Macromolecules* 18:1841-1845.

Atsumi T, Miwa Y, Kimata K, Ikawa Y. 1990. A chondrogenic cell line derived from a differentiating culture of AT805 teratocarcinoma cells. *Cell Differ Dev* 30(2):109-16.

Aukland K. 1991. Distribution volumes and macromolecular mobility in rat tail tendon interstitium. *Am J Physiol* 260(2 Pt 2):H409-19.

Aukland K, Tenstad O, Wiig H. 2001. Distribution spaces for hyaluronan and albumin in rat tail tendons. *Am J Physiol Heart Circ Physiol* 281(4):H1589-97.

Barber FA. 2003. Should allografts be used for routine anterior cruciate ligament reconstructions? *Arthroscopy* 19(4):421.

Barkhausen T, van Griensven M, Zeichen J, Bosch U. 2003. Modulation of cell functions of human tendon fibroblasts by different repetitive cyclic mechanical stress patterns. *Exp Toxicol Pathol* 55(2-3):153-8.

Baylink D, Wergedal J, Thompson E. 1972. Loss of proteinpolysaccharides at sites where bone mineralization is initiated. *J Histochem Cytochem* 20(4):279-92.

Benjamin M, Kumai T, Milz S, Boszczyk BM, Boszczyk AA, Ralphs JR. 2002. The skeletal attachment of tendons--tendon "entheses". *Comp Biochem Physiol A Mol Integr Physiol* 133(4):931-45.

Benjamin M, Ralphs JR. 1998. Fibrocartilage in tendons and ligaments--an adaptation to compressive load. *J Anat* 193 (Pt 4):481-94.

Benjamin M, Ralphs JR. 2000. The cell and developmental biology of tendons and ligaments. *Int Rev Cytol* 196:85-130.

Berthod F, Saintigny G, Chretien F, Hayek D, Collombel C, Damour O. 1994. Optimization of thickness, pore size and mechanical properties of a biomaterial designed for deep burn coverage. *Clin Mater* 15(4):259-65.

Bigerelle M, Anselme K. 2005. Bootstrap analysis of the relation between initial adhesive events and long-term cellular functions of human osteoblasts cultured on biocompatible metallic substrates. *Acta Biomater* 1(5):499-510.

Bjornsson S. 1993. Simultaneous preparation and quantitation of proteoglycans by precipitation with alcian blue. *Anal Biochem* 210(2):282-91.

Bollen S. 1998. Ligament injuries of the knee--limping forward? *Br J Sports Med* 32(1):82-4.

Brandt KD, Radin EL, Dieppe PA, van de Putte L. 2006. Yet more evidence that osteoarthritis is not a cartilage disease. *Ann Rheum Dis* 65(10):1261-4.

Bray RC, Leonard CA, Salo PT. 2003. Correlation of healing capacity with vascular response in the anterior cruciate and medial collateral ligaments of the rabbit. *J Orthop Res* 21(6):1118-23.

Brigman BE, Hu P, Yin H, Tsuzaki M, Lawrence WT, Banes AJ. 1994. Fibronectin in the tendon-synovial complex: quantitation in vivo and in vitro by ELISA and relative mRNA levels by polymerase chain reaction and northern blot. *J Orthop Res* 12(2):253-61.

Bunning TJ, Jiang H, Adams WW, Crane RL, Farmer B, Kaplan D. 1994. Applications of Silk. In: Kaplan D, Adam WW, Farmer B, Viney C, editors. *Silk Polymers*. ACS (Washington, DC) p 353-358.

Calabro A, Benavides M, Tammi M, Hascall VC, Midura RJ. 2000. Microanalysis of enzyme digests of hyaluronan and chondroitin/dermatan sulfate by fluorophore-assisted carbohydrate electrophoresis (FACE). *Glycobiology* 10(3):273-81.

Calve S, Dennis RG, Kosnik PEn, Baar K, Grosh K, Arruda EM. 2004. Engineering of functional tendon. *Tissue Eng* 10(5-6):755-61.

Canty EG, Lu Y, Meadows RS, Shaw MK, Holmes DF, Kadler KE. 2004. Coalignment of plasma membrane channels and protrusions (fibripositors) specifies the parallelism of tendon. *J Cell Biol* 165(4):553-63.

Cao Y, Liu Y, Liu W, Shan Q, Buonocore SD, Cui L. 2002. Bridging tendon defects using autologous tenocyte engineered tendon in a hen model. *Plast Reconstr Surg* 110(5):1280-9.

Cardinal RN, Aitken MRF. 2006. *Anova for the Behavioral Sciences Researcher*. Lawrence Erlbaum Associates (Florence, KY).

Charulatha V, Rajaram A. 2003. Influence of different crosslinking treatments on the physical properties of collagen membranes. *Biomaterials* 24(5):759-67.

Chen J, Altman GH, Karageorgiou V, Horan R, Collette A, Volloch V, Colabro T, Kaplan DL. 2003. Human bone marrow stromal cell and ligament fibroblast responses on RGD-modified silk fibers. *J Biomed Mater Res A* 67(2):559-70.

Chen J, Horan RL, Bramono D, Moreau JE, Wang Y, Geuss LR, Collette AL, Volloch V, Altman GH. 2006. Monitoring Mesenchymal Stromal Cell Developmental Stage to Apply On-Time Mechanical Stimulation for Ligament Tissue Engineering. *Tissue Eng*.

Chen SC, Wu YC, Mi FL, Lin YH, Yu LC, Sung HW. 2004. A novel pH-sensitive hydrogel composed of N,O-carboxymethyl chitosan and alginate cross-linked by genipin for protein drug delivery. *J Control Release* 96(2):285-300.

Chiquet-Ehrismann R, Tucker RP. 2004. Connective tissues: signalling by tenascins. *Int J Biochem Cell Biol* 36(6):1085-9.

Cho SW, Kim IK, Lim SH, Kim DI, Kang SW, Kim SH, Kim YH, Lee EY, Choi CY, Kim BS. 2004. Smooth muscle-like tissues engineered with bone marrow stromal cells. *Biomaterials* 25(15):2979-86.

Clark JM, Sidles JA. 1990. The interrelation of fiber bundles in the anterior cruciate ligament. *J Orthop Res* 8(2):180-8.

Cleland RL, Sherblom AP. 1977. Isolation and physical characterization of hyaluronic acid prepared from bovine nasal septum by cetylpyridinium chloride precipitation. *J Biol Chem* 252(2):420-6.

Cohen J. 1988. *Statistical power analysis for the behavioral sciences.* Erlbaum (Hillsdale, NJ).

Collombel C, Damour O, Gagnieu C, Poinsignon F, Echinard C, Marichy J; Centre National de la Recherche (Paris, FR), assignee. 1992. *Biomaterials with a base of mixtures of collagen, chitosan and glycosaminoglycans, process for preparing them and their application in human medicine*. USA patent 5,166,187.

Colter DC, Sekiya I, Prockop DJ. 2001. Identification of a subpopulation of rapidly self-renewing and multipotential adult stem cells in colonies of human marrow stromal cells. *Proc Natl Acad Sci U S A* 98(14):7841-5.

Cooper JA, Jr., Bailey LO, Carter JN, Castiglioni CE, Kofron MD, Ko FK, Laurencin CT. 2006. Evaluation of the anterior cruciate ligament, medial collateral ligament, achilles tendon and patellar tendon as cell sources for tissue-engineered ligament. *Biomaterials* 27(13):2747-54.

Cooper JA, Lu HH, Ko FK, Freeman JW, Laurencin CT. 2005. Fiber-based tissue-engineered scaffold for ligament replacement: design considerations and in vitro evaluation. *Biomaterials* 26(13):1523-32.

Corsi A, Xu T, Chen XD, Boyde A, Liang J, Mankani M, Sommer B, Iozzo RV, Eichstetter I, Robey PG, Bianco P, Young MF. 2002. Phenotypic effects of biglycan deficiency are linked to collagen fibril abnormalities,

are synergized by decorin deficiency, and mimic Ehlers-Danlos-like changes in bone and other connective tissues. *J Bone Miner Res* 17(7):1180-9.

Crawley MJ. 2005. *Statistics: An Introduction using R*. Wiley.

Cribb AM, Scott JE. 1995. Tendon response to tensile stress: an ultrastructural investigation of collagen:proteoglycan interactions in stressed tendon. *J Anat* 187 (Pt 2):423-8.

Cristino S, Grassi F, Toneguzzi S, Piacentini A, Grigolo B, Santi S, Riccio M, Tognana E, Facchini A, Lisignoli G. 2005. Analysis of mesenchymal stem cells grown on a three-dimensional HYAFF 11-based prototype ligament scaffold. *J Biomed Mater Res A* 73(3):275-83.

D'Ippolito G, Diabira S, Howard GA, Menei P, Roos BA, Schiller PC. 2004. Marrow-isolated adult multilineage inducible (MIAMI) cells, a unique population of postnatal young and old human cells with extensive expansion and differentiation potential. *J Cell Sci* 117(Pt 14):2971-81.

Darling EM, Athanasiou KA. 2003. Biomechanical strategies for articular cartilage regeneration. *Ann Biomed Eng* 31(9):1114-24.

De Bartolo L, Morelli S, Lopez LC, Giorno L, Campana C, Salerno S, Rende M, Favia P, Detomaso L, Gristina R, d'Agostino R, Drioli E. 2005. Biotransformation and liver-specific functions of human hepatocytes in culture on RGD-immobilized plasma-processed membranes. *Biomaterials* 26(21):4432-41.

De Bartolo L, Morelli S, Piscioneri A, Lopez LC, Favia P, d'Agostino R, Drioli E. 2006. Novel membranes and surface modification able to activate specific cellular responses. *Biomol Eng*.

Dickinson SC, Sims TJ, Pittarello L, Soranzo C, Pavesio A, Hollander AP. 2005. Quantitative outcome measures of cartilage repair in patients treated by tissue engineering. *Tissue Eng* 11(1-2):277-87.

Dobson KR, Reading L, Haberey M, Marine X, Scutt A. 1999. Centrifugal isolation of bone marrow from bone: an improved method for the recovery and quantitation of bone marrow osteoprogenitor cells from rat tibiae and femurae. *Calcif Tissue Int* 65(5):411-3.

Dodgson KS, Lloyd AG. 1957. Studies on sulphatases. XVIII. Preparation of chondroitinase-free chondrosulphatase from extracts of Proteus vulgaris. *Biochem J* 66(3):532-8.

Dopirak RM, Adamany DC, Steensen RN. 2004. A comparison of autogenous patellar tendon and hamstring tendon grafts for anterior cruciate ligament reconstruction. *Orthopedics* 27(8):837-42; quiz 843-4.

Dressler MR, Butler DL, Boivin GP. 2005. Effects of age on the repair ability of mesenchymal stem cells in rabbit tendon. *J Orthop Res* 23(2):287-93.

el Nabout R, Martin M, Remy J, Kern P, Robert L, Lafuma C. 1989. Collagen synthesis and deposition in cultured fibroblasts from subcutaneous radiation-induced fibrosis. Modification as a function of cell aging. *Matrix* 9(5):411-20.

Elbjeirami WM, Yonter EO, Starcher BC, West JL. 2003. Enhancing mechanical properties of tissue-engineered constructs via lysyl oxidase crosslinking activity. *J Biomed Mater Res* 66A(3):513-21.

Emans PJ, Pieper J, Hulsbosch MM, Koenders M, Kreijveld E, Surtel DA, van Blitterswijk CA, Bulstra SK, Kuijer R, Riesle J. 2006. Differential Cell Viability of Chondrocytes and Progenitor Cells in Tissue-engineered Constructs Following Implantation into Osteochondral Defects. *Tissue Eng* 12(6):1699-709.

Engler AJ, Sen S, Sweeney HL, Discher DE. 2006. Matrix elasticity directs stem cell lineage specification. *Cell* 126(4):677-89.

Esko J. 1999. Proteoglycans and Glycosaminoglycans. In: Varki A, Esko J, Cummings R, Esko J, Freeze H, Hart G, Marth J, editors. *Essentials of Glycobiology* Cold Spring Harbor Laboratory Press (Woodbury, NY).

Ezura Y, Chakravarti S, Oldberg A, Chervoneva I, Birk DE. 2000. Differential expression of lumican and fibromodulin regulate collagen fibrillogenesis in developing mouse tendons. *J Cell Biol* 151(4):779-88.

Fermor B, Urban J, Murray D, Pocock A, Lim E, Francis M, Gage J. 1998. Proliferation and collagen synthesis of human anterior cruciate ligament cells in vitro: effects of ascorbate-2-phosphate, dexamethasone and oxygen tension. *Cell Biol Int* 22(9-10):635-40.

Field A. 2005. *Discovering Statistics Using SPSS* SAGE Publications Ltd (London).

Fini M, Motta A, Torricelli P, Giavaresi G, Nicoli Aldini N, Tschon M, Giardino R, Migliaresi C. 2005. The healing of confined critical size cancellous defects in the presence of silk fibroin hydrogel. *Biomaterials* 26(17):3527-36.

Fleming BC, Renstrom PA, Beynnon BD, Engstrom B, Peura GD, Badger GJ, Johnson RJ. 2001. The effect of weightbearing and external loading on anterior cruciate ligament strain. *J Biomech* 34(2):163-70.

Fu FH, Bennett CH, Lattermann C, Ma CB. 1999. Current trends in anterior cruciate ligament reconstruction. Part 1: Biology and biomechanics of reconstruction. *Am J Sports Med* 27(6):821-30.

Fu FH, Bennett CH, Ma CB, Menetrey J, Lattermann C. 2000. Current trends in anterior cruciate ligament reconstruction. Part II. Operative procedures and clinical correlations. *Am J Sports Med* 28(1):124-30.

Fujii K, Yamagishi T, Nagafuchi T, Tsuji M, Kuboki Y. 1994. Biochemical properties of collagen from ligaments and periarticular tendons of the human knee. *Knee Surg Sports Traumatol Arthrosc* 2(4):229-33.

Fukubayashi T, Torzilli PA, Sherman MF, Warren RF. 1982. An in vitro biomechanical evaluation of anterior-posterior motion of the knee. Tibial displacement, rotation, and torque. *J Bone Joint Surg Am* 64(2):258-64.

Garvin J, Qi J, Maloney M, Banes AJ. 2003. Novel system for engineering bioartificial tendons and application of mechanical load. *Tissue Eng* 9(5):967-79.

Ge Z, Goh JC, Lee EH. 2005. Selection of cell source for ligament tissue engineering. *Cell Transplant* 14(8):573-83.

Gelberman RH, Steinberg D, Amiel D, Akeson W. 1991. Fibroblast chemotaxis after tendon repair. *J Hand Surg [Am]* 16(4):686-93.

Goulet F, Rancourt D, Cloutier R, Germain L, Poole AR, Auger FA. 2000. Tendons and ligaments. In: Lanza RP, Langer R, Vacanti J, editors.

Principles of Tissue Engineering. Second ed. Academic Press (Burlington, MA).
Ha SW, Tonelli AE, Hudson SM. 2005. Structural studies of bombyx mori silk fibroin during regeneration from solutions and wet fiber spinning. *Biomacromolecules* 6(3):1722-31.
Hae Yoon J, Brooks R, Hwan Kim Y, Terada M, Halper J. 2003. Proteoglycans in chicken gastrocnemius tendons change with exercise. *Arch Biochem Biophys* 412(2):279-86.
Hankemeier S, Keus M, Zeichen J, Jagodzinski M, Barkhausen T, Bosch U, Krettek C, Van Griensven M. 2005. Modulation of proliferation and differentiation of human bone marrow stromal cells by fibroblast growth factor 2: potential implications for tissue engineering of tendons and ligaments. *Tissue Eng* 11(1-2):41-9.
Harley BA, Spilker MH, Wu JW, Asano K, Hsu HP, Spector M, Yannas IV. 2004. Optimal degradation rate for collagen chambers used for regeneration of peripheral nerves over long gaps. *Cells Tissues Organs* 176(1-3):153-65.
Harris MT, Butler DL, Boivin GP, Florer JB, Schantz EJ, Wenstrup RJ. 2004. Mesenchymal stem cells used for rabbit tendon repair can form ectopic bone and express alkaline phosphatase activity in constructs. *J Orthop Res* 22(5):998-1003.
Hattori H, Sato M, Masuoka K, Ishihara M, Kikuchi T, Matsui T, Takase B, Ishizuka T, Kikuchi M, Fujikawa K. 2004. Osteogenic potential of human adipose tissue-derived stromal cells as an alternative stem cell source. *Cells Tissues Organs* 178(1):2-12.
Haubeck HD, Kock R, Fischer DC, Van de Leur E, Hoffmeister K, Greiling H. 1995. Transforming growth factor beta 1, a major stimulator of hyaluronan synthesis in human synovial lining cells. *Arthritis Rheum* 38(5):669-77.
Hays WL. 1994. *Statistics*. Thomson Learning (Fort Worth, TX).
Hern DL, Hubbell JA. 1998. Incorporation of adhesion peptides into nonadhesive hydrogels useful for tissue resurfacing. *J Biomed Mater Res* 39(2):266-76.
Hildebrand A, Romaris M, Rasmussen LM, Heinegard D, Twardzik DR, Border WA, Ruoslahti E. 1994. Interaction of the small interstitial proteoglycans biglycan, decorin and fibromodulin with transforming growth factor beta. *Biochem J* 302 (Pt 2):527-34.
Hoemann CD, Sun J, Chrzanowski V, Buschmann MD. 2002. A multivalent assay to detect glycosaminoglycan, protein, collagen, RNA, and DNA content in milligram samples of cartilage or hydrogel-based repair cartilage. *Anal Biochem* 300(1):1-10.
Horan RL, Antle K, Collette AL, Wang Y, Huang J, Moreau JE, Volloch V, Kaplan DL, Altman GH. 2005a. In vitro degradation of silk fibroin. *Biomaterials* 26(17):3385-93.
Horan RL, Collette AL, Lee C, Antle K, Chen J, Altman GH. 2005b. Yarn design for functional tissue engineering. *J Biomech*.
Howard PS, Kucich U, Taliwal R, Korostoff JM. 1998. Mechanical forces alter extracellular matrix synthesis by human periodontal ligament fibroblasts. *J Periodontal Res* 33(8):500-8.

Hsieh AH, Tsai CM, Ma QJ, Lin T, Banes AJ, Villarreal FJ, Akeson WH, Sung KL. 2000. Time-dependent increases in type-III collagen gene expression in medical collateral ligament fibroblasts under cyclic strains. *J Orthop Res* 18(2):220-7.

Huang D, Chang TR, Aggarwal A, Lee RC, Ehrlich HP. 1993. Mechanisms and dynamics of mechanical strengthening in ligament-equivalent fibroblast-populated collagen matrices. *Ann Biomed Eng* 21(3):289-305.

Huey G, Stair S, Stern R. 1990. Hyaluronic acid determinations: optimizing assay parameters. *Matrix* 10(2):67-74.

Hulbert SF, Young FA, Mathews RS, Klawitter JJ, Talbert CD, Stelling FH. 1970. Potential of ceramic materials as permanently implantable skeletal prostheses. *J Biomed Mater Res* 4(3):433-56.

Hung CT, Allen FD, Pollack SR, Attia ET, Hannafin JA, Torzilli PA. 1997. Intracellular calcium response of ACL and MCL ligament fibroblasts to fluid-induced shear stress. *Cell Signal* 9(8):587-94.

Im GI, Shin YW, Lee KB. 2005. Do adipose tissue-derived mesenchymal stem cells have the same osteogenic and chondrogenic potential as bone marrow-derived cells? *Osteoarthritis Cartilage*.

Imanari T, Toida T, Koshiishi I, Toyoda H. 1996. High-performance liquid chromatographic analysis of glycosaminoglycan-derived oligosaccharides. *J Chromatogr A* 720(1-2):275-93.

Inoue S, Tanaka K, Tanaka H, Ohtomo K, Kanda T, Imamura M, Quan GX, Kojima K, Yamashita T, Nakajima T, Taira H, Tamura T, Mizuno S. 2004. Assembly of the silk fibroin elementary unit in endoplasmic reticulum and a role of L-chain for protection of alpha1,2-mannose residues in N-linked oligosaccharide chains of fibrohexamerin/P25. *Eur J Biochem* 271(2):356-66.

Iozzo RV. 1998. Matrix proteoglycans: from molecular design to cellular function. *Annu Rev Biochem* 67:609-52.

Itala AI, Ylanen HO, Ekholm C, Karlsson KH, Aro HT. 2001. Pore diameter of more than 100 microm is not requisite for bone ingrowth in rabbits. *J Biomed Mater Res* 58(6):679-83.

Jackson DW, Simon TM, Lowery W, Gendler E. 1996. Biologic remodeling after anterior cruciate ligament reconstruction using a collagen matrix derived from demineralized bone. An experimental study in the goat model. *Am J Sports Med* 24(4):405-14.

Jarvinen TA, Kannus P, Jarvinen TL, Jozsa L, Kalimo H, Jarvinen M. 2000. Tenascin-C in the pathobiology and healing process of musculoskeletal tissue injury. *Scand J Med Sci Sports* 10(6):376-82.

Jepsen KJ, Wu F, Peragallo JH, Paul J, Roberts L, Ezura Y, Oldberg A, Birk DE, Chakravarti S. 2002. A syndrome of joint laxity and impaired tendon integrity in lumican- and fibromodulin-deficient mice. *J Biol Chem* 277(38):35532-40.

Johnson DH. 2003. Should allografts be used for routine anterior cruciate ligament reconstructions? No, allografts should not be used for routine ACL reconstruction. *Arthroscopy* 19(4):424-5.

Jozsa L, Lehto M, Kannus P, Kvist M, Reffy A, Vieno T, Jarvinen M, Demel S, Elek E. 1989. Fibronectin and laminin in Achilles tendon. *Acta Orthop Scand* 60(4):469-71.

Juncosa-Melvin N, Boivin GP, Galloway MT, Gooch C, West JR, Sklenka AM, Butler DL. 2005. Effects of cell-to-collagen ratio in mesenchymal stem cell-seeded implants on tendon repair biomechanics and histology. *Tissue Eng* 11(3-4):448-57.

Juncosa-Melvin N, Boivin GP, Gooch C, Galloway MT, West JR, Dunn MG, Butler DL. 2006. The effect of autologous mesenchymal stem cells on the biomechanics and histology of gel-collagen sponge constructs used for rabbit patellar tendon repair. *Tissue Eng* 12(2):369-79.

Kagan HM. 2000. Intra- and extracellular enzymes of collagen biosynthesis as biological and chemical targets in the control of fibrosis. *Acta Trop* 77(1):147-52.

Karageorgiou V, Kaplan D. 2005. Porosity of 3D biomaterial scaffolds and osteogenesis. *Biomaterials* 26(27):5474-91.

Ker RF. 1999. The design of soft collagenous load-bearing tissues. *J Exp Biol* 202 Pt 23:3315-24.

Khor E. 1997. Methods for the treatment of collagenous tissues for bioprostheses. *Biomaterials* 18(2):95-105.

Kim BS, Mooney DJ. 2000. Scaffolds for engineering smooth muscle under cyclic mechanical strain conditions. *J Biomech Eng* 122(3):210-5.

Kim HJ, Kim UJ, Vunjak-Novakovic G, Min BH, Kaplan DL. 2005a. Influence of macroporous protein scaffolds on bone tissue engineering from bone marrow stem cells. *Biomaterials* 26(21):4442-52.

Kim SG, Akaike T, Sasagaw T, Atomi Y, Kurosawa H. 2002. Gene expression of type I and type III collagen by mechanical stretch in anterior cruciate ligament cells. *Cell Struct Funct* 27(3):139-44.

Kim UJ, Park J, Kim HJ, Wada M, Kaplan DL. 2005b. Three-dimensional aqueous-derived biomaterial scaffolds from silk fibroin. *Biomaterials* 26(15):2775-85.

Kim UJ, Park J, Li C, Jin HJ, Valluzzi R, Kaplan DL. 2004. Structure and properties of silk hydrogels. *Biomacromolecules* 5(3):786-92.

Kitamikado M, Lee YZ. 1975. Chondroitinase-producing bacteria in natural habitats. *Appl Microbiol* 29(3):414-21.

Knott L, Bailey AJ. 1998. Collagen cross-links in mineralizing tissues: a review of their chemistry, function, and clinical relevance. *Bone* 22(3):181-7.

Konttinen YT, Saari H, Nordstrom DC. 1991. Effect of interleukin-1 on hyaluronate synthesis by synovial fibroblastic cells. *Clin Rheumatol* 10(2):151-4.

Koshiishi I, Takenouchi M, Hasegawa T, Imanari T. 1998. Enzymatic method for the simultaneous determination of hyaluronan and chondroitin sulfates using high-performance liquid chromatography. *Anal Biochem* 265(1):49-54.

Kurosaki S, Otsuka H, Kunitomo M, Koyama M, Pawankar R, Matumoto K. 1999. Fibroin allergy. IgE mediated hypersensitivity to silk suture materials. *Nippon Ika Daigaku Zasshi* 66(1):41-4.

Kurpinski K, Chu J, Hashi C, Li S. 2006. Anisotropic mechanosensing by mesenchymal stem cells. *Proc Natl Acad Sci U S A* 103(44):16095-100.

Langberg H, Skovgaard D, Bulow J, Kjaer M. 1999. Negative interstitial pressure in the peritendinous region during exercise. *J Appl Physiol* 87(3):999-1002.

Langelier E, Rancourt D, Bouchard S, Lord C, Stevens PP, Germain L, Auger FA. 1999. Cyclic traction machine for long-term culture of fibroblast-populated collagen gels. *Ann Biomed Eng* 27(1):67-72.

Lee PH, Trowbridge JM, Taylor KR, Morhenn VB, Gallo RL. 2004a. Dermatan sulfate proteoglycan and glycosaminoglycan synthesis is induced in fibroblasts by transfer to a three-dimensional extracellular environment. *J Biol Chem* 279(47):48640-6.

Lee RH, Kim B, Choi I, Kim H, Choi HS, Suh K, Bae YC, Jung JS. 2004b. Characterization and expression analysis of mesenchymal stem cells from human bone marrow and adipose tissue. *Cell Physiol Biochem* 14(4-6):311-24.

Lemon G, King JR, Byrne HM, Jensen OE, Shakesheff KM. 2006. Mathematical modelling of engineered tissue growth using a multiphase porous flow mixture theory. *J Math Biol* 52(5):571-94.

Lohmander LS, Ostenberg A, Englund M, Roos H. 2004. High prevalence of knee osteoarthritis, pain, and functional limitations in female soccer players twelve years after anterior cruciate ligament injury. *Arthritis Rheum* 50(10):3145-52.

Ma Z, Kotaki M, Inai R, Ramakrishna S. 2005. Potential of nanofiber matrix as tissue-engineering scaffolds. *Tissue Eng* 11(1-2):101-9.

Maganaris CN, Narici MV, Almekinders LC, Maffulli N. 2004. Biomechanics and pathophysiology of overuse tendon injuries: ideas on insertional tendinopathy. *Sports Med* 34(14):1005-17.

Magoshi J, Magoshi Y, Nakamura S. 1994. Mechanism of Fiber Formation of Silkworm. In: Kaplan D, Adam WW, Farmer B, Viney C, editors. *Silk Polymers*. ACS (Washington, DC) p 292-310.

Mardilovich A, Craig JA, McCammon MQ, Garg A, Kokkoli E. 2006. Design of a novel fibronectin-mimetic peptide-amphiphile for functionalized biomaterials. *Langmuir* 22(7):3259-64.

McGuire DA. 2003. Should allografts be used for routine anterior cruciate ligament reconstructions? Yes, allografts should be used in routine ACL reconstruction. *Arthroscopy* 19(4):421-4.

Mehr D, Pardubsky PD, Martin JA, Buckwalter JA. 2000. Tenascin-C in tendon regions subjected to compression. *J Orthop Res* 18(4):537-45.

Meinel L, Betz O, Fajardo R, Hofmann S, Nazarian A, Cory E, Hilbe M, McCool J, Langer R, Vunjak-Novakovic G, Merkle HP, Rechenberg B, Kaplan DL, Kirker-Head C. 2006. Silk based biomaterials to heal critical sized femur defects. *Bone*.

Meinel L, Hofmann S, Karageorgiou V, Kirker-Head C, McCool J, Gronowicz G, Zichner L, Langer R, Vunjak-Novakovic G, Kaplan DL. 2005. The inflammatory responses to silk films in vitro and in vivo. *Biomaterials* 26(2):147-55.

Min BM, Lee G, Kim SH, Nam YS, Lee TS, Park WH. 2004. Electrospinning of silk fibroin nanofibers and its effect on the adhesion and spreading of normal human keratinocytes and fibroblasts in vitro. *Biomaterials* 25(7-8):1289-97.

Mio K, Yamashita M, Odake Y, Tamai H, Takada K. 2001. Coenzyme A stimulates collagen production in cultured fibroblasts; possible mechanisms in enzymatic and gene expression. *Arch Dermatol Res* 293(10):522-31.

Moreau J, Chen J, Kaplan D, Altman G. 2006. Sequential Growth Factor Stimulation of Bone Marrow Stromal Cells in Extended Culture. *Tissue Eng*.

Moreau JE, Chen J, Bramono DS, Volloch V, Chernoff H, Vunjak-Novakovic G, Richmond JC, Kaplan DL, Altman GH. 2005a. Growth factor induced fibroblast differentiation from human bone marrow stromal cells in vitro. *J Orthop Res* 23(1):164-74.

Moreau JE, Chen J, Horan RL, Kaplan DL, Altman GH. 2005b. Sequential growth factor application in bone marrow stromal cell ligament engineering. *Tissue Eng* 11(11-12):1887-97.

Murata K, Yokoyama Y. 1987. Liquid chromatographic assay for constituent disaccharides of hyaluronic acid and chondroitin sulphate isomers. *J Chromatogr* 415(2):231-40.

Murray AW, Macnicol MF. 2004. 10-16 year results of Leeds-Keio anterior cruciate ligament reconstruction. *Knee* 11(1):9-14.

Murray MM, Spector M. 1999. Fibroblast distribution in the anteromedial bundle of the human anterior cruciate ligament: the presence of alpha-smooth muscle actin-positive cells. *J Orthop Res* 17(1):18-27.

Mutsuzaki H, Sakane M, Nakajima H, Ito A, Hattori S, Miyanaga Y, Ochiai N, Tanaka J. 2004. Calcium-phosphate-hybridized tendon directly promotes regeneration of tendon-bone insertion. *J Biomed Mater Res* 70A(2):319-27.

Mwale F, Stachura D, Roughley P, Antoniou J. 2006. Limitations of using aggrecan and type X collagen as markers of chondrogenesis in mesenchymal stem cell differentiation. *J Orthop Res* 24(8):1791-8.

Nakamura S, Magoshi J, Magoshi Y. 1994. Thermal properties of Silk Proteins in Silkworms. In: Kaplan D, Adam WW, Farmer B, Viney C, editors. *Silk Polymers*. ACS (Washington, DC) p 211-221.

Nathanson MA. 1990. Hyaluronates in developing skeletal tissues. *Clin Orthop*(251):275-89.

Nazarov R, Jin HJ, Kaplan DL. 2004. Porous 3-D scaffolds from regenerated silk fibroin. *Biomacromolecules* 5(3):718-26.

Nomura E, Inoue M, Sugiura H. 2005. Histological evaluation of medial patellofemoral ligament reconstructed using the Leeds-Keio ligament prosthesis. *Biomaterials* 26(15):2663-70.

O'Brien FJ, Harley BA, Yannas IV, Gibson LJ. 2005. The effect of pore size on cell adhesion in collagen-GAG scaffolds. *Biomaterials* 26(4):433-41.

Olde Damink LH, Dijkstra PJ, van Luyn MJ, van Wachem PB, Nieuwenhuis P, Feijen J. 1996. Cross-linking of dermal sheep collagen using a water-soluble carbodiimide. *Biomaterials* 17(8):765-73.

Orban JM, Wilson LB, Kofroth JA, El-Kurdi MS, Maul TM, Vorp DA. 2004. Crosslinking of collagen gels by transglutaminase. *J Biomed Mater Res* 68A(4):756-62.

Park KH, Na K, Chung HM. 2005. Enhancement of the adhesion of fibroblasts by peptide containing an Arg-Gly-Asp sequence with

poly(ethylene glycol) into a thermo-reversible hydrogel as a synthetic extracellular matrix. *Biotechnol Lett* 27(4):227-31.

Parry DA, Flint MH, Gillard GC, Craig AS. 1982. A role for glycosaminoglycans in the development of collagen fibrils. *FEBS Lett* 149(1):1-7.

Pei M, Solchaga LA, Seidel J, Zeng L, Vunjak-Novakovic G, Caplan AI, Freed LE. 2002. Bioreactors mediate the effectiveness of tissue engineering scaffolds. *FASEB J* 16(12):1691-4.

Peperzak KA, Gilbert TW, Wang JH. 2004. A multi-station dynamic-culture force monitor system to study cell mechanobiology. *Med Eng Phys* 26(4):355-8.

Petersen W, Tillmann B. 1999. Structure and vascularization of the cruciate ligaments of the human knee joint. *Anat Embryol (Berl)* 200(3):325-34.

Petersen W, Varoga D, Zantop T, Hassenpflug J, Mentlein R, Pufe T. 2004. Cyclic strain influences the expression of the vascular endothelial growth factor (VEGF) and the hypoxia inducible factor 1 alpha (HIF-1alpha) in tendon fibroblasts. *J Orthop Res* 22(4):847-53.

Pieper JS, Hafmans T, Veerkamp JH, van Kuppevelt TH. 2000. Development of tailor-made collagen-glycosaminoglycan matrices: EDC/NHS crosslinking, and ultrastructural aspects. *Biomaterials* 21(6):581-93.

Pieper JS, Oosterhof A, Dijkstra PJ, Veerkamp JH, van Kuppevelt TH. 1999. Preparation and characterization of porous crosslinked collagenous matrices containing bioavailable chondroitin sulphate. *Biomaterials* 20(9):847-58.

Pornprasertsuk S, Duarte WR, Mochida Y, Yamauchi M. 2004. Lysyl hydroxylase-2b directs collagen cross-linking pathways in MC3T3-E1 cells. *J Bone Miner Res* 19(8):1349-55.

Price FM, Levick JR, Mason RM. 1996. Glycosaminoglycan concentration in synovium and other tissues of rabbit knee in relation to synovial hydraulic resistance. *J Physiol* 495 (Pt 3):803-20.

Prockop DJ, Sieron AL, Li SW. 1998. Procollagen N-proteinase and procollagen C-proteinase. Two unusual metalloproteinases that are essential for procollagen processing probably have important roles in development and cell signaling. *Matrix Biol* 16(7):399-408.

Pulkki K. 1986. The effects of synovial fluid macrophages and interleukin-1 on hyaluronic acid synthesis by normal synovial fibroblasts. *Rheumatol Int* 6(3):121-5.

Puxkandl R, Zizak I, Paris O, Keckes J, Tesch W, Bernstorff S, Purslow P, Fratzl P. 2002. Viscoelastic properties of collagen: synchrotron radiation investigations and structural model. *Philos Trans R Soc Lond B Biol Sci* 357(1418):191-7.

Raper SE, Chirmule N, Lee FS, Wivel NA, Bagg A, Gao GP, Wilson JM, Batshaw ML. 2003. Fatal systemic inflammatory response syndrome in a ornithine transcarbamylase deficient patient following adenoviral gene transfer. *Mol Genet Metab* 80(1-2):148-58.

Redaelli A, Vesentini S, Soncini M, Vena P, Mantero S, Montevecchi FM. 2003. Possible role of decorin glycosaminoglycans in fibril to fibril force transfer in relative mature tendons--a computational study from molecular to microstructural level. *J Biomech* 36(10):1555-69.

Reddy GK. 2003. Glucose-mediated in vitro glycation modulates biomechanical integrity of the soft tissues but not hard tissues. *J Orthop Res* 21(4):738-43.

Reed CC, Iozzo RV. 2002. The role of decorin in collagen fibrillogenesis and skin homeostasis. *Glycoconj J* 19(4-5):249-55.

Rees JD, Wilson AM, Wolman RL. 2006. Current concepts in the management of tendon disorders. *Rheumatology (Oxford)* 45(5):508-21.

Reiser K, McCormick RJ, Rucker RB. 1992. Enzymatic and nonenzymatic cross-linking of collagen and elastin. *FASEB J* 6(7):2439-49.

Riechert K, Labs K, Lindenhayn K, Sinha P. 2001. Semiquantitative analysis of types I and III collagen from tendons and ligaments in a rabbit model. *J Orthop Sci* 6(1):68-74.

Riley GP, Harrall RL, Cawston TE, Hazleman BL, Mackie EJ. 1996. Tenascin-C and human tendon degeneration. *Am J Pathol* 149(3):933-43.

Riley GP, Harrall RL, Constant CR, Chard MD, Cawston TE, Hazleman BL. 1994. Glycosaminoglycans of human rotator cuff tendons: changes with age and in chronic rotator cuff tendinitis. *Ann Rheum Dis* 53(6):367-76.

Robinson PS, Lin TW, Jawad AF, Iozzo RV, Soslowsky LJ. 2004a. Investigating tendon fascicle structure-function relationships in a transgenic-age mouse model using multiple regression models. *Ann Biomed Eng* 32(7):924-31.

Robinson PS, Lin TW, Reynolds PR, Derwin KA, Iozzo RV, Soslowsky LJ. 2004b. Strain-rate sensitive mechanical properties of tendon fascicles from mice with genetically engineered alterations in collagen and decorin. *J Biomech Eng* 126(2):252-7.

Rodriguez-Guzman M, Montero JA, Santesteban E, Ganan Y, Macias D, Hurle JM. 2007. Tendon-muscle crosstalk controls muscle bellies morphogenesis, which is mediated by cell death and retinoic acid signaling. *Dev Biol* 302(1):267-80.

Ross JJ, Hong Z, Willenbring B, Zeng L, Isenberg B, Lee EH, Reyes M, Keirstead SA, Weir EK, Tranquillo RT, Verfaillie CM. 2006. Cytokine-induced differentiation of multipotent adult progenitor cells into functional smooth muscle cells. *J Clin Invest* 116(12):3139-49.

Sahoo S, Ouyang H, Goh JC, Tay TE, Toh SL. 2006. Characterization of a novel polymeric scaffold for potential application in tendon/ligament tissue engineering. *Tissue Eng* 12(1):91-9.

Saini S, Wick TM. 2004. Effect of low oxygen tension on tissue-engineered cartilage construct development in the concentric cylinder bioreactor. *Tissue Eng* 10(5-6):825-32.

Sakane M, Fox RJ, Woo SL, Livesay GA, Li G, Fu FH. 1997. In situ forces in the anterior cruciate ligament and its bundles in response to anterior tibial loads. *J Orthop Res* 15(2):285-93.

Sakuma K, Mizuta H, Kai K, Takagi K, Iyama K. 1993. Ultrastructural changes of collagen fibers in the anterior cruciate ligament of bipedal rats after enforced running. *Nippon Seikeigeka Gakkai Zasshi* 67(7):655-61.

Sampaio S, Taddei P, Monti P, Buchert J, Freddi G. 2005. Enzymatic grafting of chitosan onto Bombyx mori silk fibroin: kinetic and IR vibrational studies. *J Biotechnol* 116(1):21-33.

Sander EA, Nauman EA. 2003. Permeability of musculoskeletal tissues and scaffolding materials: experimental results and theoretical predictions. *Crit Rev Biomed Eng* 31(1-2):1-26.

Scott JE. 1992. Supramolecular organization of extracellular matrix glycosaminoglycans, in vitro and in the tissues. *FASEB J* 6(9):2639-45.

Scott JE. 2003. Elasticity in extracellular matrix 'shape modules' of tendon, cartilage, etc. A sliding proteoglycan-filament model. *J Physiol* 553(Pt 2):335-43.

Scott JE, Orford CR, Hughes EW. 1981. Proteoglycan-collagen arrangements in developing rat tail tendon. An electron microscopical and biochemical investigation. *Biochem J* 195(3):573-81.

Screen HR, Lee DA, Bader DL, Shelton JC. 2003. Development of a technique to determine strains in tendons using the cell nuclei. *Biorheology* 40(1-3):361-8.

Screen HR, Lee DA, Bader DL, Shelton JC. 2004. An investigation into the effects of the hierarchical structure of tendon fascicles on micromechanical properties. *Proc Inst Mech Eng [H]* 218(2):109-19.

Screen HR, Shelton JC, Bader DL, Lee DA. 2005a. Cyclic tensile strain upregulates collagen synthesis in isolated tendon fascicles. *Biochem Biophys Res Commun*.

Screen HR, Shelton JC, Chhaya VH, Kayser MV, Bader DL, Lee DA. 2005b. The influence of noncollagenous matrix components on the micromechanical environment of tendon fascicles. *Ann Biomed Eng* 33(8):1090-9.

Scutt A, Bertram P. 1995. Bone marrow cells are targets for the anabolic actions of prostaglandin E2 on bone: induction of a transition from nonadherent to adherent osteoblast precursors. *J Bone Miner Res* 10(3):474-87.

Sekiya I, Larson BL, Smith JR, Pochampally R, Cui JG, Prockop DJ. 2002. Expansion of human adult stem cells from bone marrow stroma: conditions that maximize the yields of early progenitors and evaluate their quality. *Stem Cells* 20(6):530-41.

Silver FH, Freeman JW, Seehra GP. 2003. Collagen self-assembly and the development of tendon mechanical properties. *J Biomech* 36(10):1529-53.

Skandalis SS, Theocharis AD, Papageorgakopoulou N, Zagris N. 2003. Glycosaminoglycans in early chick embryo. *Int J Dev Biol* 47(4):311-4.

Snell RS. 2000. *Clinical anatomy for medical students*. Lippincott Williams & Wilkins (Philadelphia).

Sofia S, McCarthy MB, Gronowicz G, Kaplan DL. 2001. Functionalized silk-based biomaterials for bone formation. *J Biomed Mater Res* 54(1):139-48.

Spindler KP, Kuhn JE, Freedman KB, Matthews CE, Dittus RS, Harrell FE, Jr. 2004. Anterior cruciate ligament reconstruction autograft choice: bone-tendon-bone versus hamstring: does it really matter? A systematic review. *Am J Sports Med* 32(8):1986-95.

Stewart K, Monk P, Walsh S, Jefferiss CM, Letchford J, Beresford JN. 2003. STRO-1, HOP-26 (CD63), CD49a and SB-10 (CD166) as markers of primitive human marrow stromal cells and their more differentiated progeny: a comparative investigation in vitro. *Cell Tissue Res* 313(3):281-90.

Strem BM, Hedrick MH. 2005. The growing importance of fat in regenerative medicine. *Trends Biotechnol* 23(2):64-6.

Suh SW, Shin JY, Kim J, Kim J, Beak CH, Kim DI, Kim H, Jeon SS, Choo IW. 2002. Effect of different particles on cell proliferation in polymer scaffolds using a solvent-casting and particulate leaching technique. *Asaio J* 48(5):460-4.

Sung HW, Chang WH, Ma CY, Lee MH. 2003. Crosslinking of biological tissues using genipin and/or carbodiimide. *J Biomed Mater Res A* 64(3):427-38.

Sung HW, Huang RN, Huang LL, Tsai CC, Chiu CT. 1998. Feasibility study of a natural crosslinking reagent for biological tissue fixation. *J Biomed Mater Res* 42(4):560-7.

Suzuki S, Saito H, Yamagata T, Anno K, Seno N, Kawai Y, Furuhashi T. 1968. Formation of three types of disulfated disaccharides from chondroitin sulfates by chondroitinase digestion. *J Biol Chem* 243(7):1543-50.

Takai S, Woo SL, Livesay GA, Adams DJ, Fu FH. 1993. Determination of the in situ loads on the human anterior cruciate ligament. *J Orthop Res* 11(5):686-95.

Tognana E, Padera RF, Chen F, Vunjak-Novakovic G, Freed LE. 2005. Development and remodeling of engineered cartilage-explant composites in vitro and in vivo. *Osteoarthritis Cartilage*.

Toole BP, Munaim SI, Welles S, Knudson CB. 1989. Hyaluronate-cell interactions and growth factor regulation of hyaluronate synthesis during limb development. *Ciba Found Symp* 143:138-45; discussion 145-9 281-5.

Tsai CC, Huang RN, Sung HW, Liang HC. 2000. In vitro evaluation of the genotoxicity of a naturally occurring crosslinking agent (genipin) for biologic tissue fixation. *J Biomed Mater Res* 52(1):58-65.

Tsai SW, Liu RL, Hsu FY, Chen CC. 2006. A study of the influence of polysaccharides on collagen self-assembly: nanostructure and kinetics. *Biopolymers* 83(4):381-8.

Um IC, Kweon H, Lee KG, Ihm DW, Lee JH, Park YH. 2004. Wet spinning of silk polymer. I. Effect of coagulation conditions on the morphological feature of filament. *Int J Biol Macromol* 34(1-2):89-105.

Unger RE, Wolf M, Peters K, Motta A, Migliaresi C, James Kirkpatrick C. 2004. Growth of human cells on a non-woven silk fibroin net: a potential for use in tissue engineering. *Biomaterials* 25(6):1069-75.

Unsworth BR, Lelkes PI. 2000. Assembly in Microgravity. In: Lanza RP, Langer R, Vacanti J, editors. *Principles of Tissue Engineering*. Second ed (Burlington, MA).

van der Pauw MT, Klein-Nulend J, van den Bos T, Burger EH, Everts V, Beertsen W. 2000. Response of periodontal ligament fibroblasts and gingival fibroblasts to pulsating fluid flow: nitric oxide and

prostaglandin E2 release and expression of tissue non-specific alkaline phosphatase activity. *J Periodontal Res* 35(6):335-43.

van Eijk F, Saris DB, Riesle J, Willems WJ, van Blitterswijk CA, Verbout AJ, Dhert WJ. 2004. Tissue engineering of ligaments: a comparison of bone marrow stromal cells, anterior cruciate ligament, and skin fibroblasts as cell source. *Tissue Eng* 10(5-6):893-903.

van Wachem PB, van Luyn MJ, Olde Damink LH, Dijkstra PJ, Feijen J, Nieuwenhuis P. 1994. Biocompatibility and tissue regenerating capacity of crosslinked dermal sheep collagen. *J Biomed Mater Res* 28(3):353-63.

Vickers SM, Squitieri LS, Spector M. 2006. Effects of cross-linking type II collagen-GAG scaffolds on chondrogenesis in vitro: dynamic pore reduction promotes cartilage formation. *Tissue Eng* 12(5):1345-55.

Volpi N. 1994. Fractionation of heparin, dermatan sulfate, and chondroitin sulfate by sequential precipitation: a method to purify a single glycosaminoglycan species from a mixture. *Anal Biochem* 218(2):382-91.

Volpi N. 2000. Hyaluronic acid and chondroitin sulfate unsaturated disaccharides analysis by high-performance liquid chromatography and fluorimetric detection with dansylhydrazine. *Anal Biochem* 277(1):19-24.

Von Porat A, Roos EM, Roos H. 2004. High prevalence of osteoarthritis 14 years after an anterior cruciate ligament tear in male soccer players: a study of radiographic and patient relevant outcomes. *Br J Sports Med* 38(3):263.

Voytik-Harbin SL, Brightman AO, Kraine MR, Waisner B, Badylak SF. 1997. Identification of extractable growth factors from small intestinal submucosa. *J Cell Biochem* 67(4):478-91.

Vunjak-Novakovic G, Altman G, Horan R, Kaplan DL. 2004. Tissue engineering of ligaments. *Annu Rev Biomed Eng* 6:131-56.

Vynios DH, Karamanos NK, Tsiganos CP. 2002. Advances in analysis of glycosaminoglycans: its application for the assessment of physiological and pathological states of connective tissues. *J Chromatogr B Analyt Technol Biomed Life Sci* 781(1-2):21-38.

Wallace DG, Rosenblatt J. 2003. Collagen gel systems for sustained delivery and tissue engineering. *Adv Drug Deliv Rev* 55(12):1631-49.

Walmsley AR, Batten MR, Lad U, Bulleid NJ. 1999. Intracellular retention of procollagen within the endoplasmic reticulum is mediated by prolyl 4-hydroxylase. *J Biol Chem* 274(21):14884-92.

Wang C, Luosujarvi H, Heikkinen J, Risteli M, Uitto L, Myllyla R. 2002. The third activity for lysyl hydroxylase 3: galactosylation of hydroxylysyl residues in collagens in vitro. *Matrix Biol* 21(7):559-66.

Wang H, Pieper J, Peters F, van Blitterswijk CA, Lamme EN. 2005a. Synthetic scaffold morphology controls human dermal connective tissue formation. *J Biomed Mater Res A* 74(4):523-32.

Wang Y, Kim HJ, Vunjak-Novakovic G, Kaplan DL. 2006. Stem cell-based tissue engineering with silk biomaterials. *Biomaterials*.

Wang Y, Kim UJ, Blasioli DJ, Kim HJ, Kaplan DL. 2005b. In vitro cartilage tissue engineering with 3D porous aqueous-derived silk scaffolds and mesenchymal stem cells. *Biomaterials* 26(34):7082-94.

Weitzel PP, Richmond JC, Altman GH, Calabro T, Kaplan DL. 2002. Future direction of the treatment of ACL ruptures. *Orthop Clin North Am* 33(4):653-61.

Wells AF, Klareskog L, Lindblad S, Laurent TC. 1992. Correlation between increased hyaluronan localized in arthritic synovium and the presence of proliferating cells. A role for macrophage-derived factors. *Arthritis Rheum* 35(4):391-6.

Wilkins RJ, Hall AC. 1995. Control of matrix synthesis in isolated bovine chondrocytes by extracellular and intracellular pH. *J Cell Physiol* 164(3):474-81.

Woo SL, Livesay GA, Runco TJ, Young EP. 1997. Structure and Function of Tendons and Ligaments. In: Mow VC, Hayes WC, editors. *Basic Orthopaedic Biomechanics*. Second ed. Lippincott-Raven (Philadelphia) p 209-251.

Woodfield TB, Van Blitterswijk CA, De Wijn J, Sims TJ, Hollander AP, Riesle J. 2005. Polymer scaffolds fabricated with pore-size gradients as a model for studying the zonal organization within tissue-engineered cartilage constructs. *Tissue Eng* 11(9-10):1297-311.

Wren TA, Beaupre GS, Carter DR. 2000. Mechanobiology of tendon adaptation to compressive loading through fibrocartilaginous metaplasia. *J Rehabil Res Dev* 37(2):135-43.

Xia Q, Zhou Z, Lu C, Cheng D, Dai F, Li B, Zhao P, Zha X, Cheng T, Chai C, Pan G, Xu J, Liu C, Lin Y, Qian J, Hou Y, Wu Z, Li G, Pan M, Li C, Shen Y, Lan X, Yuan L, Li T, Xu H, Yang G, Wan Y, Zhu Y, Yu M, Shen W, Wu D, Xiang Z, Yu J, Wang J, Li R, Shi J, Li H, Su J, Wang X, Zhang Z, Wu Q, Li J, Zhang Q, Wei N, Sun H, Dong L, Liu D, Zhao S, Zhao X, Meng Q, Lan F, Huang X, Li Y, Fang L, Li D, Sun Y, Yang Z, Huang Y, Xi Y, Qi Q, He D, Huang H, Zhang X, Wang Z, Li W, Cao Y, Yu Y, Yu H, Ye J, Chen H, Zhou Y, Liu B, Ji H, Li S, Ni P, Zhang J, Zhang Y, Zheng H, Mao B, Wang W, Ye C, Wong GK, Yang H. 2004. A draft sequence for the genome of the domesticated silkworm (Bombyx mori). *Science* 306(5703):1937-40.

Yagi M, Wong EK, Kanamori A, Debski RE, Fu FH, Woo SL. 2002. Biomechanical analysis of an anatomic anterior cruciate ligament reconstruction. *Am J Sports Med* 30(5):660-6.

Yagishita K, Sekiya I, Sakaguchi Y, Shinomiya K, Muneta T. 2005. The effect of hyaluronan on tendon healing in rabbits. *Arthroscopy* 21(11):1330-6.

Yahia LH, Desrosiers EA, Rivard CH. 1991. A computer-controlled apparatus for in vitro mechanical stimulation and characterization of ligaments. *Biomed Mater Eng* 1(4):215-22.

Yahia LH, Drouin G. 1989. Microscopical investigation of canine anterior cruciate ligament and patellar tendon: collagen fascicle morphology and architecture. *J Orthop Res* 7(2):243-51.

Yamagata T, Saito H, Habuchi O, Suzuki S. 1968. Purification and properties of bacterial chondroitinases and chondrosulfatases. *J Biol Chem* 243(7):1523-35.

Yamamoto E, Hayashi K, Yamamoto N. 1999. Mechanical properties of collagen fascicles from the rabbit patellar tendon. *J Biomech Eng* 121(1):124-31.

Yamamoto Y, Hsu WH, Woo SL, Van Scyoc AH, Takakura Y, Debski RE. 2004. Knee stability and graft function after anterior cruciate ligament reconstruction: a comparison of a lateral and an anatomical femoral tunnel placement. *Am J Sports Med* 32(8):1825-32.

Yang S, Leong KF, Du Z, Chua CK. 2001. The design of scaffolds for use in tissue engineering. Part I. Traditional factors. *Tissue Eng* 7(6):679-89.

Yannas IV, Lee E, Orgill DP, Skrabut EM, Murphy GF. 1989. Synthesis and characterization of a model extracellular matrix that induces partial regeneration of adult mammalian skin. *Proc Natl Acad Sci U S A* 86(3):933-7.

Young MF, Bi Y, Ameye L, Chen XD. 2002. Biglycan knockout mice: new models for musculoskeletal diseases. *Glycoconj J* 19(4-5):257-62.

Zavahir F, McGrouther DA, Misra A, Smith K, Brown RA, Mudera V. 2001. A study of the cellular response to orientated fibronectin material in healing extensor rat tendon. *J Mater Sci Mater Med* 12(10-12):1005-11.

Zayas JR, Schwarz RI. 1992. Evidence supporting the role of a proteinaceous, loosely bound extracellular molecule in the cell density signaling between tendon cells. *In Vitro Cell Dev Biol* 28A(11-12):745-54.

Zebrower M, Kieras FJ, Heaney-Kieras J. 1991. High pressure liquid chromatographic identification of hyaluronic acid and chondroitin sulphate disaccharides. *Glycobiology* 1(3):271-6.

Zeeman R. 1998. Cross-linking of collagen based materials: University of Twente.

Zhang Y, Lin HK, Frimberger D, Epstein RB, Kropp BP. 2005. Growth of bone marrow stromal cells on small intestinal submucosa: an alternative cell source for tissue engineered bladder. *BJU Int* 96(7):1120-5.

Zhao C, Yao J, Masuda H, Kishore R, Asakura T. 2003. Structural characterization and artificial fiber formation of Bombyx mori silk fibroin in hexafluoro-iso-propanol solvent system. *Biopolymers* 69(2):253-9.

Zhou L, Chen X, Dai W, Shao Z. 2006. X-ray photoelectron spectroscopic and Raman analysis of silk fibroin-Cu(II) films. *Biopolymers* 82(2):144-51.

Zhou L, Chen X, Shao Z, Zhou P, Knight DP, Vollrath F. 2003. Copper in the silk formation process of Bombyx mori silkworm. *FEBS Lett* 554(3):337-41.

Zhou P, Xie X, Knight DP, Zong XH, Deng F, Yao WH. 2004. Effects of pH and calcium ions on the conformational transitions in silk fibroin using 2D Raman correlation spectroscopy and 13C solid-state NMR. *Biochemistry* 43(35):11302-11.

Zohar R, Sodek J, McCulloch CA. 1997. Characterization of stromal progenitor cells enriched by flow cytometry. *Blood* 90(9):3471-81.

Zong XH, Zhou P, Shao ZZ, Chen SM, Chen X, Hu BW, Deng F, Yao WH. 2004. Effect of pH and copper(II) on the conformation transitions of silk fibroin based on EPR, NMR, and Raman spectroscopy. *Biochemistry* 43(38):11932-41.

Appendix A – Reagent preparation

A.1. Analytical reagents

A.1.1. Papain buffer

Stored at 4°C for up to three months

1.42g sodium phosphate, dibasic
0.0788g cysteine hydrochloride
0.1861 ethylenediamine tetraacetic acid (EDTA)
1M hydrochloride acid for pH adjustment

The sodium phosphate, cysteine hydrochloride, and EDTA were dissolved in 90ml of roH_2O. The pH was adjusted to 6.5 with the 1M Hydrochloric acid, and then the volume was topped up to 100ml.

A.1.2. Hydroxyproline assay buffer

Stored at 4°C in a dark bottle for up to two months

13.3g Citric acid (1H_2O)
3.2ml Glacial acetic acid
32g Sodium acetate (3H_2O)
9.1g Sodium Hydroxide
80ml Propan-*1*-ol

The reagents above are combined and made up to 300ml with roH_2O. The pH is adjusted to 6.0-6.5 with 0.2M sodium hydroxide, and the volume made up to 400ml with roH_2O.

A.1.3. Oxidizing solution

Use instantly

1.41g Chloramine T

Chloramine-T is dissolved in 100ml roH_2O.

A.1.4. Ehrlich's reagent

Use within 1 hour

7.5g *p*-dimethylaminobenzaldehyde
30ml Propan-*1*-ol
11.5ml 70% Perchloric acid

Reagents are combined and volume is increased to 50ml with roH2O.